# The 4th International Workshop on Nonhydrostatic Numerical Models (NHM2016)

**Nov. 30 – Dec. 2, 2016**

# The 4th International Workshop on Nonhydrostatic Numerical Models (NHM2016)

Nov. 30 - Dec. 2, 2016
at Prince Hakone Lake Ashinoko,
Kanagawa, Japan

Website http://157.82.240.172/~nhm/
E-mail nhm2016@aori.u-tokyo.ac.jp

Local Organizing Committee:
Masaki Satoh, Tomoki Miyakawa (Atmosphere and Ocean Research Institute, The University of Tokyo)
Hirofumi Tomita (RIKEN Advanced Institute for Computational Science)

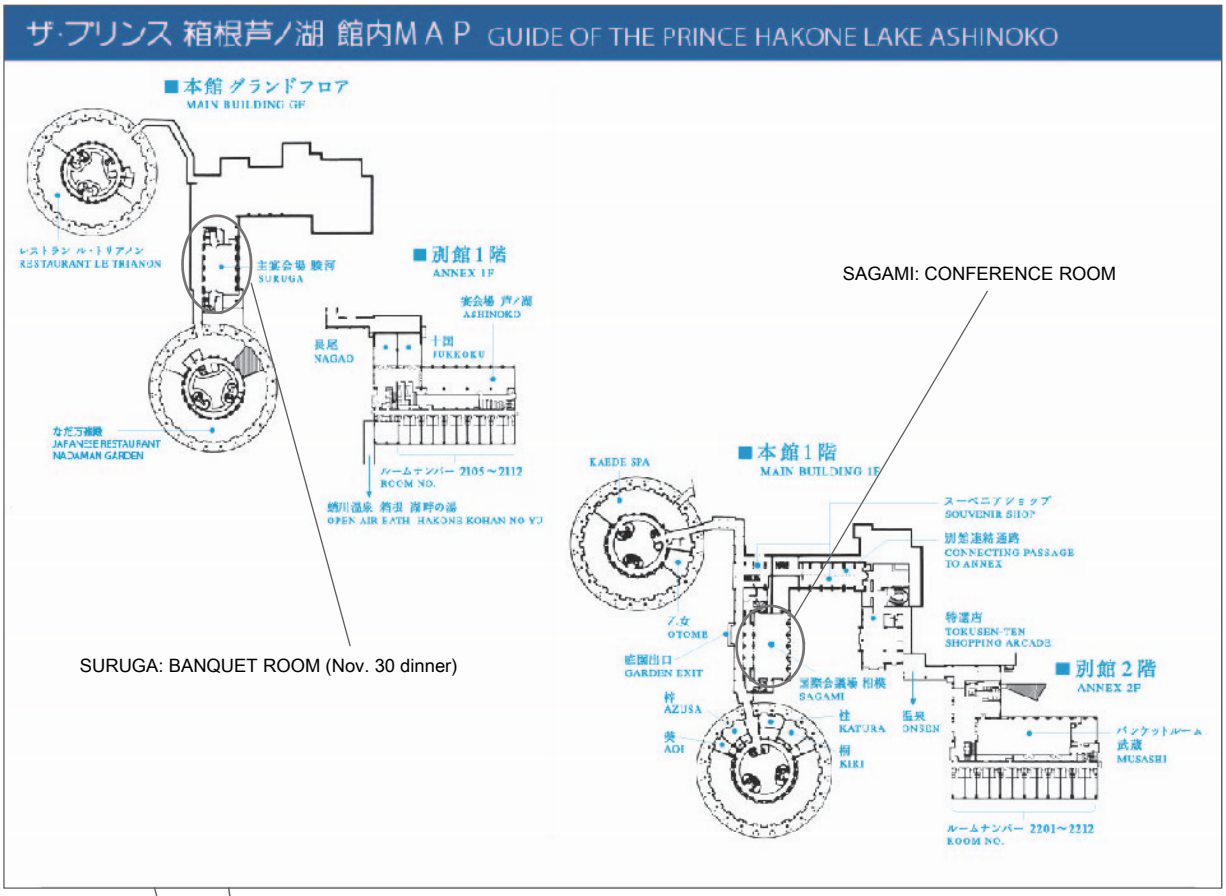


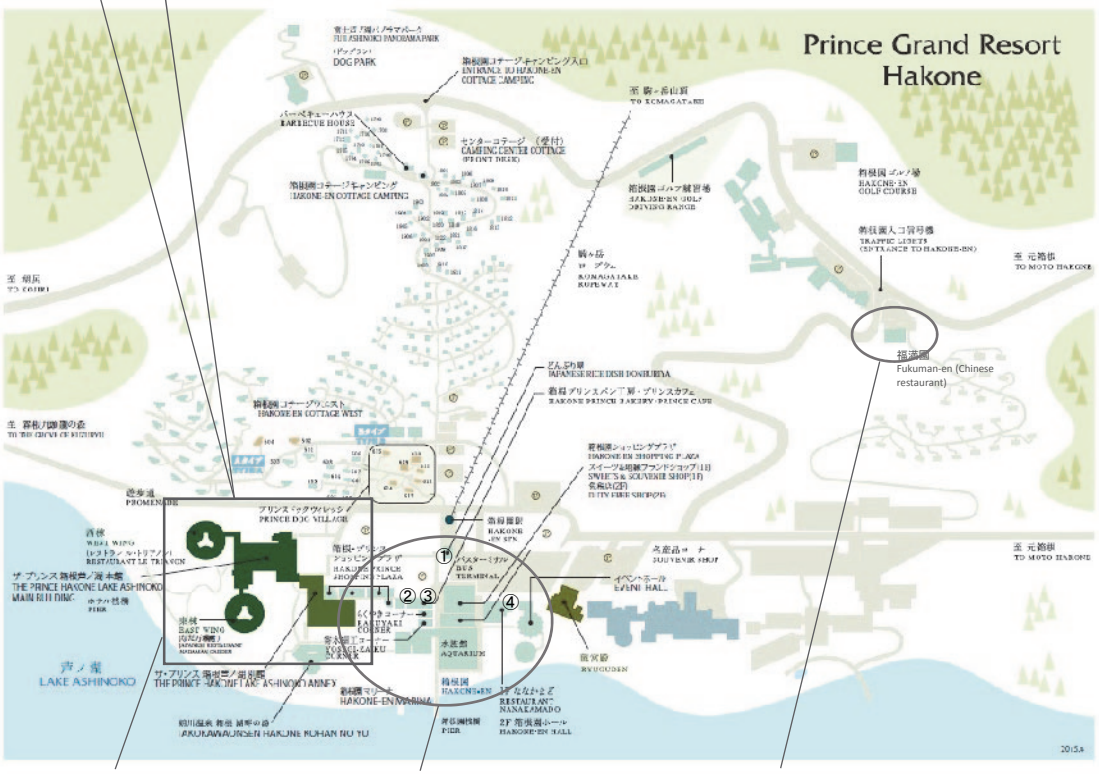


**The Prince Hakone Lake Ashinoko**
144 Motohakone,
Hakone-machi,
Ashigara-shimo-gun
Kanagawa,
250-0592, Japan
Tel: 81-(0)460-83-1111

**Hakone-en restaurants**
① Japanese rice dish Donburiya
② Curry & Ramen Mugiwaraya
③ Bakery Prince Cafe
④ Restaurant Nanakamado

**Fukuman-en Hakone** (Chinese restaurant)
（Dec. 1, banquet)
138 Motohakone, Hakone-machi,
Ashigara-shimo-gun Kanagawa, 250-0522
Tel: 81-(0)460-83-1888


**The Prince Hakone Lake Ashinoko**
144 Motohakone, Hakone-machi,
Ashigara-shimo-gun Kanagawa, 250-0592, Japan
Tel: 81-(0)460-83-1111

**Fukuman-en Hakone** (Chinese restaurant)
（Dec. 1, banquet)
138 Motohakone, Hakone-machi,
Ashigara-shimo-gun Kanagawa, 250-0522
Tel: 81-(0)460-83-1888


**Hakone-en Restaurants**

⑨ **Restaurant Nanakamado**
⑪ **Japanese rice dish Donburiya**
⑫ **Bakery Prince Cafe**
⑬ **Curry & Ramen Mugiwaraya**

## The 4th International Workshop on Nonhydrostatic Models

Nov. 30 (Wed) - Dec. 2 (Fri), 2016

The Prince Hakone Lake Ashinoko, Hakone, Japan

## Program

**November 30 (Wed)**

13:30-13:40 Masaki Satoh: Opening

Deep convection: Chair: Eigo Tochimoto

13:40-14:00 Hisashi Yashiro, Yoshiyuki Kajikawa, Yoshiaki Miyamoto, Tsuyoshi Yamaura, Ryuji Yoshida, and Hirofumi Tomita
Resolution dependence of the diurnal cycle of precipitation over land in the tropics simulated by a global cloud permitting model

14:00-14:20 Didier Ricard, Antoine Verrelle, Christine Lac, and Nicolas Rochetin
Representation of turbulence in simulations of deep convective clouds

14:20-14:40 Christopher Moseley, Cathy Hohenegger, Peter Berg, and Jan O. Haerter
Intensification of convective extremes driven by cloud–cloud interaction

14:40-15:00 Marat Khairoutdinov
Statistics of clusters of tropical convection in global cloud-resolving simulations of aqua-planet with SAM

15:00-15:30 Break

Deep convection, meso: Chair: Hisashi Yashiro

15:30-15:50 Thomas Schwitalla
Convection permitting latitude belt simulation with the WRF model

15:50-16:10 Kengo Matsubayashi, Tabito Hara, Kohei Aranami, and Kohei Kawano
An update of convection scheme in 5km resolution operational system

16:10-16:30 Eigo Tochimoto, Sho Yokota, Hiroshi Niino, and Wataru Yanase
Mesoscale vortex that caused marine accidents due to a sudden gusty wind in the southwestern part of the sea of Japan on 1 September 2015

16:30-16:50 Teruyuki Kato
Influence of horizontal resolution on structure changes of atmospheric stratification in the 2015 Hiroshima heavy rainfall

16:50-18:00 Poster display

18:00 Reception (Suruga)

**December 1 (Thu)**

Dynamical cores/numerical schemes: Chair: Tomoki Miyakawa

8:40-9:00 David Randall, Ross Heikes, and Celal Konor
A global vector vorticity model on a geodesic grid

9:00-9:20 Chien-Ming Wu
Development of a Taiwan full-physics vector vorticity equation model (VVM)

9:20-9:40 John L. McGregor
Cubed-sphere modelling activities at CSIRO

9:40-10:00 Kazushi Takemura, Keiichi Ishioka, and Shoichi Shige
Development of a non-hydrostatic atmospheric model using the Chimera grid method for a steep terrain

10:00-10:20 Kohei Kawano, Kohei Aranami, Tabito Hara, Kengo Matsubayashi, Masami Sakamoto, and Yuji Kitamura
Improving computational stability with time-splitting of vertical advection considering 3-dimensional CFL condition

10:20-10:50 Break

Numerical schemes, MJO/field exp.: Chair: Chien-Ming Wu

10:50-11:10 Lian-Ping Wang, Wojciech W. Grabowski, Zhaoli Guo, and Ryo Onishi
Development of a mesoscopic simulation method for atmospheric convection

11:10-11:30 Yuki Nishikawa, and Masaki Satoh
Topographic representation scheme using a thin-wall approximation in terrain-following coordinates

11:30-11:50 Chung-Hsiung Sui, Yi-An Chen, and Shu-Yu Hou
Simulated convective-radiative properties in the MJO during DYNAMO/CINDY

11:50-12:10 Kazuyoshi Kikuchi, Chihiro Kodama, Tomoki Miyakawa, Tomoe Nasuno, and Masaki Satoh
Multiscale structure of the MJO: Does it matter?

12:10-13:40 Lunch

MJO/field exp., assimilation: Chair: Kazuyoshi Kikuchi

13:40-14:00 Tomoki Miyakawa
Current status of MJO simulations using NICAM and its 3D-ocean coupled version NICOCO

14:00-14:20 Tomoe Nasuno
Near real-time forecasts using a global nonhydrostatic model NICAM for field campaigns

14:20-14:40 Takemasa Miyoshi, Guo-Yuan Lien, Masaru Kunii, Juan Ruiz, Yasumitsu Maejima, Shigenori Otsuka, Keiichi Kondo, Hiromu Seko,Shinsuke Satoh, Tomoo Ushio, Kotaro Bessho, Hirofumi Tomita, and Yutaka Ishikawa
"Big Data Assimilation" for 30-second-update 100-m-mesh Numerical Weather Prediction

14:40-15:00 Takuya Kawabata, Hiroshi Yamauchi, Nobuhiro Nagumo, and Ahoro Adachi
Development of assimilation methods for polarimetric radar data

15:00-15:30 Break

Assimilation: Chair: Takuya Kawabata

15:30-15:50 Yasutaka Ikuta
Impact of flow-dependent assimilation using adjoint model including 3-ice microphysics scheme

15:50-16:10 Takumi Honda, Guo-Yuan Lien, Yasumitsu Maejima, Kozo Okamoto, and Takemasa Miyoshi
Assimilating all-sky himawari-8 satellite infrared radiances: A case of Kanto-Tohoku heavy rainfall in 2015

16:10-16:30 Koji Terasaki, Keiichi Kondo, Takemasa Miyoshi
Assimilating satellite radiances with the NICAM-LETKF system

16:30-18:00 Poster display

19:00 Banquet (Fukuman-en)

**December 2 (Fri)**

Assimilation, cloud schemes: Chair: Yosuke Sato

8:40-9:00 Shunji Kotsuki, Koji Terasaki, Hisashi Yashiro, Hirofumi Tomita, Masaki Satoh, and Takemasa Miyoshi
Model parameter estimation using ensemble data assimilation: A case with the nonhydrostatic icosahedral atmospheric model NICAM and the global satellite mapping of precipitation data

9:00-9:20 Wojciech W. Grabowski
Modeling condensation in nonhydrostatic cloud-scale models

9:20-9:40 Hugh Morrison
An accurate, efficient method for calculating hydrometeor advection in multi-moment bulk and bin microphysics schemes

9:40-10:00 Akihiro Hashimoto, Ryohei Misumi, and Narihiro Orikasa
Examination of the classification of hydrometeor types in a bulk microphysics scheme

10:00-10:20 Yoshinori Yamada
Development of a two-moment three-ice bulk microphysical model for ice

10:20-10:50 Break

Cloud schemes, clouds/aerosols/LES: Chair: Junshi Ito

10:50-11:10 Chia Rui Ong
Water droplet simulation by the immersed boundary method

11:10-11:30 Kozo Nakamura, Yasushi Fujiyoshi, Kazuhisa Tsuboki, and Naomi Kuba
Development of a bulk parameterization scheme of warm rain using bin scheme model results

11:30-11:50 Mike Pritchard, Hossein Parishani, Chris Bretherton, and Marat Khairoutdinov
Towards low cloud permitting superparameterization

11:50-12:10 Yousuke Sato
Current-generation global climate models inevitably underestimate pollutant transports to the Arctic

12:10-13:40 Lunch

Clouds/aerosols/LES: Chair: Akihiro Hashimoto

13:40-14:00 Tatsuya Seiki, Chihiro Kodama, Masaki Satoh, Tempei Hashino, Yuichiro Hagihara, and Hajime Okamoto
Effect of topographical resolution on cirrus clouds using a high-resolution GCM

14:00-14:20 Junshi Ito
Numerical simulation of a local valley wind “Hijikawa-Arashi”

14:20-14:40 Akira T. Noda, Tatsuya Seiki, Masaki Satoh, and Yohei Yamada
High cloud size dependency in the applicability of the fixed anvil temperature hypothesis using global nonhydrostatic simulations

14:40-15:00 Hiromasa Nakayama, and Tetsuya Takemi
Large-eddy simulation of a diurnal cycle of atmospheric turbulent boundary layer flows over an urban area by coupling with a meso-scale meteorological simulation model

15:00-15:20 Takanobu Yamaguchi, Graham Feingold, and Vincent E. Larson
Framework for improvement by vertical enhancement: a simple approach to improve low and high level clouds in large scale models

15:20-15:30 Closing

**Posters**

P1 Seiya Nishizawa, Sachiho A. Adachi, Yoshiyuki Kajikawa, Tsuyoshi Yamaura, Kazuto Ando, Ryuji Yoshida, Hisashi Yashiro, and Hirofumi Tomita
Decomposition of the large-scale atmospheric state driving downscaling

P2 Sachiho A. Adachi, Fujio Kimura, Hiroshi G. Takahashi, Masayuki Hara, Xieyao Ma, and Hirofumi Tomita
How does utilization of high-resolution SST give impact to regional climate simulation?

P3 Shun-ichi Watanabe, and Hiroshi Niino
An idealized numerical experiment of Japan sea polar air mass convergence zone

P4 Hoang-Hai Bui, Eriko Nishimoto, and Shigeo Yoden
Effects of environment shear on convective systems in a minimal model of QBO-like oscillation

P5 Hiromu Seko
Introduction of the project 'Innovative numerical weather predictions and advanced weather disaster prevention based on damage-level estimation' and data assimilation experiment of radio occultation refractivity data by using a mesoscale LETKF system

P6 Tomoki Ohno, and Masaki Satoh
Sensitivity studies of cloud responses on SSTs in RCE experiments using a high-resolution global nonhydrostatic model

P7 Didier Ricard, and Antoine Verrelle
Simulations of deep convection as a testbed for two non-hydrostatic models

P8 Ryuji Yoshida, Tsuyoshi Yamaura, Sachiho A. Adachi, Seiya Nishizawa, Hisashi Yashiro, Yousuke Sato, and Hirofumi Tomita
A computationally cost effective online nesting procedure for regional atmospheric/climate models

P9 Hiroyasu Kubokawa, Masaki Satoh, Takashi Arakawa, and Hiroyasu Hasumi
Development of the stretch-atmosphere and ocean model to study air-sea interaction associated with tropical cyclone

P10 Shin Fukui, Toshiki Iwasaki, Kazuo Saito, Hiromu Seko, and Masaru Kunii

A comparison of precipitations reproduced with regional reanalysis assimilating only conventional observations and dynamical downscaling

P11 Michiko Otsuka

Assimilation experiments of himawari-8 rapid scan atmospheric motion vectors

P12 Sho Yokota, Masaru Kunii, Kazumasa Aonashi, and Seiji Origuchi

4D-EnVAR with iterative calculation of non-linear model

P13 Woosub Roh, and Masaki Satoh

Evaluations of cloud properties in NICAM using CALIPSO and CloudSat

P14 Yousuke Sato

Impacts of spatial grid resolution on the cloud cover of marine shallow cumulus

P15 Daisuke Takasuka, and Masaki Satoh

Initiation processes and structures of intraseasonal variability simulated in an aqua-planet

P16 Masuo Nakano, Akiyoshi Wada, Masahiro Sawada, Hiromasa Yoshimura, Ryo Onishi, Shintaro Kawahara, Wataru Sasaki, Tomoe Nasuno, Munehiko Yamaguchi, Takeshi Iriguchi, Masato Sugi, and Yoshiaki Takeuchi

Global 7-km mesh nonhydrostatic Model Intercomparison Project for improving TYphoon forecast (TYMIP-G7)

P17 Chihiro Kodama, Bjorn Stevens, Thorsten Mauritsen, Tatsuya Seiki, and Masaki Satoh

Future projection of extratropical cyclone simulated by a 14 km mesh global atmospheric model

P18 Masaki Satoh, Tomoki Ohno, Allison Wing, Sandrine Bony, and Bjorn Stevens

RCEMIP: Radiative Convective Equilibrium Model Inter-comparison Project

[Day 1, 13:40-14:00]

# Resolution dependence of the diurnal cycle of precipitation over land in the tropics simulated by a global cloud permitting model

Hisashi Yashiro[1], Yoshiyuki Kajikawa[1,2], Yoshiaki Miyamoto[1,3], Tsuyoshi Yamaura[1], Ryuji Yoshida[1,2], Hirofumi Tomita[1]

1. RIKEN Advanced Institute for Computational Science, Kobe, Japan
2. Research Center for Urban Safety and Security, Kobe University, Kobe, Japan
3. Rosenstiel School of Marine and Atmospheric Science, University of Miami, Miami, Florida

Email: h.yashiro@riken.jp

## Abstract

Resolution dependence was found in the simulated diurnal precipitation cycle over land in the tropics. We conducted a series of grid refinement experiments of the atmosphere from 14 km to 0.87 km using the non-hydrostatic icosahedral atmospheric model (NICAM, Satoh et al. 2014) without any convection parameterizations. The precipitation peak appeared around midnight in the lower resolution simulations (Figure 1, left panel), whereas the TRMM observed precipitation peak appeared in the late afternoon. In those experiment, the diurnal amplitudes of the column maximum vertical velocity were small (Figure 1, right panel), and the precipitation peak was later than the peak of convective available potential energy. These results suggest that the orographic lift of water vapor plays an important role for the diurnal precipitation cycle in the experiments at grid spacing of around 10 km without any convection parameterizations. With increasing horizontal resolution, the peak time became earlier and the amplitude became larger. The two highest resolution experiments better reproduced the observed time of precipitation peak. Both precipitation and column maximum vertical velocity were started early in these simulations. This result suggests that the high resolution simulation have the ability to reproduce weak convection with precipitation in the late morning, which is important process for effective representation of the diurnal precipitation cycle. The characteristics of the simulated diurnal precipitation cycle changed with grid spacing of less than 2–3 km. This

fundamental change is related to the different representation of convection at resolutions less than 2–3 km, shown by Miyamoto et al. (2013) and Kajikawa et al. (2016).

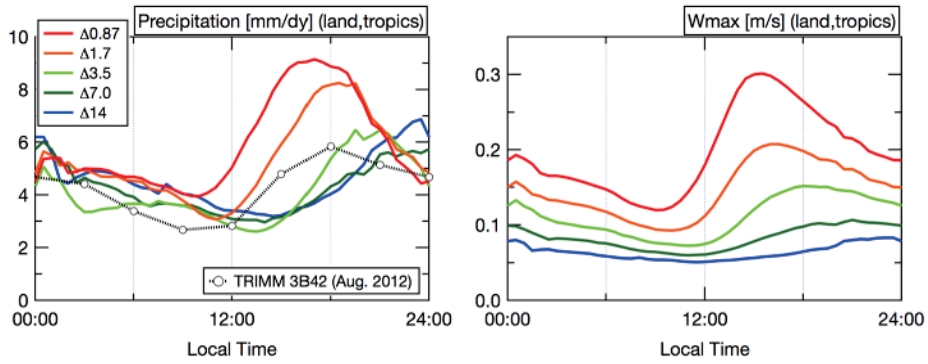


Figure 1. Simulated diurnal cycle of precipitation over land (left panel) and column maximum vertical velocity (right panel) in the tropics (15°S–15°N) for five horizontal resolutions: 14km(Δ14), 7km(Δ7), 3.5km(Δ3.5), 1.7km(Δ1.7), and 0.87km(Δ0,87). The average diurnal precipitation cycle of August 2012, obtained from TRMM 3B42 dataset (Huffman et al. 2007), is also shown for reference in the left panel.

## References:


Huffman, G. J., D. T. Bolvin, E. J. Nelkin, D. B. Wolff, R. F. Adler, G. Gu, Y. Hong, K. P. Bowman, and E. F. Stocker, 2007: The TRMM Multisatellite Precipitation Analysis (TMPA): Quasi-global, multiyear, Combined-sensor precipitation estimates at fine scales. *J. Hydrometeor*, 8, 38–55, doi:10.1175/JHM560.1.

Kajikawa, Y., Y. Miyamoto, R. Yoshida, T. Yamaura, H. Yashiro, and H. Tomita, 2016: Resolution dependence of deep convections in a global simulation from over 10-kilometer to sub-kilometer grid spacing. *Progress in Earth and Planetary Science*, 3:16, doi:10.1186/s40645-016-0094-5.

Miyamoto, Y., Y. Kajikawa, R. Yoshida, T. Yamaura, H. Yashiro, and H. Tomita, 2013: Deep moist atmospheric convection in a subkilometer global simulation. *Geophys. Res. Lett.*, 40, 4922–4926, doi:10.1002/grl.50944.

Satoh, M., H. Tomita, H. Yashiro, H. Miura, C. Kodama, T. Seiki, A. T. Noda, Y. Yamada, D. Goto, M. Sawada, T. Miyoshi, Y. Niwa, M. Hara, T. Ohno, S. Iga, T. Arakawa, T. Inoue and H. Kubokawa, 2014: The Non-hydrostatic Icosahedral Atmospheric Model: description and development. *Progress in Earth and Planetary Science*, 1:18. doi: 10.1186/s40645-014-0018-1

[Day 1, 14:00-14:20]

# Representation of turbulence in simulations of deep convective clouds

Didier Ricard, Antoine Verrelle, Christine Lac, Nicolas Rochetin

CNRM (Météo-France, CNRS), Toulouse, France

Email: didier.ricard@meteo.fr

## Abstract

Although turbulence processes have been extensively studied for the boundary layer, there are few studies that evaluate the turbulence parameterization inside convective clouds in atmospheric models. Yet, turbulence can be strong inside cumulus and cumulonimbus. This study aims at evaluating and improving the parameterization of subgrid turbulence in deep convective clouds simulated by numerical cloud resolving model at kilometer scale.

First, we have characterized the turbulence representation in deep convective clouds. For that, a Large-Eddy Simulation (LES) using simplified atmospheric conditions has been performed with the Meso-NH model (Lafore et al, 1997) to serve as a reference simulation of deep convection (Figure 1). This LES with a 50-m grid spacing is used to compute the turbulent fluxes at different coarser horizontal resolutions (500 m, 1 km, and 2 km). Vertical turbulent fluxes of liquid-ice water potential temperature and total non-precipitating water mixing ratio exhibit counter-gradient structures, indicative of nonlocal turbulence.

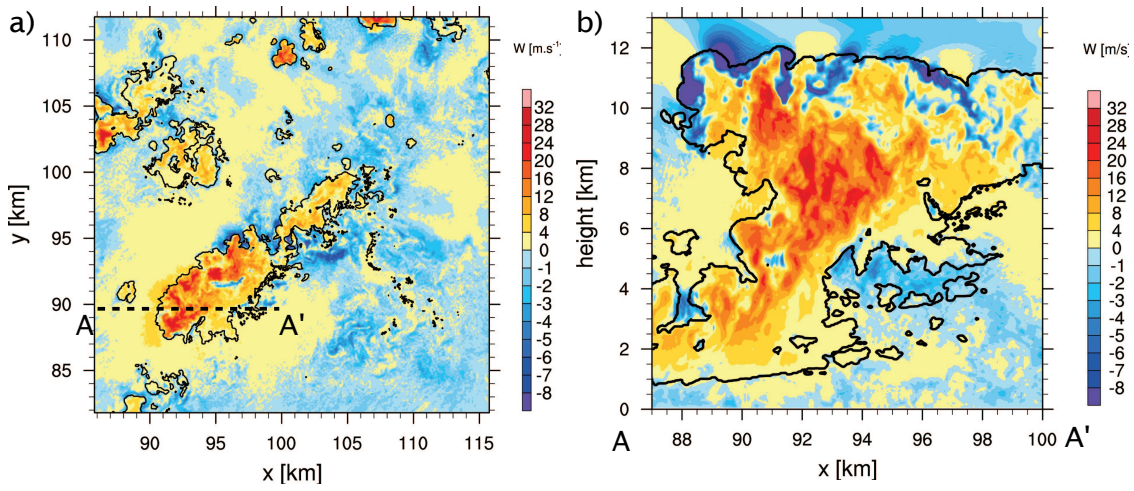


*Figure 1: LES (50-m grid spacing) of deep convection: (a) horizontal cross section (at 6 km AGL) and (b) vertical cross section (along AA') of vertical velocities (m $s^{-1}$, shading) and cloud boundaries represented as the sum of cloud and ice water mixing ratios (above 0.001 g $kg^{-1}$, black contours).*

Second, a diagnostic assessment, from the reference LES fields, of the current turbulence parameterization (Cuxart et al, 2000) used in the Meso-NH model at these coarser resolutions shows that turbulent kinetic energy is largely underestimated in the clouds, related to an underestimation of thermal production. The counter-gradient structures of vertical turbulent fluxes are not reproduced, indeed, the local K-gradient

formulation is not suitable. Alternative parametrizations of some turbulent fluxes are then tested. In particular, a parameterization based on horizontal gradients of resolved variables as proposed by Moeng (2014), gives a better representation of the thermal production of turbulence in the clouds.

Third, the on-line evaluation from model runs with 2-km, 1-km, and 500-m horizontal grid spacing confirms the improvement when using the modified scheme (Figure 2), with an increase of subgrid turbulence and a decrease of vertical velocities in convective clouds.

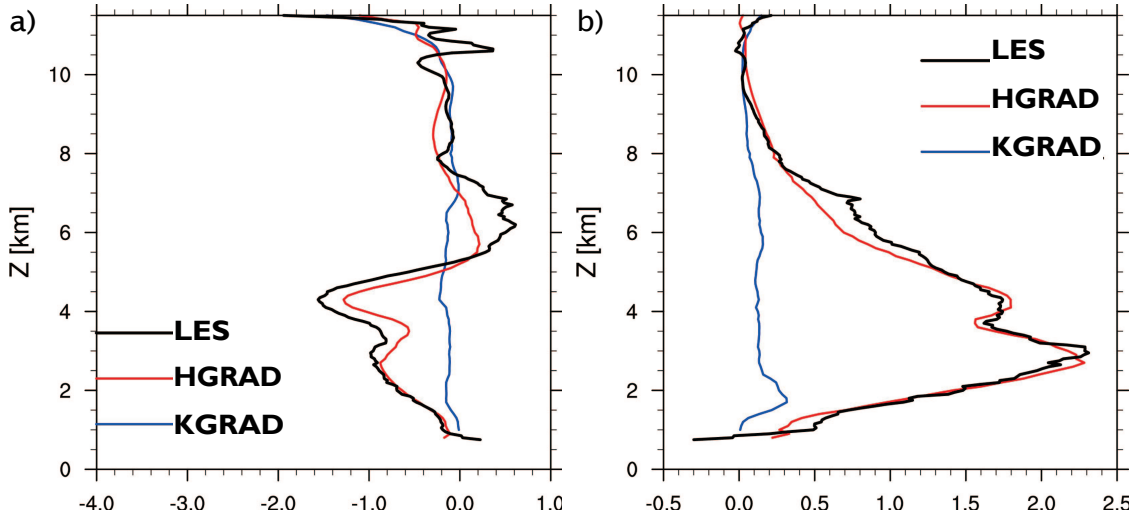


*Figure 2: Vertical profiles averaged inside the clouds of the turbulent vertical fluxes of heat (K m $s^{-1}$) (a) and total non-precipitating water mixing ratio (g $kg^{-1}$m $s^{-1}$) (b): reference fluxes from the LES (black lines) obtained by 1-km box filtering, parameterized fluxes from the K-gradient formulation (KGRAD, blue lines) and from the product of horizontal gradients (HGRAD, red lines) for 1-km runs.*

Further evaluation is currently conducted on the convective systems observed during the HyMeX field campaign that took place over the northwestern Mediterranean in fall 2012 (Ducrocq et al. 2014).

**References:**


Ducrocq, V., and Coauthors, 2014: HyMeX-SOP1: The field campaign dedicated to heavy precipitation and flash flooding in the Northwestern Mediterranean. *Bulletin of the American Meteorological Society, 95 (7), 10831100, doi:10.1175/bams-d-12-00244.1, URL* http://dx.doi.org/10.1175/BAMS-D-12-00244.1

Lafore, J. P., J. Stein, N. Asencio, P. Bougeault, V. Ducrocq, J. Duron, C. Fischer, P. Hereil, P. Mascart, J. P. Pinty, J. L. Redelsperger, E. Richard, and J. Vila-Guerau de Arellano, 1998: The Meso-NH Atmospheric Simulation System. Part I: Adiabatic formulation and control simulations. *Annales Geophysicae, 16, 90-109*

Cuxart, J., P. Bougeault, and J.-L. Redelsperger, 2000: A turbulence scheme allowing for mesoscale and large-eddy simulations. *Quarterly Journal of the Royal Meteorological Society, 126 (562), 1–30*

Moeng, C.-H., 2014: A closure for updraft-downdraft representation of subgrid-scale fluxes in cloud-resolving models. *Monthly Weather Review, 142 (2), 703–715, doi:10.1175/mwr-d-13-00166.1, URL* http://dx.doi.org/10.1175/MWR-D-13-00166.1

[Day 1, 14:20-14:40]

# Intensification of convective extremes driven by cloud–cloud interaction

Christopher Moseley[1], Cathy Hohenegger[1], Peter Berg[2], Jan O. Haerter[3]

1. Max-Planck-Institute for Meteorology, Hamburg, Germany

2. Swedish Meteorological and Hydrological Institute, Norrköping, Sweden

3. Niels Bohr Institute, University of Copenhagen, Denmark

Email: christopher.moseley@mpimet.mpg.de

## Abstract

In a changing climate, a key role may be played by the response of convective-type clouds and precipitation systems to temperature changes (e.g. Kendon *et al.*, 2014). Yet, it is unclear if convective precipitation intensities will increase mainly due to thermodynamic or dynamical processes (Westra et al., 2014). Here we perform idealized large eddy simulations (LES) of convection by imposing a realistic diurnal cycle of surface temperature and solar insolation, representative for mid-latitude climate.

We find convective events to gradually self-organize into larger cloud clusters and those events occurring late in the day to produce the highest precipitation intensities. Tracking rain cells throughout their life cycles, we show that events which result from collisions respond strongly to changes in boundary conditions, such as temperature changes, but also to large-scale influences like moisture convergence and vertical uplifting. Conversely, isolated events not resulting from collisions remain largely unaffected by the boundary conditions. Increased surface temperature indeed leads to more interaction between events and stronger precipitation extremes. However, comparable intensification occurs when leaving temperature unchanged but simply granting more time for self-organization.

Our findings imply that the convective field as a whole acquires a memory of past precipitation and inter-cloud dynamics, driving extremes. For global climate model projections, our results suggest that the interaction between convective clouds must be

incorporated into convection parametrizations to simulate convective extremes and the diurnal cycle more realistically.

**References:**

Kendon, E. J., N. M. Roberts, H. J. Fowler, M. J. Roberts, S. C. Chan, and C. A. Senior: Heavier summer downpours with climate change revealed by weather forecast resolution model. *Nat. Clim. Change* **4**, 570–576 (2014).

Westra, S., H. J. Fowler, J. P. Evans, L. V. Alexander, P. Berg, F. Johnson, E. J. Kendon, G. Lenderink, and N. M. Roberts: Future changes to the intensity and frequency of short-duration extreme rainfall. *Rev. Geophys.* **52**, 522–555 (2014).

Moseley, C., C. Hohenegger, P. Berg, and J. O. Haerter: Intensification of convective extremes driven by cloud–cloud interaction. *Nat. Geosci.* **9**, 748–752 (2016)

[Day 1, 14:40-15:00]

# Statistics of clusters of tropical convection in global cloud-resolving simulations of aqua-planet with SAM

Marat Khairoutdinov

1. School of Marine and Atmospheric Sciences, Stony Brook University, New York, USA

Email: marat.khairoutdinov@stonybrook.edu

## Abstract

The global cloud-resolving simulations of aqua-planet are analyzed using a global version of the System for Atmospheric Modeling. The model uses latitude-longitude grid with grid-spacing of 4 km at the equator. We use the sea-surface temperature profiles from the Aqua-Planet Experiment (APE). The radiation is interactive with diurnal cycle. The pdf of cluster area and degree of aggregation are compared to the previous studies based on satellite observations. The response of the net outgoing radiation to the degree of aggregation is examined. The results of sensitivity experiment in which the SST is uniformly increased by 4 K are also discussed.

[Day 1, 15:30-15:50]

# Convection permitting latitude belt simulation with the WRF model

Thomas Schwitalla[1]

1. Institute of Physics and Meteorology, University of Hohenheim, Stuttgart, Germany

Email: thomas.schwitalla@uni-hohenheim.de

## Abstract

In contrast to global climate models, regional climate models are usually applied as limited area models with 10 to 50 km resolution and the domain centered over the region of interest due to limited computing resources. However, the boundary relaxation zone can deteriorate the representation of synoptic features. At longer time scales, these errors can penetrate into the model domain and impact the results of the higher resolution domain.

In order to study the effect of very high resolution climate modeling we applied the WRF model for a northern hemisphere latitude belt between 20 °– N and 65 °– N to omit boundary effects and to study the interaction of small-to-large scale processes with CP resolution.

The model was operated both at 12 km and 3 km resolution for July and August 2013. The model was forced with ECMWF operational analyses data at the northern and southern boundary. No additional data assimilation was performed.

We demonstrate the benefit of a very high resolution by validating both simulations with respect to temperature, moisture and wind at different altitudes including surface variables.

Due to the better representation of orographic features, the CP simulation shows a more realistic mesoscale circulation and produces more realistic precipitation patterns as compared to the 12 km simulation. Also the large-scale situation over the North Atlantic and Central Europe is better captured at the CP resolution.

A highlight of the CP experiment is the realistic simulation of Typhoon Soulik at July 10, 2013. The predicted typhoon track is in accordance with the observation with a delay of 6 hours and a track error of approx. 250 km with 10 days lead time.

[Day 1, 15:50-16:10]

# An update of convection scheme in 5km resolution operational system

Kengo Matsubayashi, Tabito Hara, Kohei Aranami and Kohei Kawano

Numerical Prediction Division, Japan Meteorological Agency

Email: kengomatsubayashi@met.kishou.go.jp

## 1 Introduction

The Japan Meteorological Agency (JMA) has been operating the Meso-Scale Model (MSM) with 5-km horizontal resolution since 2006, and it still plays a crucial role to provide information on disaster prevention caused by severe weather as well as aviation weather. JMA plans to replace the current operational model with a newly developed non-hydrostatic model called ASUCA soon.

In the 5-km model, the convection scheme plays an important role because it strongly affects prediction accuracy. A number of defects have been spotted in its convection scheme through the development, and modifications give significantly large impacts.

## 2 An update of convection scheme in MSM

In the initial stage of convection scheme development in MSM, behaviour of its convection scheme (based on Kain Fritsch 1990, hereafter KF) was thoroughly analyzed not only in 3D model but also in single-column model. Some of the exposed problems are listed below.

1. Magnitudes of tendencies are quite different between shallow and deep convection defined in KF scheme.
2. Cloud top height of parameterized convection is often excessively higher than that estimated by satellite observations.
3. Parameterized convection tends to be too frequently initiated at windward of mountains and it brings too much precipitation.

The problem 1 is related to difference of the closure assumption between shallow and deep convection. While cloud base mass flux (CBMF) is diagnosed by the CAPE closure in deep convection, shallow convection assumes almost constant CBMF, which is significantly larger than that of deep convection. By changing CBMF in shallow convection, discontinuity of CBMF between deep and shallow convection is removed. With the modification, dry bias over the lower layer is partially improved.

The problem 2 is highly associated to entrainment rate in sub-grid scale convection. Excessively higher cloud top in the scheme implies that entrainment rate is too small. By comparing cloud top in the scheme and varying the entrainment rate, an appropriate entrainment rate, which is larger than the original one, was finally found. The modification also led to improvement of dry bias over the lower layer.

The inordinate precipitation described in the problem 3 is linked to the triggering of convection in the scheme. When this kind of excessively intense precipitation is predicted, the precipitation system comes from offshore and CAPE is highly accumulated there. According to the corresponding observation, relatively heavy precipitation is often seen even on the sea, however, the model predicts almost no precipitation there. Because the convection scheme assumes that larger vertical velocity gives more frequent convection initiation, it is difficult for the convection scheme to trigger convection in the place where forced lifting necessary for convective initiation is relatively hard to

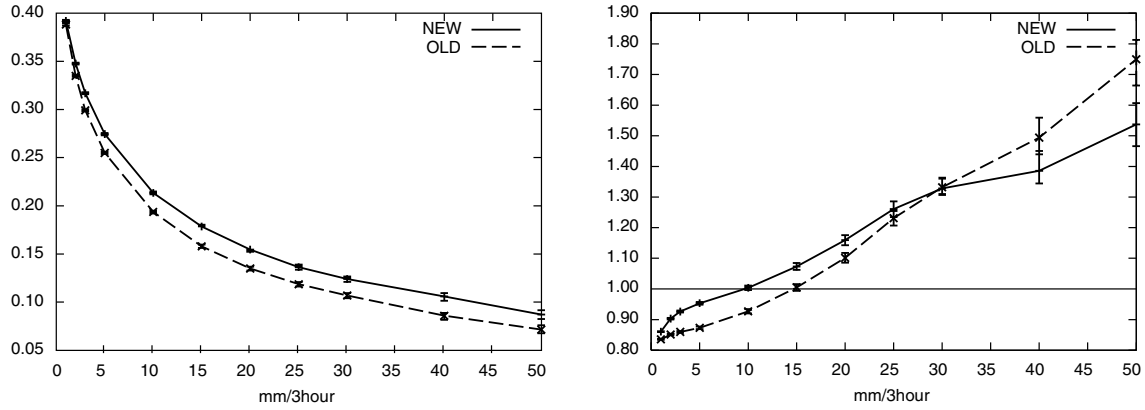


Figure 1: Threat score (left) and Bias score (right) in precipitation forecast.

occur. In the model, CAPE accumulated on the sea is suddenly released just after the precipitation system lands on because vertical velocity is strengthened by horizontal wind convergence driven by difference of roughness between land and sea and/or orographic effects. The newly implemented trigger function highly depends on buoyancy near the surface and convective velocity scale, and is not sensitive to grid mean vertical velocity.

## 3 Results and Discussion

The model enhanced by the improvements described above demonstrates remarkable improvement in the precipitation forecast accuracy (Figure 1). Also dry bias over the lower layer is well reduced.

However, the bias score indicates that prediction frequency is still higher than observation in relatively heavy precipitation forecast while the improved model removes instability more than the original. As an attempt one experiment in which convection parameterization stabilizes further more aggressively was conducted, and its result showed that excessive prediction frequency in relatively heavy precipitation was reduced and accuracy of precipitation forecasts measured by the threat score was more enhanced. Although the aggressive scheme has not been incorporated into the operational candidate because dry bias over the lower layer became more serious and the extended dry bias affected some post processing using its forecasts. The experimental fact might be linked to lack of small scale phenomena such as entrainment in resolved convective transport. Entrainment weakens convection activity by incorporating dry air outside cumuli and dilutes moist air inside, which is taken into account in many convection schemes. However, entrainment driven by small scale turbulence is not resolved in models with several kilometer horizontal gridspacing. Once it is explicitly initiated, convection can be too strong because one of the processes weakening convection is not resolved. It is sort of the Grey Zone problem where resolved and unresolved scales co-exist. These considerations imply that even if vertical transport, which is the main feedback of convection, is resolved in high resolution models, smaller unresolved phenomena around convection should be still parameterized to control convection properly.

## References:

Kain, J. S. and J. M. Fritsch, 1990: A one-dimensional entraining/detraining plume model and its application in convective parameterization. J. Atmos. Sci. 47, 2784-2802.

[Day 1, 16:10-16:30]

# Mesoscale Vortex that Caused Marine Accidents due to a Sudden Gusty Wind in the Southwestern Part of the Sea of Japan on 1 September 2015

Eigo Tochimoto[1], Sho Yokota[2], Hiroshi Niino[1], and Wataru Yanase[1]
1. Atmosphere and Ocean Research Institute, the University of Tokyo, Japan
2. Meteorological Research Institute, Tsukuba, Japan

Email:tochimoto@aori.u-tokyo.ac.jp

## Abstract

A sudden gusty wind accompanied by a mesoscale vortex of 30km diameter occurred in the Tsushima Strait at the southwest part of the Sea of Japan between 0300 and 0400 JST (Japan Standard Time) on 1 September 2015. It upset 6 fishery boats, causing 4 fatalities and 2 missing people. Some of the survived fishermen reported that they were hit by a waterspout. The mesoscale vortex was located near the warm front about 300 km northeast of the center of an extratropical cyclone. The structure and evolution of this mesoscale vortex are examined using observational data set and a numerical simulation.

A C-band Doppler radar of Japan Meteorological Agency (JMA), which is located at Fukuoka, about 130km south east of the area of the marine accidents, detected a spiral-shaped reflectivity pattern associated with a convective system to the east of Tsushima island at around 0300 JST. The convective system propagated northward with time. At 0320 JST, a couplet of positive and negative Doppler velocities exceeding 50 m $s^{-1}$ started to be observed near the center of the spiral-shaped reflectivity pattern, which later transformed into a circular reflectivity pattern with an eye-like weak echo region at the center by 0400 JST.

A numerical simulation using JMA Non-hydrostatic Model (JMANHM) with horizontal resolution of 2km and 50 vertical levels successfully reproduced the mesoscale vortex. The simulated vortex had a diameter of about 10-50 km, and was formed in the northeast quadrant of the extratropical cyclone at around 0300 JST. It had a warm core structure at low levels. The vortex developed between 0330 and 0400 JST and the associated wind exceeded 20 m $s^{-1}$ near the surface.

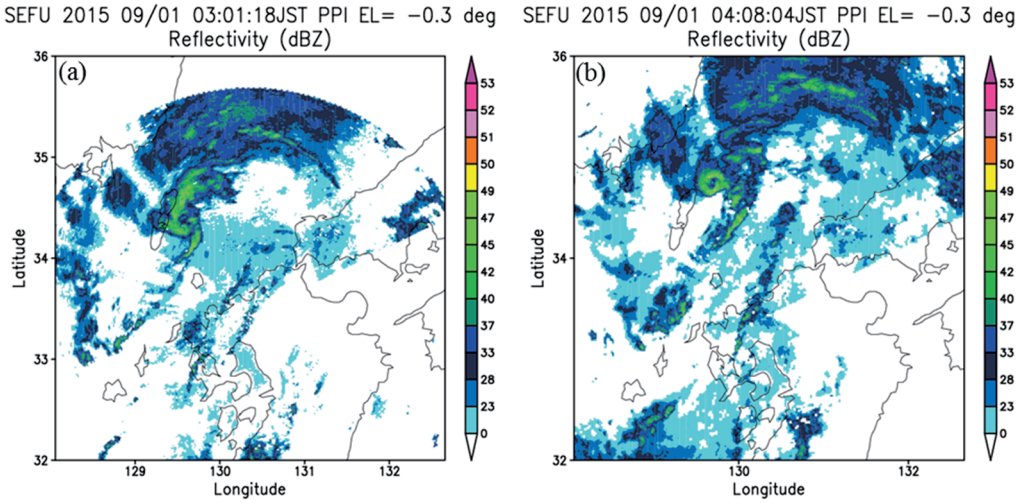


Fig. 1 Radar reflectivity (dBZ) observed by a C-band radar with -0.3 elevation angle at (a) 0301JST and (b) 0408JST on 1 September 2015.

An additional numerical simulation with a finer horizontal resolution have been performed to clarify more detailed structure and evolution of the vortex and to reproduce small-scale features that caused the damaging gusty wind. A simulation with 50 m horizontal resolution well reproduced mesoscale vortex with spiral-shaped precipitation system. Smaller scale vortices developed within the mesoscale vortex. It is suggested that these vortices formed with shear instability. The maximum of vorticity and wind speed occasionally exceeds 50 m $s^{-1}$ and 1 $s^{-1}$, respectively, during the simulation.

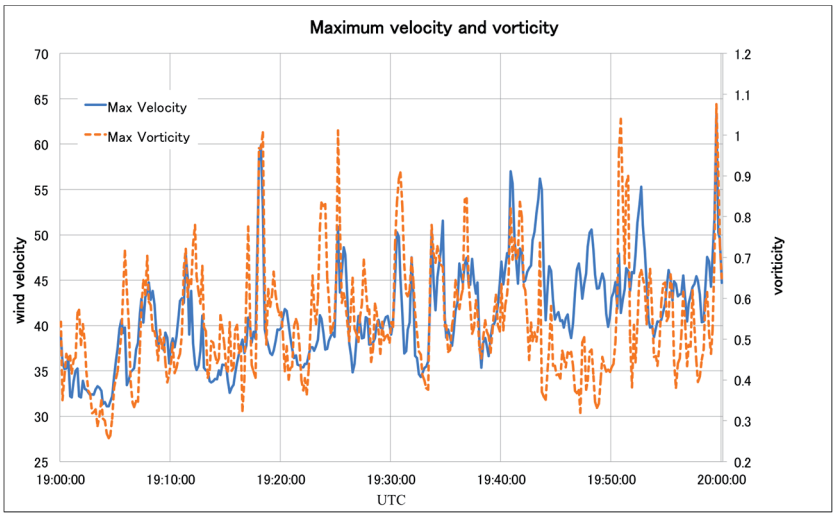


Fig. 2 Time series of the maximum velocity and vorticity for the NHM simulation with 50 m horizontal grid spacing.

[Day 1, 16:30-16:50]

# Influence of horizontal resolution on structure changes of atmospheric stratification in the 2015 Hiroshima heavy rainfall

Teruyuki Kato[1]

[1]Meteorological Research Institute/Japan Meteorological Agency

(Email: tkato@mri-jma.go.jp)

## 1. Introduction

On 20 August 2014, heavy rainfall exceeding 200 mm $3h^{-1}$ occurred in Hiroshima, western Japan. The rainfall was caused by a band-shaped precipitation system (BPS) with a hierarchical structure consisting of convective cells and band-shaped multi-cell clusters that stagnated for 4 hours. The BPS had a back-building type formation, as well as the multi-cell clusters, in which new multi-cell clusters successively formed upstream of the pre-existing ones, and it consequently extended northeastward with a width of 20~30 km and a length of about 100 km (Fig. 1a). These features were quantatively and qualitatively well reproduced by JMA nonhydrostatic model (NHM: Saito et al. 2007) with a horizontal resolution of 250 m (Fig. 1c). Even 2km-resolution NHM (Fig. 1b) also well reproduced horizontal distribution of rainfall, although it cannot simulate a BPS with a hierarchical structure.

In this study, the dependency of horizontal resolution on structure changes of atmospheric stratification is examined focusing on vertical profiles of appearance frequency (AF) of equivalent potential temperature (θe) and vertical velocity exceeding some thresholds.

## 2. Experimental designs

Half-day forecasts with 2km, 1km, 500m and 250m NHMs from 18 JST (=UTC+ 9hs) 19 August 2014 were conducted using initial and boundary conditions produced from hourly available JMA local analyses with a horizontal resolution of 5 km. Forecast horizontal domain was 1000x800 km for 2km, 1km and 500mNHMs, and 250mNHM with a domain of 412x330 km was run nested within 2kmNHM forecasts. A bulk-type microphysics parameterization scheme in which two moments were treated only for ice hydrometeors was used for precipitation processes. The turbulence closure scheme of Mellor-Yamada-Nakanishi-Niino level-3 (MYNN: Nakanishi and Niino 2006) was used. The other settings including numerical diffusion are the same for all NHMs.

## 3. Appearance frequency (AF) of θe

To understand the change of atmospheric structure caused by convective activities, vertical AF profiles of θe exceeding threshold values are examined (Fig. 2). High θe exceeding 355 K, found below a 1-km height, is conserved when environmental air is not entrained into lifted air. The AF of such high θe is almost the same in 2km and 250mNHMs, although it is very low (0.01~0.001 %) at middle and upper levels. The AF of moderate θe (~350 K) found at middle levels is, however, about twice higher in 2kmNHM than in 250mNHM. This could be smaller entrainment of environmental air due to bigger horizontal scales of convection in 2kmNHM. This feature is relaxed in 1kmNHM (Fig. 3a), but AF of high θe in 500mNHM (Fig. 3b) considerably decreases compared with the other NHMs. This indicates that high resolution do not always help improve forecasts; 250mNHM is suitable while 500mNHM should be avoided.

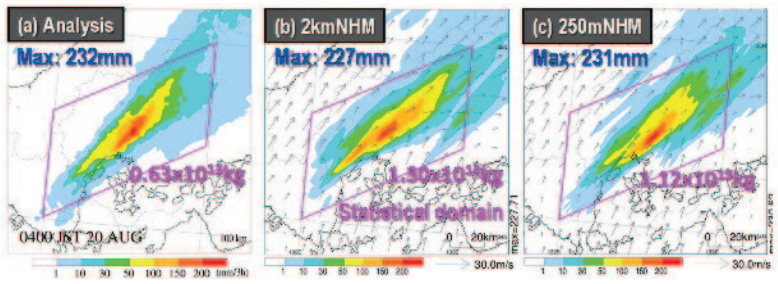


Fig. 1 (a) Distribution of 3-hour accumulated rainfall amounts, estimated using rain gauge and radar observations between 01 and 04 JST 20 August 2014. Same as (a), but (b) 2kmNHM and (c) 250mNHM forecasts. Blue (pink) numbers show the maximum value (total amounts) within pink rectangles.

The change of atmospheric structure from the developing stage to mature stage of convective activities in 250mNHM is shown in Fig. 4. The AF of high θe increases by a factor of about 10 (0.001->0.01 %), and that of moderate θe is doubled (0.3->0.6 %). These increases are, however, very small for the whole amount. This indicates that even strong

convective activities weakly changes the atmospheric structure, and such a large stabilization as that assumed in the Kain-Fritsch convection parameterization scheme, in which convective available potential energy (CAPE) is reduced up to 15 %, does not occur.

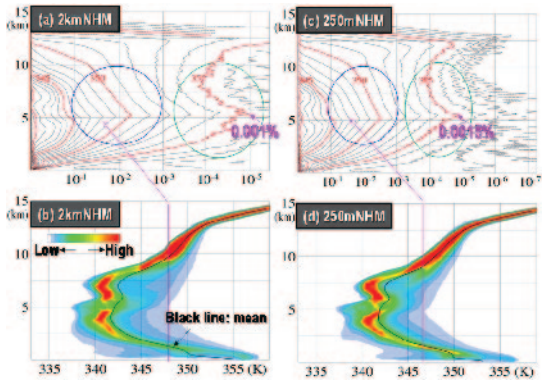


Fig. 2 (a) Vertical AF profiles of θe exceeding threshold values, shown by contours with intervals of 1 K, and (b) vertical AF distribution of θe within pink rectangles in Fig. 1 between 23 JST 19 and 04 JST 20 August 2014 that are estimated from 1-min interval output of 2kmNHM. (c) and (b) Same as (a) and (b), but for 250mNHM.

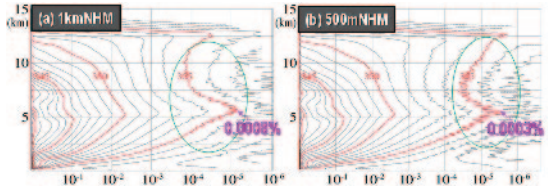


Fig. 3 Same as Fig. 2a, but in (a) 1kmNHM and (b) 500mNHM.

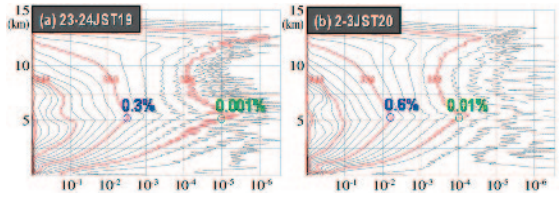


Fig. 4 Same as Fig. 2c, but between (a) 23 and 24 JST 19 (developing stage) (b) 02 and 03 JST 20 August 2014 (mature stage).

## 4. AF of strong vertical velocity

The maximum updraft and its appearance height are examined related to horizontal resolutions (Fig. 5). The maximum updraft exceeding 18 m $s^{-1}$ is found just below a 10-km height in 2kmNHM. On the other hand, 250mNHM has strong updrafts exceeding 35 m $s^{-1}$ that is about half of an estimated updraft from CAPE (~ 2000 J $kg^{-1}$). The strong updrafts are majorly found a few kilometers below the level of neutral buoyancy (LNB) that is estimated when air with low-level θe of 355 K is lifted. Strong updrafts are also found above the LNB, which indicates that 250mNHM can simulate overshoots. The maximum updraft and its appearance height in 1km and 500mNHMs are illustrated as intermediate features between 2km and 250mNHMs. This shows that a height with the maximum updraft appears lower for lower horizontal resolutions. Noted that AF of moderate updrafts (~ 5 m $s^{-1}$) at middle levels little depends on horizontal resolutions.

The features of downdraft AF are largely different for 2km and 250mNHMs. Strong downdrafts found around a 10-km height in 250mNHM are produced as compensation for strong updrafts. Meanwhile, such strong downdrafts are not found in 2kmNHMs.

Since low-level high θe with large CAPE can produce strong updrafts, AF of vertical velocity is examined for θe > 355 K (Fig. 6). Vertical motions are accelerated upward with height, as θe is almost conserved even in 2kmNHM. Above a 10-km height, AF of θe > 355 K (pink line in Fig. 6) decreases rapidly, while strong updrafts remain. This indicates that mixing with environmental field becomes larger, but an examination on detail processes is a future work.

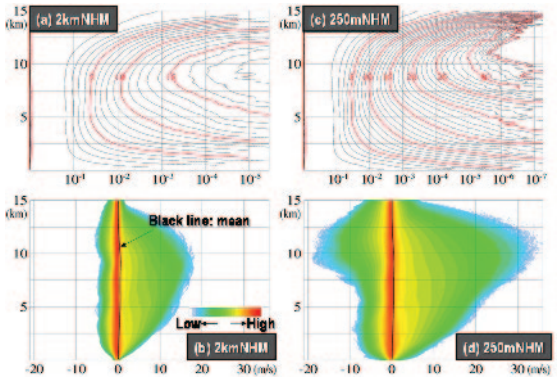


Fig. 5 (a) and (b) Same as Figs. 2a and 2c, but for vertical velocity. (c) and (b) Same as (a) and (b), but in 250mNHM. Contour intervals in (a) and (c) are 1 m $s^{-1}$.

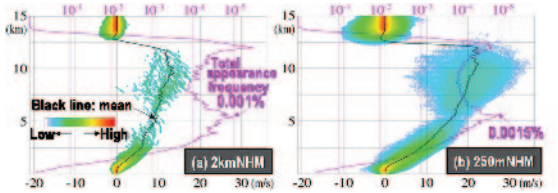


Fig. 6 (a) and (b) Same as Figs. 5b and 5d, but for θe > 355 K.

## References

Saito, K., J. Ishida, K. Aranami, T. Hara, T. Segawa, M. Nareta, and Y. Honda, 2007: *J. Meteor. Soc. Japan*, **85B**, 271-304.

[Day 2, 8:40-9:00]

# A Global Vector Vorticity Model on a Geodesic Grid

David Randall, Ross Heikes, Celal Konor
Department of Atmospheric Science, Colorado State University
Fort Collins, Colorado USA

## Abstract

We have created a non-hydrostatic global atmospheric model based on the "vector vorticity model" (VVM) of Jung and Arakawa (2008), which is based on the horizontal vorticity vector, and also using the "Unified System" of equations discussed by Arakawa and Konor (2009), which filters vertically propagating sound waves. The model uses the geodesic grid of Heikes et al. (2013). To avoid computational modes on the geodesic grid, we adapt the ideas of Randall (1994) to predict the curl and divergence of the horizontal vorticity vector, rather than the horizontal vorticity vector itself. Results will be shown from several DCMIP cases.

### References:

Arakawa, A., and C. S. Konor, 2009: Unification of the anelastic and quasi- hydrostatic systems of equations. *Mon. Wea. Rev.,* **137**, 710-726.

Heikes, R. P., D. A. Randall, and C. S. Konor, 2013: Optimized icosahedral grids: Performance of finite-difference operators and multigrid solver. *Mon. Wea. Rev.*, **141**, 4450-4469.

Jung, J.-H., and A. Arakawa, 2008: A Three-Dimensional Anelastic Model Based on the Vorticity Equation. *Mon. Wea. Rev.*, **136**, 276-294.

Randall, D. A., 1994: Geostrophic adjustment and the finite-difference shallow-water equations. *Mon. Wea. Rev.,* **122**, 1371-1377.

[Day 2, 9:00-9:20]

# Development of a Taiwan full-physics vector vorticity equation model (VVM)

Chien-Ming Wu

Department of Atmospheric Sciences, National Taiwan University

## Abstract

In this study, a high-resolution (500 m in the horizontal) vorticity equation based cloud resolving model covering the whole Taiwan area is developed with the following features:

Representation of surface topography in the vector vorticity equation model (VVM) is updated with a partial step approach using the immersed boundary method. Compared with the full step approach, the partial step approach provides additional topography forcing to represent micro mountains while preserving the same grid structure through interpolating from adjacent grid points. It maintains the characteristics of dynamics and physics of VVM and improves the representation of gentle slope topography without increasing vertical resolution. This approach produces reasonable results on the simulation of classical mountain waves with coarse vertical resolution. Additional experiments are performed to verify our approach including density driven flow using a cold bubble and 3-D orographic precipitation over a ridge. The results show that vorticity fields in the partial step approach have a smoother response to the gentle slopes due to the improvement in the topography representation.

Representation of land surface processes is updated with the Noah land surface model (LSM) using the surface properties in 500 m horizontal resolution in Taiwan. This approach produces reasonable diurnal cycle evolution of boundary layer and local circulation which is crucial in the development of local afternoon thunderstorms. Two idealized experiments are performed to demonstrate the importance of land atmosphere interactions in which the coupled experiment is conducted by using the VVM/LSM coupling system, while the uncoupled experiment is conducted by VVM solely with prescribed surface fluxes from the coupled experiment. The results show that with identical diurnal evolution of surface fluxes, the accumulated precipitation is less in the uncoupled experiment. This is caused by the surface fluxes and precipitation are not matched with each other after the development of convective systems. The shifted surface heat fluxes would weaken the strength of cold pool below the convective systems and prohibit further development of the convective systems.

References:

Chien, M.-H., and C.-M. Wu (2016), Representation of topography by partial steps using the immersed boundary method in a vector vorticity equation model (VVM), J. Adv. Model. Earth Syst., 8, 212–223, doi:10.1002/2015MS000514.

Lin, H.-C., M.-H. Chien, C.-M. Wu and F.-Y. Cheng (2016), Impact of land-atmosphere interaction on afternoon thunderstorm simulations in a vector vorticity equation model (VVM) by implementing Noah land surface model. In preparation.

[Day 2, 9:20-9:40]

# Cubed-Sphere Modelling Activities at CSIRO

John L. McGregor
CSIRO Oceans and Atmosphere, Melbourne 3195, Australia
Email: John.McGregor@csiro.au

## Abstract

The Conformal-Cubic Atmospheric Model (CCAM; McGregor 2005a) was the first atmospheric GCM to be formulated on a cubed grid and it has been used at CSIRO for the past 18 years. CCAM employs semi-Lagrangian, semi-implicit dynamics, which handles the somewhat finer resolution near the vertices without a time step penalty. It also uses reversible staggering in the horizontal (McGregor 2005b) to achieve good dispersion properties and good kinetic energy spectra. The Miller and White equations permit a very economical treatment of non-hydrostatic behaviour for CCAM.

Recently the Variable-Cubic Atmospheric Model (VCAM) has also been developed at CSIRO. Originally formulated on the equiangular cubed grid, there are several advantages obtained by using the uniform Jacobian grid. VCAM uses the primitive equations in conservative form, which is attractive for climate studies and for modelling trace gases and chemistry. Both CCAM and VCAM can be run in variable-resolution mode by employing the Schmidt transformation.

VCAM uses split-explicit time stepping, with small time steps for the “fast” gravity waves processes and longer time steps for the “slow” advective processes and the physical parameterizations. Flux-corrected-transport is employed to better preserve any sharp gradients in the advected fields. The reversible staggering technique is also adopted to transform the contravariant wind components of VCAM to/from an Arakawa-C configuration. Using the Uniform Jacobian grid avoids grid imprinting effects. The Coriolis terms require special treatment to provide good computational efficiency.

### References:

McGregor, J. L., 2005a: C-CAM: Geometric aspects and dynamical formulation. CSIRO Atmospheric Research Tech. Paper No. 70, 43 pp.

McGregor, J. L., 2005b: Geostrophic adjustment for reversibly staggered grids. *Mon. Wea. Rev.*, **133**, 1119-1128.

[Day 2, 9:40-10:00]

# Development of a non-hydrostatic atmospheric model using the Chimera grid method for a steep terrain

Kazushi Takemura[1], Keiichi Ishioka1, Shoichi Shige[1]

1. Graduate School of Science, Kyoto University, Japan

Email: k_takemura@kugi.kyoto-u.ac.jp

## 1. Introduction

Recent developments in computing have rapidly increased atmospheric models' resolution. In high-resolution models, the terrain is resolved in more detail, and thus steeper and more complex terrain can be resolved. The terrain-following coordinates, which are commonly used to represent the terrain, do not have orthogonality on the such steep terrain. It is known that the less orthogonality induces serious errors. Satomura (1989) used numerically generated coordinates, which have high orthogonality, and succeeded in reducing this error. However, this coordinate system cannot be generated over complex terrain in which the slope angle changes abruptly: e.g. a cliff.

In this paper, we present a non-hydrostatic atmospheric model that uses the Chimera grid method to represent steep and complex terrain (Takemura et al. 2016).

## 2. Chimera grid method

The Chimera grid method is mainly used in the field of CFD to represent complex topography. In the field of the earth science, the Chimera grid method is used as Yin-Yang grid to represent the globe (Kageyama and Sato 2004). The computational region is represented by a composite of overlapping grid; a local grid and a global grid (Fig.1). Interaction between grids is accomplished by interpolating boundary point values each other.

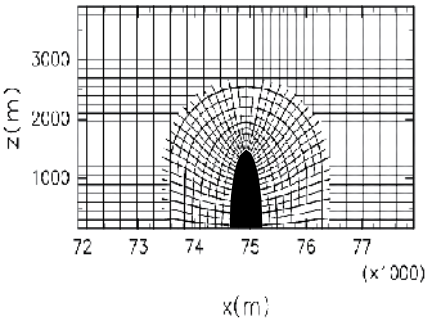


Fig.1 Representation of a tall semi-elliptic mountain of height H=1500m and width B=300m.

## 3. Description of the model

This model adopted the momentum equation, the continuity equation, the thermodynamic equation and the state equation as governing equation. Model equations were described in the fully-compressible form and the advective form. Taking into the

stratification, thermodynamic variables are separated into the perturbation component and the basic component (depending on only the height). In introducing the Chimera grid method to an atmospheric model, interpolation of thermodynamic variables at the boundary was done in the following way. The perturbation component was interpolated at the boundary and the basic component was set constant. Interpolation method was the bi-linear interpolation.

## 4. Simulation of mountain wave

Mountain wave was simulated over a tall semi-elliptical mountain of height H=1500m and width B=300m. As the slope is very steep and changes sharply at the foot of the mountain, terrain following coordinates and numerically generated coordinates cannot properly simulate this mountain. As the initial condition, the atmosphere has a constant Brunt-Vaisala frequency, N = 0.01[1/s], and a constant horizontal velocity, U = 10[m/s]. The time integration was done for 60 minutes. The coordinates were set to numerically generated coordinates for the local grid and Cartesian coordinates for the global grid as shown in Fig.1. The result is shown in Fig.2. This result is qualitatively consistent with the analytical solution of a mountain wave over similar mountain by Huppert and Miles (1969). Thus it is evident that the Chimera grid method can simulate the flow appropriately over a very steep mountain for which the numerical coordinates cannot be generated.

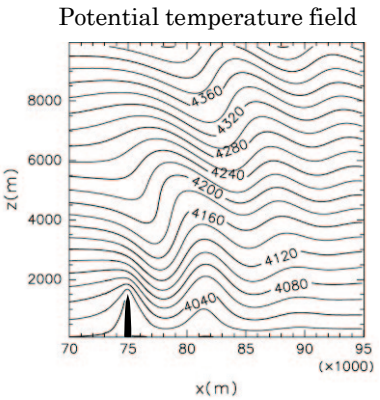


Fig.2 Potential temperature field. Surface Potential Temperature is 4000K to mimic Bousinessq system. The contour interval is 20K

## References:


Satomura, T. (1989), *J. Meteor. Soc. Japan*, **67**, 473-482.

Takemura, K., K. Ishioka and S. Shige (2016), Development of a non-hydrostatic atmospheric model using the Chimera grid method for a steep terrain. *Atmos. Sci. Lett.*, **17**, 109-114, doi:10.1002/asl.633.

Kageyama, A. and T. Sato, (2004), *Geochem. Geophys. Geosyst.,* **5**(9), 15

Huppert, H.E. and J.W. Miles (1969), *J. Fluid Mech.*, **35**(3), 481-496

[Day 2, 10:00-10:20]

# Improving computational stability with time-splitting of vertical advection considering 3-dimensional CFL condition

Kohei Kawano[1], Kohei Aranami[1], Tabito Hara[1], Kengo Matsubayashi[1], Masami Sakamoto[1] and Yuji Kitamura[2]

1. Numerical Prediction Division, Japan Meteorological Agency
2. Meteorological Research Institute

Email: k_kawano@met.kishou.go.jp

## 1 Motivation

ASUCA, a newly developed nonhydrostatic model of the Japan Meteorological Agency, employs the third-order upwind scheme with the flux limiter function proposed by Koren (1993) for advection. As a time integration method of the system, the Runge-Kutta (RK3) scheme (Wicker and Skamarock 2002), as shown in Fig.1, is adopted. With these schemes, grid spacings and time steps are restricted by the CFL condition of 3-dimensional advection such as $C_x + C_y + C_z < 1.25$ ( where $C_x$ is the Courant number in direction $x$, etc.), which can be confirmed through an idealized test of 2-dimensional scalar advection(Fig. 3(a)). The 3-dimensional CFL condition can be severe to be met because it depends not only on wind velocity but also on horizontal wind direction. For example, the case where U=V=40 m/s requires severer limitation on the vertical velocity than the case where U=$40\sqrt{2}$ m/s and V=0 m/s even though those wind velocities are identical. To overcome the restriction, a time-splitting method for advection is one of the sensible measures. Considering computational efficiency and ASUCA's memory alignment where the vertical indices are put innermost, it is more reasonable that time integration of only the vertical advection is divided into smaller substeps because the number of substeps can be determined independently from its neighboring columns.

## 2 Time-splitting of vertical advection

In the time-splitting method, dividing each of the RK3 stages into substeps is the simplest way under the restriction where field values at $t + \Delta t/3$ and $t + \Delta t/2$ are required to evaluate tendencies in the other processes. On each of columns, the number of substeps $N$ is chosen so as to satisfy $C_x+C_y+C_z/N < 1.25$ at each of the RK3 stages. Because each of the RK3 stages can be regarded as the forward time integration with timestep of $\Delta t/3$, $\Delta t/2$ and $\Delta t$, respectively, these time steps are used to evaluate the Courant numbers at each of the stages.

As mentioned above, the RK3 consists of three forward form integrations, resulting that each of the stages is restricted by the CFL condition for the forward integration with the third-order advection scheme, which is severer than that with the RK3. By replacing the forward form integration at each of the RK3 stages with the RK3 (i.e. RK3 is nested in the original RK3 time integration), the stable region in the idealized 2D advection tests is successfully expanded (a figure not shown), meaning that more stable method is established, although computational cost is more expensive.

In addition, when the time-splitting is invoked, fields are updated using the horizontal flux $F_H$ first, then the vertical flux is evaluated with the integrated field as follows.

$$\phi^{H*} = \phi^{n} - \left( F_{H}{}^{n}_{(i+1/2)} - F_{H}{}^{n}_{(i-1/2)} \right) \Delta t, \tag{1}$$

$$\phi^{n+1} = \phi^{H*} - \left( F_{V}{}^{H*}_{(k+1/2)} - F_{V}{}^{H*}_{(k-1/2)} \right) \Delta t. \tag{2}$$

Note that there is an ambiguity in the order of integrations, that is, horizontal and vertical integrations are simultaneously executed, or horizontal update should come first, or vertical first, or the order is exchanged every timestep. The choice affects resulting computational stability.

It has been confirmed that the time-splitting method expands the stable region in the idealized tests as shown in Fig. 3(b). Many real-data simulations including severe storm cases such as typhoons have also shown that the method provides sufficient computational stability for the operational use as well as practical computational efficiency.

In our presentation, we will talk about some details on our time-splitting method for vertical advection.

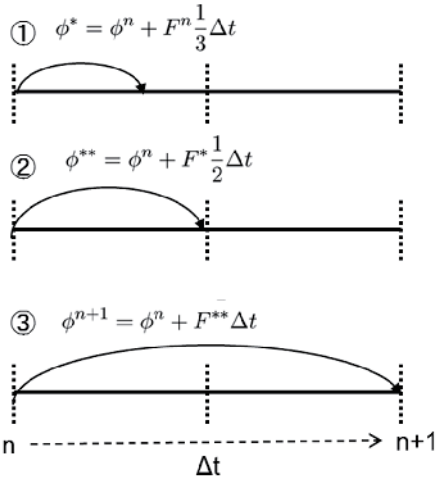


Figure 1: Schematic figure of RK3 time integration scheme.

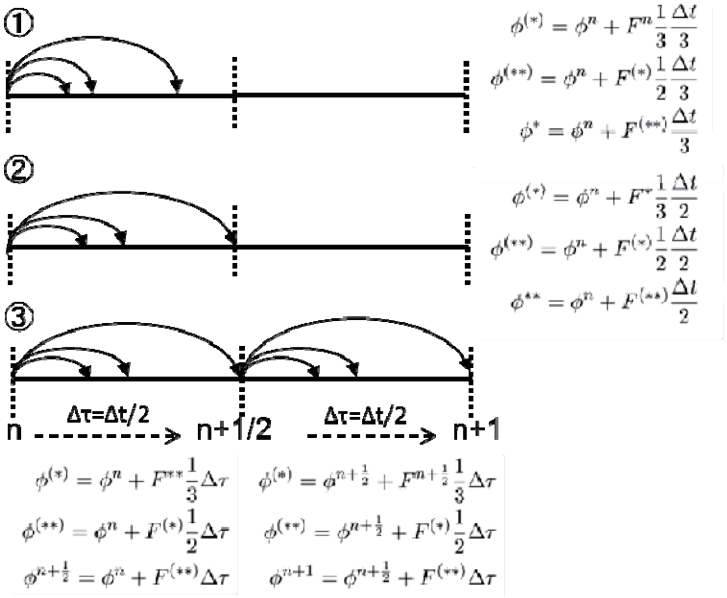


Figure 2: Schematic figure of time-splitting. The case needs to split ③ time-step into 2 substeps.

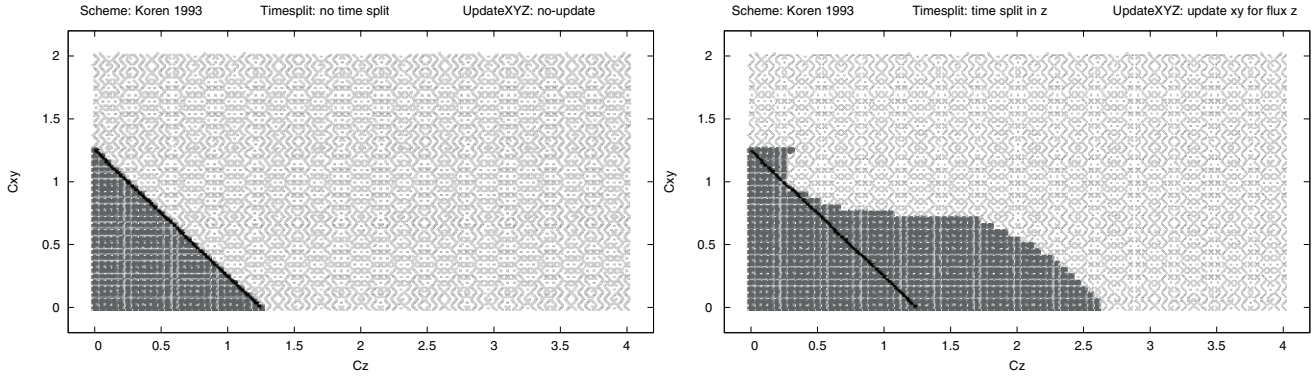


(a) Without time-splitting method.

(b) Time-splitting method is adopted to direction (Z).

Figure 3: Computational stability in the idealized 2D-advection tests with various vertical Courant numbers $C_z$ and horizontal ones $C_{xy}$. In each test, a cylinder placed at the center of the computation domain is advected and its final amplitude is checked to decide whether the computation completes stably or not. A dark-gray point indicates that the corresponding computation is stable, where the final amplitude is smaller than the initial one, and a light-gray point shows unstable. The black line in the figures depicts $C_{xy} + C_z = 1.25$.

**Acknowledgment**
This study is partly supported by SOUSEI program of MEXT Japan.

**References:**

Koren, B. 1993: A Robust Upwind Discretization Method for Advection, Diffusion and Source Terms. CWI Technical Report NM-R 9308 1993 , 1:22.

Wicker, L. and W. Skamarock, 2002: Time-Splitting Methods for Elastic Models Using Forward Time Schemes. Mon. Wea. Rev., 130, 2088:2097.

[Day 2, 10:50-11:10]

# Development of a mesoscopic simulation method for atmospheric convection

Lian-Ping Wang[1,2], Wojciech W. Grabowski[3], Zhaoli Guo[4], Ryo Onishi[2]

1. Department of Mechanical Engineering, University of Delaware, USA

2. Japan Agency for Marine-Earth Science and Technology, Japan

3. National Center for Atmospheric Division, USA

4. Huazhong University of Science and Technology, China

Email: lwang@udel.edu

## Abstract

In recent years, several mesoscopic methods based on the Boltzmann equation have been developed as an alternative computational fluid dynamics (CFD) approach for simulating turbulent flows. These methods have low numerical dissipation, are suitable for scalable computation, and can be applied to complex flow geometries. Although these mesoscopic methods are widely used in engineering applications, they are less known to the atmospheric community. Here we explore the possibility of using a mesoscopic approach known as the Discrete Unified Gas Kinetic Scheme (DUGKS) developed in Guo *et al.* (2013, 2015), as a tool to simulate atmospheric convection flows. DUGKS is designed as a finite-volume scheme of a modeled Boltzmann equation, with flexible mesh adaptation. Parallel implementation, treatment of boundary condition and external forcing, and extension to thermal flows are discussed in Wang *et al.* (2015) and Bo *et al.* (2016).

Specifically, we consider large-scale nonhydrostatic convection induced by a rising dry bubble (Carpenter et al. 1990), where both the shape and length scales change dramatically over time. Our goal is to simulate the large-scale motion and temperature field as accurately as possible with a limited grid resolution. In Navier-Stokes based finite-volume / finite-difference formulations, numerical limiters such as the piecewise parabolic method (Carpenter et al. 1990), the multidimensional positive definite

advection transport (MPDATA, Smolarkiewicz & Grabowski 1990), and the second-order weighted average flux (WAF) method (Toro 1989) with the SUPERBEE flux limiter (Roe 1981) are used to properly dissipate small scales so they do not introduce unphysical effects on the dynamics of large or resolved scales. One may view these numerical limiters as implicit sub-grid-scale models.

Similarly, we apply a numerical limiter (e.g., the van Leer limiter, see Guo et al. 2015) to DUGKS when simulating the dry bubble convection. We shall validate DUGKS by comparing the results to two independent solvers based on the Navier-Stokes equations. At the same times, we use such comparisons as a way to assess the sensitivity of results on the model details such as the type of numerical limiters. Furthermore, in the early stage of the dry bubble convection, all scales are resolved, so such comparisons can be used to compare the inherent numerical dissipation of each model. The comparisons include the center height of the dry bubble, the kinetic energy of the system, the velocity and temperature profiles, and the shape of the bubble. We will also compare the computational efficiency of these models.

**References:**


Bo, Y. T., P. Wang, Z.L. Guo and L.-P. Wang: Parallel implementation and validation of DUGKS for three-dimensional Taylor-Green vortex flow and turbulent channel flow, *Comput. & Fluids* 2016, submitted.

Carpenter, R.L., K.K. Droegemeier, P.R. Woodward and C.E. Hane: Application of the piecewise parabolic method (PPM) to meteorological modeling. *Monthly Weather Review* 1990, **118**: 586-612.

Guo, Z. L., Xu, K. and R. Wang: Discrete unified gas kinetic scheme for all Knudsen number flows: Low-speed isothermal case, Physical Review E 2013, **88**:033305.

Guo, Z.L., R. Wang and K. Xu: Discrete unified gas kinetic scheme for all Knudsen number flows. II. Thermal compressible case, *Physical Review E* 2015, **91**: 033313.

Roe, P.L. Approximate Riemann Solvers, Parameter Vectors, and Difference Schemes, *J. Comp. Phys*. 1981, **43**: 357-372

Smolarkiewicz, P.K. and W.W. Grabowski: The Multidimensional positive advection transport algorithm: nonoscillatory option, *J. Comp. Phys*. 1990, **86**: 355-375.

Toro, E. F.: A weighted average flux method for hyperbolic conservation laws. *Proc. Roy. Soc. London* 1989, **A423**: 401–418.

Wang, P., S. Tao, Z.L. Guo: A coupled discrete unified gas-kinetic scheme for Boussinesq flows. *Computers and Fluids* 2015, **120**: 70-81.

[Day 2, 11:10-11:30]

# Topographic representation scheme using a thin-wall approximation in terrain-following coordinates

Yuki Nishikawa[1] and Masaki Satoh[1]

1. Atmosphere and Ocean Research Institute, the University of Tokyo, Japan

Email: y_nishi@aori.u-tokyo.ac.jp

## Abstract

The resolution of atmospheric models has achieved under 1km even in global simulation. In such high-resolution simulation, conventional topographic schemes, terrain-following approaches, are not enough to represent steep mountains with accuracy because it induces large numerical errors over steep mountains. Thus, we have developed a topographic scheme using a thin-wall approximation in z-coordinates for such high-resolution simulation (Nishikawa and Satoh 2016). The scheme represents the steady flow over topography well. However, it blows up tracer near mountains when the topographic surface intersects except vertical levels in a model. For example, the density current is blown up by the scheme in cold bubble test with layer topography as shown Fig 1. Then, the topography is approximated as that vertical walls continuously are lined. Both schemes hold each problem as above. We introduce a thin-wall scheme to a terrain-following approach to solving those two problems; one is about terrain-following coordinates over steep mountains, and another is about the thin-wall

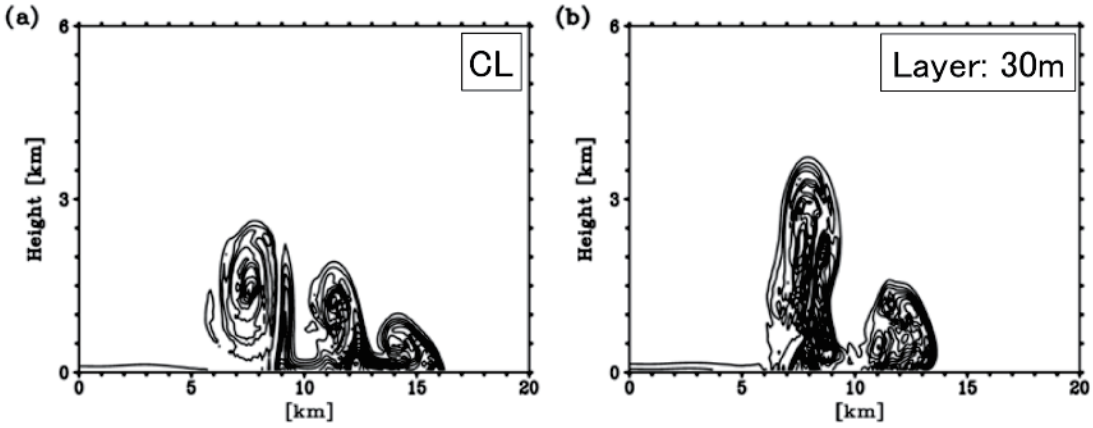


Fig. 1. Perturbation of temperature after 900 sec in cold bubble test. (a) is with no topography. (b) is with a layer topography, which is 30 m high in a whole domain. Both of horizontal and vertical resolution is 100m. Contour is 1 K.

approximation near smooth mountains as above. In the scheme, the smooth topography is represented only by terrain-following coordinates, and steep or high topography is represented by the two parts of terrain-following coordinates and a thin-wall approximation. We will talk about the separating algorithm for the steep or high mountain in a presentation. After here, we call thin-wall scheme in terrain-following coordinates as "hybrid scheme".

We implement the hybrid scheme to 2-dimensional non-hydrostatic equations and confirm its performance with a mountain wave test. The mountain profile is that the top of height is 1000m and the half width is 10km. Terrain-following coordinates in the hybrid scheme are decided by maximum gradient 0.05. Fig. 2 shows the results using terrain-following coordinates and the hybrid scheme with the smooth mountain. The hybrid scheme slightly induces numerical errors near the surface, and they appear as the spike of vertical velocity in Fig. 2 (b). However, the result of the hybrid scheme is almost consistent to that of terrain-following coordinates.

We formulate the hybrid scheme and confirm its performance with a smooth mountain. We will also talk about other test cases using the hybrid scheme.

**References:**

[1] Nishikawa, Y., Satoh, M. (2016) A conserved topographical representation scheme using a thin-wall approximation in z-coordinates. *SOLA*, **12**, 232-236, doi:10.2151/sola.2016-046

[2] Sundqvist, H., 1976: On vertical interpolation and truncation in connexion with use of sigma system models. *Atmosphere*, **14**, 37-52.

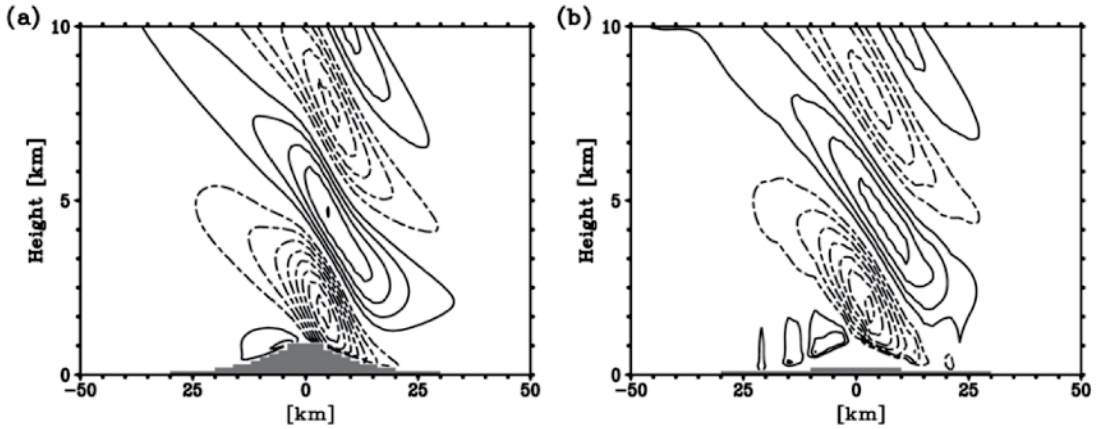


Fig. 2. Vertical velocity at 3 hours simulation. (a) is by terrain-following coordinates. (b) is by the hybrid scheme. Shaded regions show topography represented by terrain-following coordinates. In (b), the white area on shaded is the part of the thin-wall scheme. Contour is 0.2 m/s.

[Day 2, 11:30-11:50]

# Simulated Convective-Radiative Properties in the MJO during DYNAMO/CINDY

Chung-Hsiung Sui, Yi-An Chen, Shu-Yu Hou
Department of Atmospheric Sciences, National Taiwan University, Taiwan, ROC
Email: sui@ac.ntu.edu.tw

## Abstract

A model simulation is performed to analyze the recharge-discharge mechanisms of moisture and moist static energy (MSE) in the Madden Julian Oscillations observed over Indian Ocean during DYNAMO/CINDY2011 by using model for Prediction Across Scale (MPAS, Skamarock et al. 2012). The results of simulations are compared with sounding, operational assimilation and satellite data. The model captured the broad-scale features of the two MJOs in terms of wind field, outgoing long wave radiation, precipitation, hierarchical structure from low-troposphere ascending motion to deep ascending motion in the evolution of the two MJO events. But the model over-simulates the ascent, synoptic-scale disturbances and associated moistening process as revealed in the budget analysis. The moisture and MSE budget analyses reveal that the broad-scale features is dominated by moisture advection by mean-intraseasonal scale flow and moisture fields, and by diabatic process (surface flux and radiative feedback) as moisture and MSE sources in the suppressed and the cloud developing stage. Furthermore, we derive the convective-radiative properties over the NSA site over the Indian Ocean by using an offline parameterized cumulus and radiation schemes. The result shows low-troposphere moistening in the suppressed phase is primarily determined by cloud re-evaporation and cumulus moisture flux convergence. On the other hand, the condensation and cumulus moisture flux divergence are the major moisture sinks in the convective phase. This result also indicates an evolution from shallow cumulus that destabilized atmosphere by recharging columned integrated moisture to the development of deep convection that stabilized the atmosphere by discharging moisture. The bias of the simulated cumulus-radiative properties are evaluated against observations.

### References:

Skamarock, W. C., J. B. Klemp, M. G. Duda, L. Fowler, S.-H. Park, and T. D. Ringler, 2012: A multiscale nonhydrostatic atmospheric model using centroidal Voronoi tessellations and C-grid staggering. Mon. Wea. Rev., 140, 3090–3105.

[Day 2, 11:50-12:10]

# Multiscale structure of the MJO: Does it matter?

Kazu Kikuchi[1], Chihiro Kodama[2], Tomoki Miyakawa[3], Tomoe Nasuno[2], Masaki Satoh[2,3]

1. IPRC, University of Hawai'i, USA

2. Japan Agency for Marine-Earth Science and Technology, Japan

3. Atmosphere and Ocean Research Institute, the University of Tokyo, Japan

Email: kazuyosh@hawaii.edu

## Abstract

The Madden-Julian Oscillation is the predominant intraseasonal oscillation in the tropics. Despite extensive studies over the past several decades, our understanding of the dynamics and physics of the MJO remains incomplete and our ability to simulate the MJO with fidelity even in state-of-the-art numerical models remains unsatisfactory. Of the key processes associated with the initiation and maintenance of the MJO, it seems obvious that the interplay between convection and the large-scale circulation must play a crucial role, although our knowledge of these interactions is perhaps the most uncertain of all. The MJO is usually viewed as a coupled system consisting of a rather ill-defined planetary-scale convective envelope and associated large-scale circulation that move eastward at an average phase speed of 5-6 m $s^{-1}$ in the Indo-Pacific region. On the other hand, individual convective elements within the MJO envelope occur on much smaller scales, many of which are highly organized mesoscale convective systems (MCSs; e.g., Nakazawa 1988) that tend to develop in association with synoptic-scale equatorially-trapped waves; they are collectively referred to as convectively coupled equatorial waves (CCEWs; e.g., Kiladis et al. 2009).

It stands to reason that for a complete understanding of the MJO, particularly in terms of the interaction between convection and large-scale circulation, it is of critical importance to understand the relationship between the MJO and the organization of convection, particularly in terms of CCEWs, within its envelope. However, our knowledge remains limited and no consensus has been reached on the makeup of the MJO. Perhaps this is largely due to the fact that each MJO has different characteristics (i.e., MJO diversity) in its multiscale structure as well as other aspects such as phase

speed and zonal scale and that few effective approach was available to reveal the multiscale structure of the MJO. Taking advantage of the spatio-temporal wavelet transform (STWT) (Kikuchi and Wang 2010), our recent observation study with particular focus on the CINDY/DYNAMO MJOs suggests that slow Kelvin waves (3-9 m $s^{-1}$) are major building blocks of the MJO (Kikuchi et al. 2016), though the details of the multiscale structure of the MJO varies greatly from one event to another. We thus hypothesize that slow Kelvin waves play the central role in the propagation of the MJO.

In this talk, we will argue how the multiscale structure of the MJO is linked to MJO simulation fidelity based upon NICAM (Satoh et al. 2014). We use two distinct 14-km simulations: a long-term AMIP-type climate simulation (Kodama et al. 2015) and a series of 40-day hindcasts (Miyakawa et al. 2014). As in the observational study, at this stage, we limit ourselves to examining the morphological aspect based on the STWT.

**References:**


Kikuchi, K. and B. Wang, 2010: Spatiotemporal wavelet transform and the multiscale behavior of the Madden-Julian oscillation. *J. Climate*, **23,** 3814-3834.

Kikuchi, K., G. N. Kiladis, J. Dias, and T. Nasuno, 2016: Convectively coupled equatorial waves within the MJO during CINDY/DYNAMO: Slow Kelvin waves as building blocks. *Clim. Dyn.*, Submitted.

Kiladis, G. N., M. C. Wheeler, P. T. Haertel, K. H. Straub, and P. E. Roundy, 2009: Convectively coupled equatorial waves. *Rev. Geophys.*, **47,** RG2003.

Kodama, C., and Coauthors, 2015: 20-year climatology of a NICAM AMIP-type simulation. *J. Meteor. Soc. Japan*, **93,** 393-424.

Miyakawa, T., and Coauthors, 2014: Madden-Julian oscillation prediction skill of a new-generation global model demonstrated using a supercomputer. *Nature Communications*, 10.1038/ncomms4769.

Nakazawa, T., 1988: Tropical super clusters within intraseasonal variations over the western Pacific. *J. Meteor. Soc. Japan*, **66,** 823-839.

Satoh, M., and Coauthors, 2014: The Non-hydrostatic Icosahedral Atmospheric Model: Description and Development. *Progress in Earth and Planetary Science*, **1**:18.

[Day 2, 13:40-14:00]

# Current status of MJO simulations using NICAM and its 3D-ocean coupled version NICOCO

Tomoki Miyakawa[1]

1. Atmosphere and Ocean Research Institute, the University of Tokyo, Japan

Email: miyakawa@aori.u-tokyo.ac.jp

## Abstract

NICAM can now be run in a fully-coupled mode with the ocean component COCO of the MIROC model. We carried out multiple MJO simulations using this new ocean-coupled version NICAM (NICOCO) to see the impact on MJO and seasonal predictions compared to the well-performing atmospheric NICAM (Miyakawa et al. 2014). As is the case in most global models, ocean coupling frees the model from being anchored by the observed SST and allows the model climate to drift away further from reality compared to the atmospheric version of the model. Thus, it is important to evaluate the model bias, and in an initial value problem such as the seasonal extended-range prediction, it is essential to be able to distinguish the actual signal from the early transition of the model from the observed state to its own climatology. Since NICAM is a highly resource-demanding model, evaluation and tuning of the model climatology (order of years) is challenging. Here we focus on the initial 100 days to estimate the early drift of the model, and subsequently evaluate MJO prediction skills of NICOCO. Additionally, we carry out a series of simulations that targets an eastward propagating event that is perceived to have affected the termination of 1997/1998 El-Nino (Takayabu et al. 1999), and explore the merits of having a full 3D dynamical ocean.

Results show that in the initial 100 days, NICOCO forms a La-Nina like SST bias compared to observation, with a warmer Maritime Continent warm pool and a cooler equatorial central Pacific. The enhanced convection over the Maritime Continent associated with this bias project on to the real-time multi-variate MJO indices (RMM, Wheeler and Hendon 2004), and contaminate the MJO skill score. However, the bias does not appear to demolish the MJO signal severely, as the model maintains a valid MJO prediction skill up to nearly 4 weeks when evaluated after removing the early drift component estimated from the 54 simulations.

The result of 1998 event simulation series show that the model is able to capture both the eastward event and the transition from the El-Nino to La-Nina condition that occurred during the initial 100 days of the simulations. The roles of the surface flux associated with the event on the termination of El-Nino will be evaluated.

**References:**

Miyakawa, T., Satoh, M., Miura, H., Tomita, H., Yashiro, H., Noda, A. T., Yamada, Y., Kodama, C., Kimoto, M., Yoneyama, K., 2014: Madden-Julian Oscillation prediction skill of a new-generation global model. Nature Commun., 5, 3769. doi:10.1038/ncomms4769

Takayabu, Y. N., T. Iguchi, M. Kachi, A. Shibata, and H. Kanzawa, 1999: Abrupt termination of the 1997-98 El Nino in response to a Madden-Julian oscillation. Nature, 402, 279-282.

Wheeler, M. C., and H. H. Hendon, 2004: An all-season real-time multivariate MJO index: Development of an index for monitoring and prediction. Mon. Wea. Rev., 132, 1917–1932.

[Day 2, 14:00-14:20]

# Near real-time forecasts using a global nonhydrostatic model NICAM for field campaigns

Tomoe Nasuno[1]

1. Japan Agency for Marine-Earth Science and Technology, Japan

Email: nasuno@jamstec.go.jp

## Abstract

A near real-time forecast system using Nonhydrostatic Icosahedral Atmospheric Model (NICAM) (Satoh et al. 2014) have been developed at JAMSTEC since 2010. The forecast system had been operated daily during field campaigns, the CINDY/DYNAMO (October 2011-January 2012) (Yoneyama et al. 2013), PALAU2010 (May-June 2010), PALAU2013 (May-July 2013), and Pre-YMC (November-December 2015; pilot study of the Years of Maritime Continent, 2017-2019). The major target of the PALAU campaigns was the boreal summer intraseasonal variability (BSISO) and associated phenomena, whereas that in the CINDY/DYNAMO and Pre-YMC was the initiation and dynamics of the Madden-Julian Oscillation (MJO) (Madden and Julian 1971) over the Indian Ocean and multiscale interactions over the Maritime Continent. This presentation reviews the performances and updates of the forecast system.

The first version of the forecast system was constructed using the regionally stretched grid ssystem (Tomita 2008), with the finest horizontal mesh size of ~14 km in the equatorial central Indian Ocean. The simulation was initialized using the NCEP final analysis and week-long forecasts were executed. In all the simulations, moist convection was explicitly represented without using the cumulus parameterization. The forecast system was capable of capturing the intraseasonal signals despite the relatively coarse resolutions in both seasons. In the CINDY/DYNAMO case, where two prominent and one marginal MJO events took place, the real-time multivariate MJO index (Wheeler and Hendon 2004) was reasonably predicted at the average skill score ~0.8 for the week-long integrations (Nasuno 2013). Systematic biases associated with the mean low-level flow bias was also noticed. The atmospheric sounding includes dry (~ 1 g $kg^{-1}$) and warm (~ 1 K) biases in comparison with the sonde observations (Nasuno et al. 2016, in revision), which was approximately twice the magnitude of the biases in the ERA Interim (Nasuno et al. 2015). The moisture budget analysis using the forecast outputs during the CINDY/DYNAMO period indicated significant amount of vertical transport

of moisture associated with sub-daily components. As to the individual mesoscale convective events, a tendency of earlier development of low pressure systems were noticed, especially in the summertime runs.

The forecast system was upgraded in 2015 for the Pre-YMC campaign, using the global 7-km and 14-km mesh NICAM on the third generation of the Earth Simulator. During the campaign, a MJO was intensified around the observational site (southwest Sumatra). The 14-km mesh month-long forecasts simulated the evolution of the MJO approximately two weeks in advance. The 7-km mesh week-long forecasts captured the drastic change in the morphology and propagation of the convective systems before and after the amplification of the MJO. The moisture budget analysis using the forecast outputs suggested moisture accumulation associated with synoptic scale variability during the transition. The plans for the YMC campaign will be also discussed.

**References:**


Madden, R. and P. Julian, 1971: Detection of a 40–50 day oscillation in the zonal wind in the tropical Pacific. J. Atmos. Sci., 28, 702–708.

Nasuno, T., 2013: Forecast Skill of Madden-Julian Oscillation Events in a Global Nonhydrostatic Model during the CINDY2011/DYNAMO Observation Period. Scientific *Online Letters on the Atmosphere*, 9, 69–73, doi: 10.2151/sola.2013-016.

Nasuno, T., T. Li, and K. Kikuchi, 2015: Moistening processes before the convective initiation of Madden-Julian Oscillation events during the CINDY2011/DYNAMO period. *Mon. Wea. Rev.,* 143, 622-643.

Satoh, M., H. Tomita, H. Yashiro, H. Miura, C. Kodama, T. Seiki, A. T. Noda, Y. Yamada, D. Goto, M. Sawada, T. Miyoshi, Y. Niwa, M. Hara, T. Ohno, S. Iga, T. Arakawa, T. Inoue and H. Kubokawa, 2014: The Non-hydrostatic Icosahedral Atmospheric Model: description and development. *Progress in Earth and Planetary Science*, **1**:18. doi: 10.1186/s40645-014-0018-1

Tomita, H., 2008: A stretched grid on a sphere by new grid transformation, *J. Meteor. Soc. Japan*, 86A, 107–119.

Wheeler, M. C. and H. H. Hendon, 2004: An all-season real-time multivariate MJO index: Development of an index for monitoring and prediction. Mon. Wea. Rev., 132, 1917–1932.

Yoneyama, K., C. Zhang, and C. N. Long, 2013: Tracking pulses of the Madden-Julian Oscillation. *Bull. Amer. Meteor. Soc.,* 94, 1871–1891.

[Day 2, 14:20-14:40]

# "Big Data Assimilation" for 30-second-update 100-m-mesh Numerical Weather Prediction

Takemasa Miyoshi[1], Guo-Yuan Lien[1], Masaru Kunii[2,1], Juan Ruiz[3,1], Yasumitsu Maejima[1], Shigenori Otsuka[1], Keiichi Kondo[1], Hiromu Seko[2], Shinsuke Satoh[4], Tomoo Ushio[5], Kotaro Bessho[6], Hirofumi Tomita[1], Yutaka Ishikawa[1]

1. RIKEN Advanced Institute for Computational Science, Japan
2. Meteorological Research Institute, Japan
3. University of Buenos Aires, Argentina
4. National Institute of Information and Communications Technology, Japan
5. Osaka University, Japan
6. Meteorological Satellite Center (now at Forecast Department), Japan Meteorological Agency, Japan

Email: takemasa.miyoshi@riken.jp

## Abstract

A typical lifetime of a single cumulonimbus is within an hour, and radar observations often show rapid changes in only a 5-minute period. For precise prediction of such rapidly-changing local severe storms, we have developed what we call a "Big Data Assimilation" (BDA) system that performs 30-second-update data assimilation cycles at 100-m grid spacing (Miyoshi et al. 2016a; 2016b). The concept shares that of NOAA's Warn-on-Forecast (WoF), in which rapidly-updated high-resolution NWP will play a central role in issuing severe-storm warnings even only minutes in advance. The 100-m resolution and 30-second update frequency are a leap above typical recent research settings, and it was possible by the fortunate combination of Japan's most advanced supercomputing and sensing technologies: the 10-petaflops K computer and the Phased Array Weather Radar (PAWR). The X-band PAWR is capable of a dense three-dimensional volume scan at 100-m range resolution with 100 elevation angles and 300 azimuth angles, up to 60-km range within 30 seconds. The PAWR data show temporally-smooth evolution of convective rainstorms. This gives us a hope that we may

assume the Gaussian error distribution in 30-second forecasts before strong nonlinear dynamics distort the error distribution for rapidly-changing convective storms. With this in mind, we apply the Local Ensemble Transform Kalman Filter (LETKF) that considers flow-dependent error covariance explicitly under the Gaussian-error assumption. The flow-dependence would be particularly important in rapidly-changing convective weather. Using a 100-member ensemble at 100-m resolution, we have tested the BDA system in real-world cases of sudden local rainstorms, and obtained promising results. Figure 1 shows a case around Kobe on September 11, 2014. Here we can see that 100-m resolution BDA well captures the observed 3-D structure, although the 1-km resolution counterpart shows only a blur representation. Without assimilating the every 30-second PAWR data, we have no clue to simulate the observed rain system at all. In this presentation, we will present the most up-to-date progress of our BDA research.

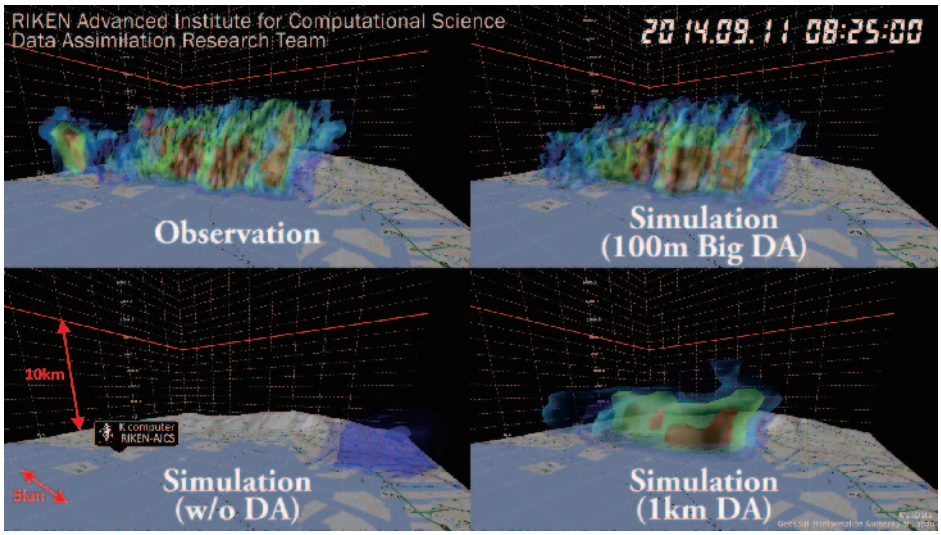


Figure 1. 3-D plot of radar reflectivity from (top left) actual PAWR observation, (top right) 100-m resolution BDA, (bottom left) 100-m resolution without BDA, and (bottom right) 1-km resolution DA.

**References:**

Miyoshi, T., G.-Y. Lien, S. Satoh, T. Ushio, K. Bessho, H. Tomita, S. Nishizawa, R. Yoshida, S. A. Adachi, J. Liao, B. Gerofi, Y. Ishikawa, M. Kunii, J. Ruiz, Y. Maejima, S. Otsuka, M. Otsuka, K. Okamoto, and H. Seko, 2016b: "Big Data Assimilation" toward Post-peta-scale Severe Weather Prediction: An Overview and Progress. *Proc. of the IEEE*, in press.

Miyoshi, T., M. Kunii, J. Ruiz, G.-Y. Lien, S. Satoh, T. Ushio, K. Bessho, H. Seko, H. Tomita, and Y. Ishikawa, 2016a: "Big Data Assimilation" Revolutionizing Severe Weather Prediction. *Bull. Amer. Meteor. Soc.*, **97**, 1347-1354. doi:10.1175/BAMS-D-15-00144.1

[Day 2, 14:40-15:00]

# Development of Assimilation Methods for Polarimetric Radar Data

Takuya Kawabata[1], Hiroshi Yamauchi[2], Nobuhiro Nagumo[1], Ahoro Adachi[1]

1. Meteorological Research Institute, Japan Meteorological Agency

2. Japan Meteorological Agency

Email: tkawabat@mri-jma.go.jp

## Abstract

### 1. Introduction

Recently, polarimetric radars have been deployed as operational radars in many countries, which are expected to contribute improving rainfall forecast skills by data assimilation. In this study, two types of assimilation methods for dual polarimetric radar data have been developed and presented.

### 2. Operators

The first operator is assimilation of observed polarimetric parameters like the horizontal reflectivity ($Z_{\mathrm{H}}$), the differential reflectivity ($Z_{\mathrm{DR}}$), and the specific differential phase ($K_{\mathrm{DP}}$). These parameters are represented by

$$Z_{\mathrm{H,V}} = \frac{4\lambda^4}{\pi^4 |K_w|^2}\left(\alpha_{h,v}^2 N_0 \Lambda^{-(2\beta_{h,v}+1)}\Gamma\left(2\beta_{h,v}+1\right)\right),$$

$$Z_{\mathrm{DR}} = Z_{\mathrm{H}} - Z_{\mathrm{V}},$$

$$K_{\mathrm{DP}} = \frac{180\lambda}{\pi} N_0 \alpha_k \Lambda^{-(\beta_k+1)}\Gamma(\beta_k+1).$$

Here, H,V, h, and v represent horizontal and vertical polarizations, $\alpha$ and $\beta$ represent fitting coefficients against scattering amplitudes, $\lambda$, $K_w$, $N_0$, $\Lambda$, and $\Gamma$ are wave length, a constant defined as $K_w = (\varepsilon - 1)/(\varepsilon + 2)$ in which $\varepsilon$ is the complex dielectric constant of water, the intercept and slope parameters, respectively.

The second is assimilation of rain water content retrieved from observed KDP as

$$\mathrm{Q}(K_{\mathrm{DP}}) = \mathrm{c}_2 \left(\frac{K_{\mathrm{DP}}}{f}\right)^{b_2},$$

c is a fitting coefficient against scattering amplitude, and f represents a wave frequency. b is the empirical constants described in Bringi and Chandrasekar (2001).

3. Result

These methods were implemented into nonhydrostatic cloud-resolving 4DVAR (NHM-4DVAR). Fig. 1 shows that the assimilation system improved the first guess filed closing to the observation. Details will be given in the presentation.

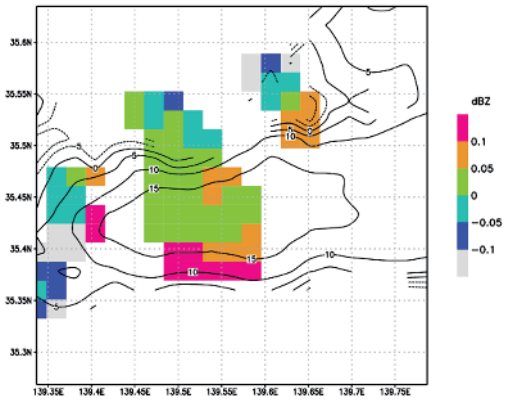


Fig. 1. Horizontal reflectivity of analysis increment (shades) and observations (contour).

**References:**

Bringi, V. N., and V. Chandrasekar, 2001, Polarimetric Doppler weather radar-principle and application. Cambridge University Press, 636 pp.

[Day 2, 15:30-15:50]

# Impact of flow-dependent assimilation using adjoint model including 3-ice microphysics scheme

Yasutaka Ikuta[1,2]

1. Japan Meteorological Agency, Japan,

2. Meteorological Research Institute, Japan

Email: ikuta@met.kishou.go.jp

## Abstract

Aiming at improvement of short-range precipitation forecasts, the Japan Meteorological Agency has been developing a new meso-scale hybrid 4D-Var data assimilation system using flow-dependent background error estimated from ensemble forecasts. This system will enable the assimilation of high temporal resolution observations. Some important data among such observations are radar reflectivity and satellite radiance, for whose assimilation the detailed information of hydrometeors is necessary.

In this regard, we have developed a tangent-linear and an adjoint model including simplified 6-class 3-ice 1-moment bulk cloud microphysics scheme. The simplification of microphysics scheme provides that the growth of perturbation in this tangent-linear model becomes similar to the growth of nonlinear perturbation during 3-hour assimilation window. The adjoint model propagates the gradient of cost function with respect to hydrometeors from observation of reflectivity and brightness temperature to the beginning of assimilation window. In most cases, ice-phase information from observation is transformed into water vapor information through the backward integration with adjoint operators of the microphysics scheme.

The impact of the assimilation of radar reflectivity and satellite radiance data using the meso-scale hybrid 4D-Var data assimilation system will be presented at the workshop.

[Day 2, 15:50-16:10]

# Assimilating All-Sky Himawari-8 Satellite Infrared Radiances: A Case of Kanto-Tohoku heavy rainfall in 2015

Takumi Honda[1], Guo-Yuan Lien[1], Yasumitsu Maejima[1], Kozo Okamoto[2,1]
Takemasa Miyoshi[1]

1. RIKEN Advanced Institute for Computational Science, Japan

2. Meteorological Research Institute, Japan Meteorological Agency, Japan

Email: takumi.honda@riken.jp

## Abstract

To predict heavy rainfalls accurately, better initial conditions through data assimilation are required. Lien et al. (2016) developed a new ensemble data assimilation system called SCALE-LETKF and showed that the Kanto-Tohoku heavy rainfall in 2015 was well replicated with only the conventional observations. However, the location and intensity of rainbands extending from the ocean showed room for improvement.

Geostationary satellites can provide precious observations over the ocean, where the number of the conventional observations is generally limited. In July 2015, full operations of the new Japanese geostationary satellite "Himawari-8" was started (Bessho et al., 2016). Himawari-8 provides high-resolution radiance observation with 16 frequency bands every 10 minutes for full disk, and every 2.5 minutes for local regions around Japan and tropical cyclones (TCs). Recently, Honda et al. (2016) assimilated all-sky Himawari-8 infrared (IR) radiance observation and showed its clear advantages for the analyses and forecasts of the strongest TC case in the Western North Pacific in 2015. The present study aims to assimilate all-sky Himawari-8 IR radiances for the Kanto-Tohoku heavy rainfall in 2015 and investigate its impact on the analyses and forecasts of the rainbands and associated heavy rainfall.

We performed two experiments with and without the Himawari-8 radiance assimilation. The results showed that assimilating the Himawari-8 observation improves the radiance analysis dramatically (Figure 1). We will show the impact on the forecasts in the presentation.

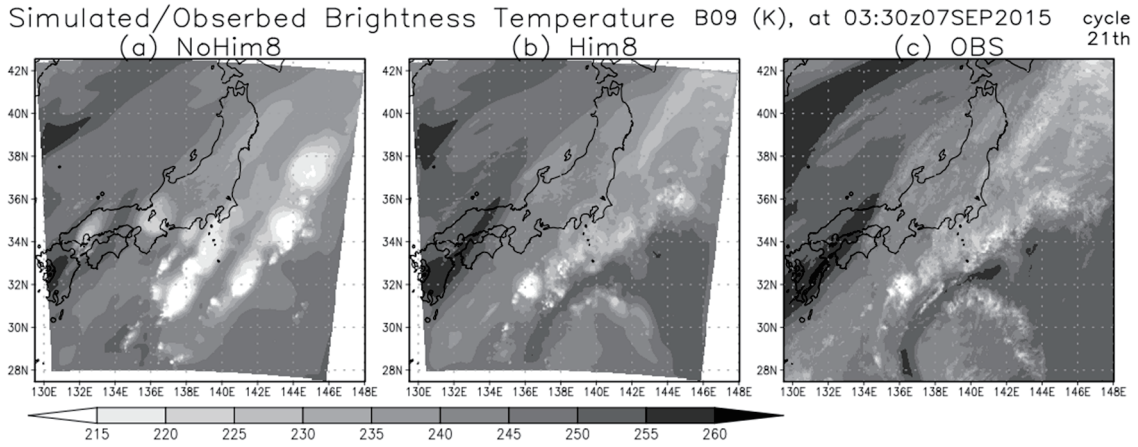


Figure 1. Horizontal maps of Himawari-8 brightness temperature (K) of band 9 (6.9 μm) at 0330 UTC 7 September (after 21 data assimilation cycles). (a) NoHim8 (without the Himawrai-8 observation) ensemble mean analysis, (b) Him8 (with the Himawrai-8 observation) ensemble mean analysis, and (c) Himawari-8 observation.

**References:**

Bessho, K., and Coauthors (2016), An introduction to Himawari-8/9 –Japan's new-generation geostationary meteorological satellites, *J. Meteor. Soc. Japan*, **94**, 151–183, doi:10.2151/jmsj.2016-009.

Honda, T., T. Miyoshi, G.-Y. Lien, S. Nishizawa, R. Yoshida, S. A. Adachi, K. Terasaki, K. Okamoto, H. Tomita, and K. Bessho (2016), Assimilating All-Sky Himawari-8 Satellite Infrared Radiances: A Case of Typhoon Soudelor (2015), submitted to *Mon. Wea. Rev.*.

Lien, G.-Y., T. Miyoshi, S. Nishizawa, R. Yoshida, H. Yashiro, S. A. Adachi, T. Yamaura, and H. Tomita (2016), Near-real-time forecasts of the heavy rainfall induced by Typhoon Etau (2015) using the SCALE-LETKF, submitted to *SOLA*.

[Day 2, 16:10-16:30]

# Assimilating satellite radiances with the NICAM-LETKF system

Koji Terasaki[1], Keiichi Kondo[1], Takemasa Miyoshi[1]

1. Advanced Institute for Computational Science, RIKEN

Email: koji.terasaki@riken.jp

## Abstract

In numerical weather prediction (NWP), data assimilation plays a key role. Terasaki et al. (2015) applied the local ensemble transform Kalman filter (LETKF) to non-hydrostatic icosahedral atmospheric model (NICAM: Satoh et al. 2014), and successfully assimilated the conventional observations. Next, the NICAM-LETKF system is improved to assimilate satellite radiances. First, we developed the NICAM-LETKF system to assimilate the AMSU-A radiance. There are several kinds of the satellite radiances observed with microwave, infrared, and so on. Advanced Microwave Sounding Unit-A (AMSU-A) is one of the microwave sounders which is installed on a lot of satellites. The AMSU-A has a larger spatial coverage compared with the other satellites. Also, it is known that AMSU-A has a large impact on the NWP compared with the other instruments. First, we developed the NICAM-LETKF system to assimilate the AMSU-A radiance.

Bias correction is an important issue on assimilating satellite radiances. In this study, we applied the online estimation of bias correction for both airmass and scan biases which depend on the atmospheric state and scan position, respectively. We performed two experiments in this study. One assimilates only the conventional observations, and the other assimilates AMSU-A radiances in addition to the conventional observations. The channels from 6 to 8 which are sensitive to the middle and upper troposphere are assimilated.

Quality control is also important to assimilate the satellite radiances. Microwave sounding data are less contaminated by the cloud and rain particles than infrared sounding data. However, the microwave sounding is known to be contaminated by the thick clouds and rain. We applied the quality control by the liquid water path computed from the channels 1 and 2 of the AMSU-A radiances (Ralf, 2002).

We confirmed that the NICAM-LETKF system assimilating AMSU-A stably ran for 2 months, and that the analysis was improved by assimilating the AMSU-A radiances in addition to the conventional observations (Fig. 1). Future studies include assimilating

the AMSU-A radiances in all-sky condition, and assimilating other satellite radiances.

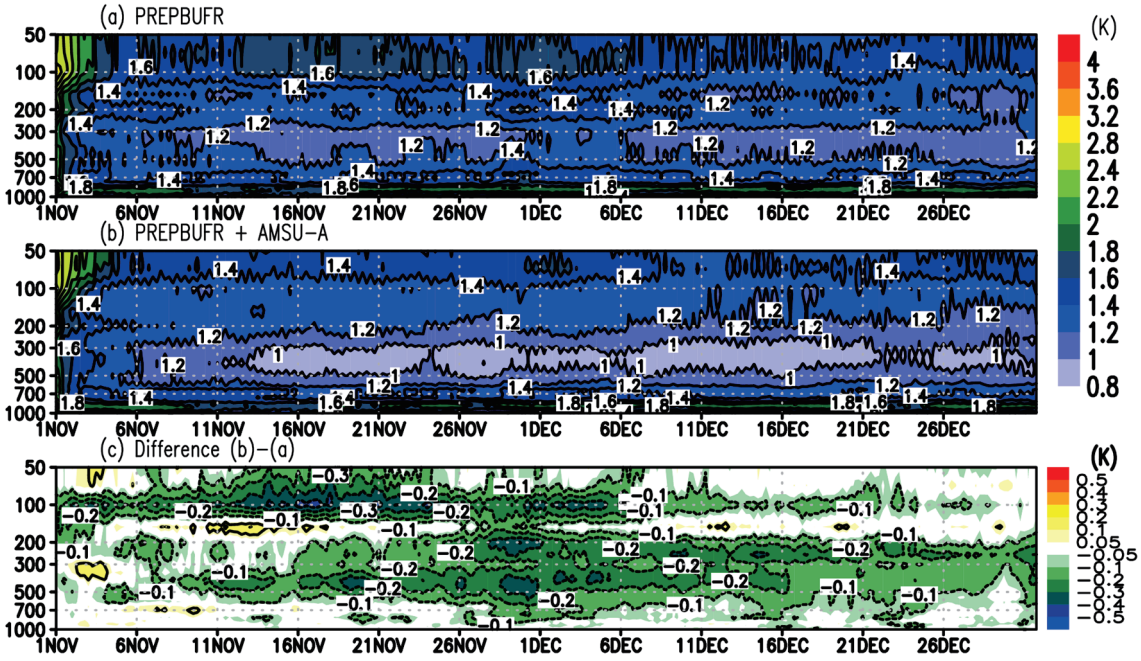


Fig. 1 Time series of the global RMSD of the air temperature relative to the ERA-interim for the experiments (a) with PREPBUFR only, (b) with additional AMSU-A. (c) shows the difference between (a) and (b), with negative values corresponding to the advantage by assimilating the AMSU-A radiances. The horizontal and vertical axes represent the date and pressure, respectively.

**References:**

Ralf Bennartz, 2002: Precipitation analysis using the Advanced Microwave Sounding Unit in support of nowcasting applications. Meteorol. Appl., 9, 177-189.

Satoh, M., H. Tomita, H. Yashiro, H. Miura, C. Kodama, T. Seiki, A. T. Noda, Y. Yamada, D. Goto, M. Sawada, T. Miyoshi, Y. Niwa, M. Hara, T. Ohno, S. Iga, T. Arakawa, T. Inoue and H. Kubokawa: The Non-hydrostatic Icosahedral Atmospheric Model: description and development. *Progress in Earth and Planetary Science* 2014, **1**:18. doi: 10.1186/s40645-014-0018-1

Terasaki, K., M. Sawada, and T. Miyoshi, 2015: Local Ensemble Transform Kalman Filter Experiments with the Nonhydrostatic Icosahedral Atmospheric Model NICAM. *SOLA*, **11**, 23-26. doi:10.2151/sola.2015-006

[Day 3, 8:40-9:00]

# Model Parameter Estimation Using Ensemble Data Assimilation: A Case with the Nonhydrostatic Icosahedral Atmospheric Model NICAM and the Global Satellite Mapping of Precipitation Data

Shunji Kotsuki[1], Koji Terasaki[1], Hisashi Yashiro[1],
Hirofumi Tomita[1], Masaki Satoh[2,3], and Takemasa Miyoshi[1,3,4]

1. RIKEN Advanced Institute for Computational Science, Japan

2. Atmosphere and Ocean Research Institute, the University of Tokyo, Japan

3. Japan Agency for Marine-Earth Science and Technology, Japan

4. Department of Atmospheric and Oceanic Science, University of Maryland, U. S.

Email: shunji.kotsuki@riken.jp

## Abstract

This study aims to improve precipitation forecasts from numerical weather prediction (NWP) models through effective use of satellite-derived precipitation data. Kotsuki et al. (2016a) successfully improved the precipitation forecasts by assimilating the Japan Aerospace eXploration Agency (JAXA)'s Global Satellite Mapping of Precipitation (GSMaP) data into the Nonhydrostatic Icosahedral Atmospheric Model (NICAM) at 112-km horizontal resolution. Kotsuki et al. mitigated the non-Gaussianity of the precipitation variables by the Gaussian transform method for observed and forecasted precipitation using the previous 30-day precipitation data.

This study extends the previous study by Kotsuki et al. and explores an online estimation of model parameters using ensemble data assimilation. We choose two globally-uniform parameters, one from the Berry's parameterization for large scale condensation and the other from the Arakawa-Schubert cumulus parameterization scheme. We perform the online-estimation of the two model parameters with an ensemble transform Kalman filter by assimilating the GSMaP precipitation data with the Gaussian transform. The parameter estimation successfully improved 6-hour precipitation forecasts (Fig. 1). The improvement is significant after two months when the estimated parameters are stabilized. In addition, the estimated parameters improve the mixing ratio in the lower troposphere (Fig. 2). Therefore, the parameter estimation would be a useful technique to improve the NWP models and their forecasts. This presentation will include the most recent progress up to the time of the workshop.

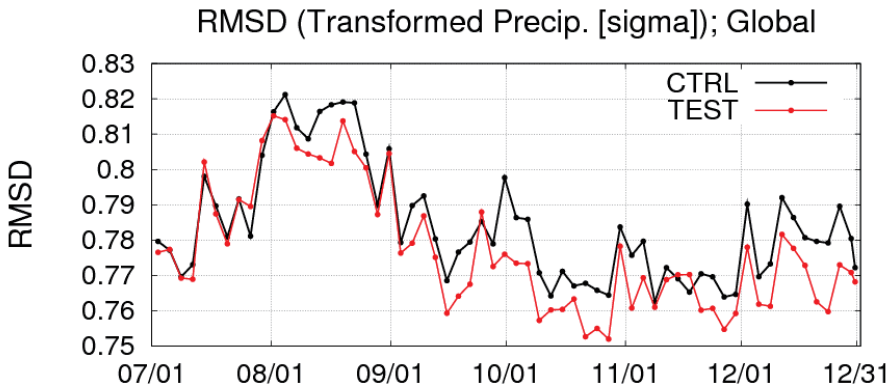


Fig. 1 Time series of the changes in 3-day average root mean square differences (RMSDs) in the 6-hr precipitation forecasts relative to the GSMaP precipitation data. Black and blue lines represent the control and parameter estimation experiments, respectively. The horizontal axes show date-month in 2014. According to Kotsuki et al. (2016b)

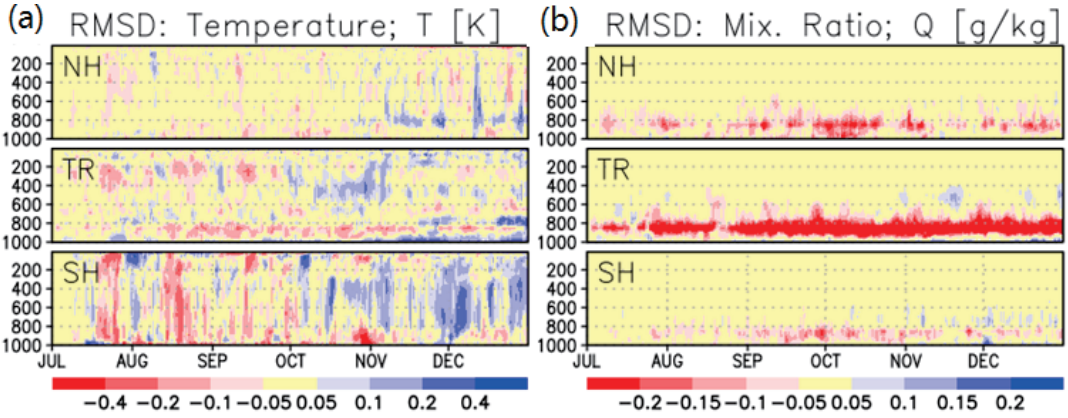


Fig. 2 Time series of the changes in RMSDs in the analyses relative to the ERA Interim reanalysis between control and parameter estimation experiments for (a) temperature (K), and (b) mixing ratio (g $kg^{-1}$). The vertical and horizontal axes show the pressure level from 1000 to 100 hPa, and date-month in 2014, respectively. Warm (cold) color represents improvement (degradation) due to the parameter estimation. According to Kotsuki et al. (2016b)

**References:**

Kotsuki, S., T. Miyoshi, K. Terasaki, G.Y. Lien, and E. Kalnay (2016a): Assimilating the Global Satellite Mapping of Precipitation Data with the Nonhydrostatic Icosahedral Atmospheric Model NICAM. *Journal of Geophysical Research-Atmospheres* (submitted)

Kotsuki, S., K. Terasaki, H. Yashiro, H. Tomita, M. Satoh, and T. Miyoshi (2016b): Model parameter estimation using ensemble data assimilation: A case with the Nonhydrostatic Icosahedral Atmospheric Model NICAM and the Global Satellite Mapping of Precipitation Data. (in preparation)

[Day 3, 9:00-9:20]

# Modeling condensation in nonhydrostatic cloud-scale models

Wojciech W. Grabowski
Mesoscale and Microscale Meteorology Laboratory
National Center for Atmospheric Research, Boulder, USA
Email: grabow@ucar.edu

## Abstract

Condensation of water vapor to form and grow cloud droplets is the fundamental process of cloud and precipitation formation. It drives convective dynamics through the release of latent heat and determines the strength of convective updrafts. Cloud-scale models simulate condensation by applying two drastically different methods. The first one is the bulk condensation, where cloud water is assumed to exist only in saturated conditions and evaporates instantaneously when the air becomes sub-saturated. Bulk condensation is computationally efficient because it does not constrain the model time step and allows straightforward implementation of the centered-in-time time stepping. Computational implementation of the bulk condensation typically involves a procedure that is referred to as the saturation adjustment because volumes with cloud water are to be at saturation at the completion of the model time step. The second approach involves prediction of the in-cloud super- or sub-saturation and is typically associated with models that predict not only condensate mass but also relevant features of the droplet size distribution (e.g., models with the 2-moment microphysics or with the bin microphysics). However, predicting in-cloud super- or sub-saturation is numerically cumbersome. The question is whether the difference between the two approaches has a noticeable impact on convective dynamics. To answer this question, we apply a novel modeling methodology, the microphysical piggybacking (Grabowski 2014, 2015; Grabowski and Jarecka 2015; Grabowski and Morrison 2016). The main idea is to use two sets of thermodynamic variables driven by two microphysical schemes or by the same scheme with different scheme parameters. One set is coupled to the dynamics and drives the simulation, and the other set piggybacks the simulated flow, that is, responds to the simulated flow but does not affect it. By switching the two sets (i.e., the set driving the simulation becomes the piggybacking one, and vice versa), the impact on the cloud dynamics can be isolated from the purely microphysical effect. Application of this methodology to the daytime deep convection development over land based on the observations during the

Large-scale Biosphere–Atmosphere (LBA) field project in Amazonia (Grabowski et al. 2006) will be discussed applying a double-moment microphysics scheme with either the saturation adjustment or predicting the in-cloud super- and sub-saturation. The results document a significant dynamical impact of finite supersaturations on deep convection and a strong microphysical effect associated with upper-tropospheric anvils. Implications of these results for modeling of convective dynamics will be discussed and a possible intermediate modeling methodology will be suggested.

**References:**


Grabowski, W. W., 2014: Extracting microphysical impacts in large eddy simulations of shallow convection. *J. Atmos. Sci.*, **71**, 4493-4499.

Grabowski, W. W., 2015: Untangling microphysical impacts on deep convection applying a novel modeling methodology. *J. Atmos. Sci.*, **72**, 2446-2464.

Grabowski, W. W., and D. Jarecka, 2015: Modeling condensation in shallow nonprecipitating convection. *J. Atmos. Sci.*, **72**, 4661-4679.

Grabowski, W. W., and H. Morrison, 2016: Untangling microphysical impacts on deep convection applying a novel modeling methodology. Part 2: Double-moment microphysics. *J. Atmos. Sci.*, (in press; available on EOR; should be published by the time of the meeting).

Grabowski, W. W., and Coauthors, 2006: Daytime convective development over land: a model intercomparison based on LBA observations. *Quart. J. Roy. Met. Soc.*, **132**, 317-344.

[Day 3, 9:20-9:40]

# An accurate, efficient method for calculating hydrometeor advection in multi-moment bulk and bin microphysics schemes

Hugh Morrison

1. MMM Laboratory, National Center for Atmospheric Research, Boulder, USA

Email: morrison@ucar.edu

## Abstract

A new, efficient flux-based method for calculating the advection of coupled cloud hydrometeor quantities, similar to Vector Transport applied previously in aerosol modeling, will be presented. In this method, called Scaled Flux Vector Transport (SFVT), lead scalars (the mass mixing ratios in bulk microphysics schemes) are advected using the host model's unmodified advection scheme and secondary scalars (e.g., number mixing ratios in bulk schemes) are advected by appropriately scaling the lead scalar fluxes. By design, SFVT retains linear relationships between the advected scalars. Analytic tests reveal that mean errors using SFVT are similar to those incurred using the traditional approach of separately advecting each variable. SFVT is applied to the multi-moment Predicted Particle Properties (P3) bulk microphysics scheme in idealized two-dimensional squall line simulations using the Weather Research and Forecasting model. The computational cost in total wall clock run time is reduced by 10-15% while producing solutions very similar to the traditional approach. Thus, SFVT can reduce the overall cost of using multi-moment bulk microphysics schemes, making them competitive with simpler schemes having fewer prognostic variables. Extension of the SFVT method to a bin microphysics scheme will also be discussed. For the bin scheme, SFVT produces similar solutions compared to the traditional approach of separately advecting each bin scalar, but with even greater reduction in total model wall clock run time of 15-25%.

[Day 3, 9:40-10:00]

# Examination of the classification of hydrometeor types in a bulk microphysics scheme

Akihiro Hashimoto[1], Ryohei Misumi[2], Narihiro Orikasa[1]

1. Forecast Research Department, Meteorological Research Institute, Japan

2. National Research Institute for Earth Science and Disaster Resilience, Japan

Email: ahashimo@mri-jma.go.jp

## Abstract

Hydrometeors in the atmosphere, in particular, solid hydrometeors, have a large diversity of characteristics such as size, shape and density. In contrast, bulk microphysics schemes which are implemented in nonhydrostatic models usually have only several classes to represent the characteristics of the hydrometeors. In order to find implications for the optimal classification of solid hydrometeors in a bulk microphysics scheme, we conducted adiabatic parcel lifting simulations, using a multi-dimensional microphysics model (Misumi et al., 2010). Initial temperature and humidity were 8 $^{o}$C and 95 %, respectively. We gave 4 m s$^{-1}$ or 1 m s$^{-1}$ for the ascending rate of air parcel. The simulation results show a wide variety of size, shape and density of ice particles (Fig. 1). The variation enlarged depending on the ascending rate (Fig. 2). The range of variation was large enough to affect the growth rate and fall velocity of particles,

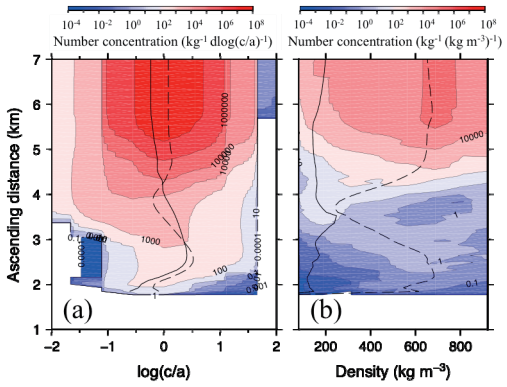


Fig. 1: Vertical profiles of the (a) aspect ratio and (b) density of ice particles, in the case of w = 4 m s$^{-1}$. Broken and solid lines indicate the average and standard deviation, respectively.

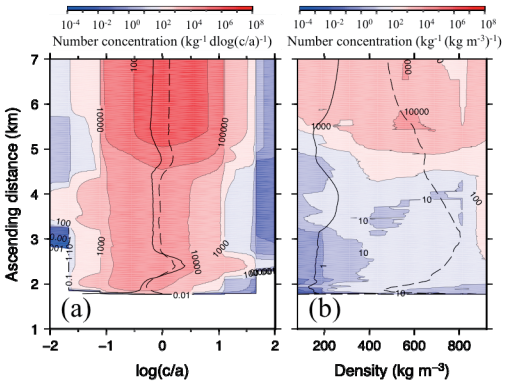


Fig. 2: Same as Fig. 1, but for w = 1 m s$^{-1}$.

which supports that an appropriate classification is necessary for bulk microphysical modeling. We will discuss about an optimal classification of solid hydrometeors for application to a bulk microphysics scheme.

## References

Misumi et al., 2010: Microphysical structure of a developing convective snow cloud simulated by an improved version of the multi-dimensional bin model. *Atmos. Sci. Let.*, **11**, 186-191. doi:10.1002/asl.268

[Day 3, 10:00-10:20]

# Development of a two-moment three-ice bulk microphysical model for ice

Yoshinori Yamada

Meteorological Research Institute, Tsukuba, Ibaraki, 305-0052, Japan

E-mail: yyamada@mri-jma.go.jp

## Abstract

### 1. Introduction

A two-moment three-ice bulk microphysical model for ice is developed, as one of the options of the Japan Meteorological Agency non-hydrostatic model (hereafter, JMA-NHM: Saito et al. 2006), aiming at better representation of snow clouds and the associated snowfalls. This paper briefly describes the outline of the new bulk microphysical model and results of preliminary tests.

### 2. Outline of the new microphysical model

The newly developed bulk microphysical model predicts both the mixing ratios and the number concentrations of cloud ice, snow, and graupel. Main features of the new model are as follows: (a) Size distributions are represented by Gamma function. (b) Mass-size relations are expressed by power laws. (c) Conversion from cloud ice to snow is computed in the following two processes: mass and number fluxes resulting from the depositional growth across a prescribed size of cloud ice (Harrington et al. 1995) and a transfer of cloud ice of larger size to snow. (d) Formation of graupel by riming of cloud ice and snow is modeled by introducing a bin-like idea, in which the graupel formation is determined by the riming rates of cloud ice and snow. Their size distributions are divided into certain number of bins first, then riming rates of particles (cloud ice or snow) in each bin are computed based on the continuous growth model. (e) The aggregation of cloud ice and snow is modeled by a strict solutions using temperature-dependent collection efficiencies.

### 3. Results of a preliminary test

The new bulk microphysical model described in section 2 was tested for snow clouds associated with cold-air outbreaks over Ishikari Bay and Ishikari Plane in Hokkaido, Japan. Figure 1 shows a radar-derived accumulated precipitation corresponding to a heavy snow fall event on Dec. 15, 2014, indicating that this snowfall was brought about a band-like snow clouds. Daily precipitation and the daily accumulated snow fall amount at Sapporo Observatory were 25 mm in water equivalence and 39 cm,

respectively. The performance of the new model was investigated by several experiments at 1-km and 5-km resolutions. Results from the 5-km resolution model are shown here.

Experiments were made by employing JMA-NHM of a domain size of 2000 km x 2000 km centered at the location of Sapporo city. Number of vertical layers was 50, and the top of the model domain was set to 21.8 km. The model run started at the initial time of 18 UTC on Dec. 14 up to 18 hours. The initial and boundary conditions were supplied from the global analysis of JMA. Except for the bulk microphysical models, other model setting was common to all experiments. As shown in Fig.2, the new model represents a band-like precipitation pattern similar to the observation in Fig. 1, relative to the current one. The relative contribution of snow and graupel to the total snowfall will also be discussed.

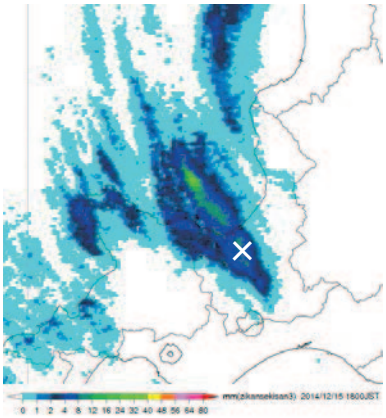

Figure 1 Accumulated precipitation for three hours (shaded area) between 16 and 18 JST from JMA radars. The position of Sapporo is marked by a cross mark. Light blue color indicates precipitation less than 1 mm in water equivalent.

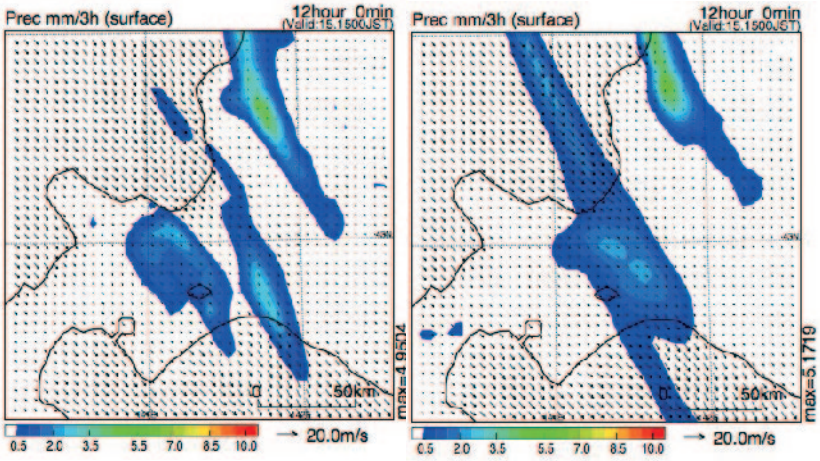


Figure 2 Accumulated precipitation for three hours (shaded area) from the current (left panel) and the new (right panel) models, respectively.

*Acknowledgement*

This work was supported by MEXT KAKENHI Grant Number 26242036.

The program for computing the incomplete Gamma function was developed in the cooperative study on photovoltaic power generation between Meteorological Research Institute and National Institute of Advanced Industrial Science and Technology.

**References:**

Harrington, J. Y., M. P. Meyers, R. L. Walko, and W. R. Cotton, 1995: Parameterization of ice crystal conversion processes due to vapor deposition for mesoscale models using double-moment basis functions. Part I: Basic formulation and parcel model results. J. Atmos. Sci., **52**, 4344-4366.

Saito, K., T. Fujita, Y. Yamada, J. Ishida, Y. Kumagai, K. Aranami, S. Ohmori, R. Nagasawa, S. Kumagai, C. Muroi, T. Kato, H. Eito, and Y. Yamazaki, 2006: The Operational JMA Nonhydrostatic Mesoscale Model. *Mon. Wea. Rev.*, **134**, 1266-1298.

[Day 3, 10:50-11:10]

# Water Droplet Simulation by the Immersed Boundary Method

Ong Chia Rui, Hiroaki Miura
University of Tokyo, Japan
Email: ong.chiarui@eps.s.u-tokyo.ac.jp

## Abstract

The multiphase flow simulation has been a subject of intensive research in the Computational Fluid Dynamics (CFD) field. It is not only important in engineering field, but also in meteorology because the capability of multiphase flow simulation may help us understand more about the motion of ice particles, raindrops, and surface ocean wave, so that their impacts on large scale fluid motions can be analyzed systematically. However, the treatment of complex moving boundary is an extremely time consuming, formidable task in a traditional boundary conforming fluid solver. A number of workarounds have been proposed such as the volume-of-fluid method (VOF), the level set method (LS), and the immersed boundary method (IBM). These methods provide a relatively efficient way to simulate multiphase flow on fixed rectangular grids, without a necessity to regenerate a complex mesh system that conforms to the interface at every time step. So far many multiphase flow simulations using these so-called "mixed Eulerian-Lagrangian methods" have been carried out and demonstrated to agree with the experimental results to some extent. However, most of the simulations are confined to lab-scale fluid flow with moderate-to-low density ratio. It is still very difficult to perform long time scale multiphase flow simulations of high density ratio such as water-air interaction. Therefore, a successful simulation of a free-fall water droplet in the air until it reaches its terminal velocity is an important cornerstone for successful large scale, high density-ratio multiphase flow simulations and future applications in the atmospheric science.

In this work, a multigrid finite volume Direct Numerical Simulation (DNS) solver implemented with the IBM was developed to tackle the problem of water droplet simulations. In the IBM, the interfacial jump conditions are replaced by adding a forcing term into the Navier-Stokes equations that spreads across a few grid cells by the

discretized delta function. The interface is tracked by a series of connected Lagrangian markers. However, we found that the pointwise behavior of the discretized delta function on Cartesian grid causes the unphysical parasitic currents tangential to the interface. These spurious currents are a consequence of the discretization error of delta function. In particular, a discretized delta function must satisfy the non-solenoidal condition to eliminate the parasitic currents. A new method is proposed in which the parasitic currents are completely removed. It is verified through some standard test cases. Due to instability, success has been limited to simulations for free-fall water droplets with diameter smaller than 1.0 mm in 2D and 0.1mm in axis-symmetric flow. Simulations of oscillating and free-fall droplet with small density ratio have been carried out as well. Besides some progresses have been achieved in this work, there remains problems that need to be addressed in the future such as improving its stability. Coalescence and phase transfer are other needs to be incorporated into the IBM in the future for widening its application in the atmospheric science.

[Day 3, 11:10-11:30]

# Development of a bulk parameterization scheme of warm rain using bin scheme model results

Kozo Nakamura[1], Yasushi Fujiyoshi, Kazuhisa Tsuboki[1,2], and Naomi Kuba[3]

1. Japan Agency for Marine-Earth Science and Technology, Japan

2. Institute for Space-Earth Environmental Research, Nagoya University, Japan

3. Atmosphere and Ocean Research Institute, the University of Tokyo, Japan

Email: nakamura@jamstec.go.jp

## Abstract

Boundary layer clouds have a large effect on global radiation budget, and the improvement of their modeling is important for climate study. We have developed a bin microphysical model for warm rain, which was applied to 'Rain In Cumulus over the Ocean' (RICO) measurement campaign, and the results are used for developing a new bulk scheme model which can be used in large-scale cloud resolving models.

The model we are using is CReSS (Cloud Resolving Storm Simulator). The details of the model can be found in Tsuboki and Sakakibara (2002, 2007). We incorporate a two-moment bin microphysical scheme for warm rain, in which 71 bins for radii between 0.001mm and 3.25 mm are used. The condensation and coalescence are calculated in the semi-Lagrangian framework by using the two-moment bin method developed by Chen and Lamb (1994). The initial cloud droplet size distribution is determined by the parameterization scheme proposed by Kuba and Fujiyoshi (2006) in terms of CCN (cloud condensation nuclei) number concentration and vertical velocity.
The model setting is the same as the one for the GCSS intercomparison experiment (http://www.knmi.nl/samenw/rico/). A 24 hour run was performed and our bin model works generally well. However, there are few problems in the results. In the original version of the model, in which there is no activation in clouds, the average value of the cloud number concentration in clouds decreases too rapidly with height. Therefore, in the new version, we modified to allow the activation of CCN in clouds if the moistening effect due to upward motion is larger than the drying effect due to condensational growth of the existing cloud droplets. The number concentration of activated CCN is

determined in terms of the difference between the moistening and drying effects. The results indicate that the cloud number density in the upper cloud layer is not so small as in the old version's results. So we are using the results for developing a bulk model formulation.

For the first step, we consider a two groups and two moments bulk scheme. The condensed water are classified into two groups, i.e., cloud and rain, by its radius, and their mixing ratios and number concentrations are used as prognostic variables. All microphysical processes and physical variables at every grid point are stored. Then at first, a log-linear fitting for each process as a function of physical variables are tested and we determine the combination which gives the largest correlation coefficient for each process. As an example, if we consider the process called autoconversion, i.e., producing rain by the collision between cloud droplets, the combination of number concentration of cloud droplets ($n_c$) and mixing ratio of cloud water ($q_c$) gives the best result. The figure shows the relation between these variables, although only vary small number of data are plotted. However, if we use the best result of fitting in the log scale in the autoconversion rate, the RICO simulation gives very small rainfall rate, because it is affected by the large number of small autoconversion rate results. If we use the fitting results which gives the smallest root mean square error in the linear scale, it gives much better results in the RICO simulation.

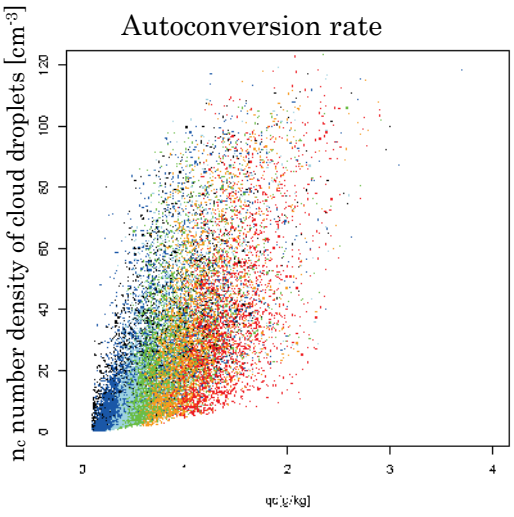


Figure. Scatter diagram of autoconversion rate in terms of $q_c$ and $n_c$. The colors indicate the autoconversion rate, $1x10^{-9}$< black<$1x10^{-8}$ < blue < $1x10^{-7}$ < light blue< $2x10^{-7}$ < green < $4x10^{-7}$ < orange < $8x10^{-7}$ < red [g/kg/s].

**References:**


Chen, J. -P. and Lamb, D., 1994: Simulation of cloud microphysics and chemical processes using a multicomponent framework. Part I Description of the microphysical model, *J. Atmos. Sci.*, **51**, 2613--2630.

Kuba, N., and Y. Fujiyoshi, 2006: Development of a cloud microphysical model and parameterizations to describe the effect of CCN on warm cloud. *Atmos. Chem. Phys.*, **6**, 2793–2810.

Tsuboki, K., and A. Sakakibara, 2002: Large-scale parallel computing of cloud resolving

storm simulator. High Performance Computing, H. P. Zima et al., Eds., Springer, 243–259.

[Day 3, 11:30-11:50]

# Towards low cloud permitting superparameterization

Mike Pritchard[1], Hossein Parishani[1], Chris Bretherton[2], Marat Khairoutdinov[3]

1. Department of Earth System Sciences, University of California, Irvine, CA, USA

2. Department of Atmospheric Sciences, University of Washington, Seattle, WA, USA

3. School of Marine and Atmospheric Sciences, Stony Brook University, Stony Brook, NY, USA

Email: mspritch@uci.edu

## Abstract

Systematic biases in the representation of boundary layer clouds are a leading source of uncertainty in modern climate projections. A variation on superparameterization (SP) called ``ultraparameterization'' (UP) is developed, in which the grid spacing of the cloud-resolving models (CRMs) is fine enough (250 m by 20 m) to explicitly capture the outer scales of boundary layer turbulence, associated clouds and entrainment in a global climate model capable of multi-year simulations. UP is implemented within the Community Atmosphere Model using 2 degree resolution (~14,000 embedded CRMs) and exhibits excellent parallel scalability. Despite being 200 times more expensive than SP, UP is computationally feasible today and promising for exascale computers.

Short duration global UP hindcasts are compared with SP and matched satellite observations of top-of-atmosphere radiation and cloud vertical structure. The most encouraging improvement is a deeper boundary layer and more realistic vertical structure of subtropical stratocumulus (Sc) and shallow cumulus (Cu) clouds, due to much stronger vertical eddy motions that promote more entrainment.

Ongoing issues in this UP implementation include excess ITCZ liquid water path, overly bright midlatitude low clouds due to efficient aerosol nucleation in strong updrafts and hence high cloud droplet concentrations, and 'burstiness' of turbulence and cloud within individual cloud-resolving models. Nevertheless, UP makes global eddy-permitting simulation a feasible alternative to conventionally parameterized GCMs for studying

boundary-layer cloud-climate and cloud-aerosol feedback.

**References:**

Parishani, H., M. Pritchard, C. Bretherton and M. Khairoutdinov. Towards low cloud permitting superparameterization, submitted October 2016 to *Journal of Advances in Modeling Earth Systems*.

[Day 3, 11:50-12:10]

# Current-generation Global Climate Models inevitably underestimate pollutant transports to the Arctic.

Yousuke Sato[1], Hiroaki Miura[2], Hisashi Yashiro[1], Daisuke Goto[3], Toshihiko Takemura[4], Hirofumi Tomita[1], and Teruyuki Nakajima[5]

1. RIKEN Advanced Institute for Computational Science, Japan

2. Department of Earth and Planetary Science, The University of Tokyo, Japan

3. National Institute of Environmental Studies, Japan

4. Research Institute for Applied Mechanics, Kyushu University, Japan

5. Earth Observation Research Center, Japan Aerospace Exploration Agency, Japan

Email: yousuke.sato@riken.jp

## Abstract

Black carbon aerosol (BCA) in the Arctic has attracted substantial attention from climate scientists due to its unique and profound impacts on the global climate system. BCA is mainly emitted from the burning of fossil fuels, biomass, and agricultural waste. It not only interacts with sunlight through absorption and scattering in the air but also changes the reflectance of snow-covered surfaces (Bond et al., 2013). Recent studies have demonstrated that BCA in the Arctic is transported mainly from mid-latitudes (Stohl, 2006; Koch and Hansen, 2005; Shindell et al., 2008). General circulation models (GCMs) are powerful tools for estimating the impacts of BCA on climate, but they tend to underestimate the levels of BCA in the Arctic region (Koch et al., 2009). Previous studies have attempted to address this underestimation by improving the accuracy of the removal and/or aging process of BCA (Liu et al., 2011). Although these attempts have been partially successful, resolving the fine structure of mid-latitude low-pressure systems, including warm and cold frontal systems, could lead to significant further improvements. Low-pressure systems represent one of the main mechanisms for the transport of BCA to the Arctic (Stohl, 2006), but have not yet been studied rigorously because the grid resolution of GCMs (Eckhardt et al., 2015) is too coarse to resolve them. Here, we conducted a global aerosol transport simulation with a horizontal grid resolution of 3.5 km, which is sufficiently fine to resolve low-pressure systems. The higher resolution significantly enhanced the representation of low-pressure systems, and reduced the underestimation of BCA levels in the Arctic. The BCA mass concentration in the Arctic simulated with the 3.5-km grid resolution was 4.2-fold larger than that simulated with a coarse (56-km) grid resolution (as shown in Figure 1). Our results suggest that global simulations using kilometre-order horizontal resolution can

lead to more accurate estimations of the distribution of pollutants in the Arctic and reduce uncertainties regarding the effects of aerosols on global climate.

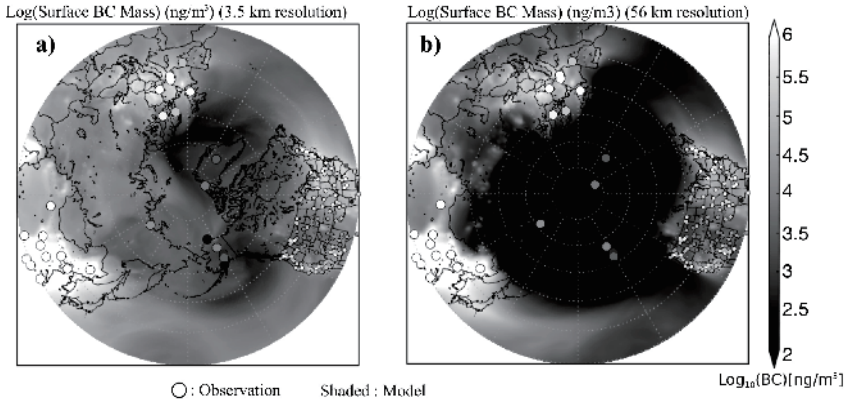


Figure 1: (Shaded) Mass concentration of BCA averaged over the last 10 days of simulation and (circle) those observed surface observation site averaged during November 2011. Cited from (Sato et al., 2016) and rearranged.

## References:


Bond, T. C. et al., Bounding the role of black carbon in the climate system: A scientific assessment, *J. Geophys. Res.*, 2013,**118**, 5380–5552, doi:10.1002/jgrd.50171.

Eckhardt, S. et al., Current model capabilities for simulating black carbon and sulfate concentrations in the Arctic atmosphere: a multi-model evaluation using a comprehensive measurement data set, *Atmos. Chem. Phys.*, 2015, **15**, 9413–9433

Koch, D., and J. Hansen, Distant origins of Arctic black carbon: A Goddard Institute for Space Studies Model Eexperiment, *J. Geophys. Res.*, 2005, **110**, 1–14, doi:10.1029/2004JD005296.

Koch, D. et al., Evaluation of black carbon estimations in global aerosol models, *Atmos. Chem. Phys.*, 2009, **9**, 9001–9026, doi:10.5194/acp-9-9001-2009.

Liu, J., S. Fan, L. W. Horowitz, and H. Levy (2011), Evaluation of factors controlling long-range transport of black carbon to the Arctic, *J. Geophys. Res.*, 2011, **116**, doi:10.1029/2010JD015145.

Sato, Y., H. Miura, H. Yashiro, D. Goto, T. Takemura, H. Tomita, and T. Nakajima, Unrealistically pristine air in the Arctic produced by current global scale models, 2016, *Sci. Rep.*, **6**, 26561, doi:10.1038/srep26561.

Shindell, D. T. et al., A multi-model assessment of pollution transport to the Arctic, *Atmos. Chem. Phys.*, 2008, **8**, 5353–5372, doi:10.5194/acp-8-5353-2008.

Stohl, A., Characteristics of atmospheric transport into the Arctic troposphere, *J. Geophys. Res.*, 2006, **111**, D11306, doi:10.1029/2005JD006888.

[Day 3, 13:40-14:00]

# Effect of topographical resolution on cirrus clouds using a high-resolution GCM

Tatsuya Seiki, Chihiro Kodama, Masaki Satoh, Tempei Hashino, Yuichiro Hagihara, Hajime Okamoto

1. Japan Agency for Marine-Earth Science and Technology, Japan

2. Atmosphere and Ocean Research Institute, the University of Tokyo, Japan

3. Research Institute for Applied Mechanics, Kyushu University

4. The Earth Observation Research Center, Japan Aerospace Exploration Agency

Email: tseiki@jamstec.go.jp

## Abstract

This study investigated the sensitivity of cirrus clouds induced by orographic gravity waves to the smoothness of topography and the horizontal resolution ($\Delta x$ = 28, 14, and 7 km) of a global non-hydrostatic model. To examine the effects of strength of the orographic gravity waves on cirrus clouds, we analyzed the amplitude of the vertical velocity and the nucleated ice number concentration. We found that a numerical diffusion filter used to smooth topography strongly weakened the orographic gravity waves and induced less orographic cirrus clouds. Column integrated number concentration of the sum of cloud ice and snow over mountainous regions significantly increased by turning off the numerical filter for topography as well as by an increase in the horizontal resolution. The change in global averaged value of outgoing longwave radiative flux due to the topographical effect was significant at a horizontal resolution of 28 km. The vertical profiles of the number concentration of the sum of cloud ice and snow were evaluated by comparing them to CALIPSO and CloudSat satellite observations. The ice number concentration was found to be underestimated over all the experiments, but the bias was partly reduced by a higher horizontal resolution without the numerical filter for topography. Furthermore, we found that the effect of topography on orographic cirrus clouds became more localized as the horizontal resolution increased, so that the global average value of the ice number concentration did not significantly change at a horizontal resolution of 14 km or less.

[Day 3, 14:00-14:20]

# Numerical Simulation of a Local Valley Wind "Hijikawa-Arashi"

Junshi Ito[1], Masaru Kurosaka[2], Toshiyuki Nagoshi [2]

1. Meteorological Research Institute, Japan

2. Iwate University, Japan

Email: junshi@aori.u-tokyo.ac.jp

## Abstract

A local valley wind, "Hijikawa-Arashi", is occasionally observed at the estuary of Hjijikwa River (Ozu-city, Ehime, Japan) in the morning of the autumn and early winter. A cold air is accumulated in the Ozu basin, which locates upstream of the Hijikawa River, during a night in a fine weather due to the radiative cooling. The cold air-mass flows out through a very narrow valley whose minimum width is several hundred meters near the estuary. The wind is significantly accelerated just behind the narrowest part of the valley. The surface wind speed at the estuary reaches about 10 m/s (Ohashi et al. 2015). A very remarkable feature of Hijikawa-Arashi is that the valley wind is visualized by fog formed in the Ozu basin (Figure 1).

This study conducts fine resolution numerical simulations of Hijikawa-Arashi. We employ a regional weather prediction model, Japan Meteorological Agency's Non-Hydrostatic Model (JMANHM) (Saito et al. 2006), which includes realistic topography, cloud physics, and so on to reproduce several real cases of Hjijikawa-Arashi. The Meso-Analysis provided by JMA (MANL) is used for initial and boundary conditions.

Setting the horizontal resolution to be 400 m, the numerical grid is managed to resolve the steep valley and basin. If the vertical resolution at the bottom grid is 40 m, moderately strong winds (~10 m/s) occur near the estuary, but the fog in the basin do not form. If the vertical resolution is improved to be 10 m, the radiation fog in the night does appear owing to about 5 K difference in the surface temperature. As a result, stronger surface winds are found near the estuary.

We increase also increase horizontal resolution up to 80 m. With the finer horizontal resolution, the model can reproduce the realistic Hjijikawa-Arashi: the strong winds near the estuary accompany the fog (Figure 2).

A vertical cross-section along with Hijikawa River exhibits characteristics of the

hydraulic jump just behind the narrowest part of the valley. We will also compare with available aerial videos and surface observation data of wind speeds and temperature at the estuary.

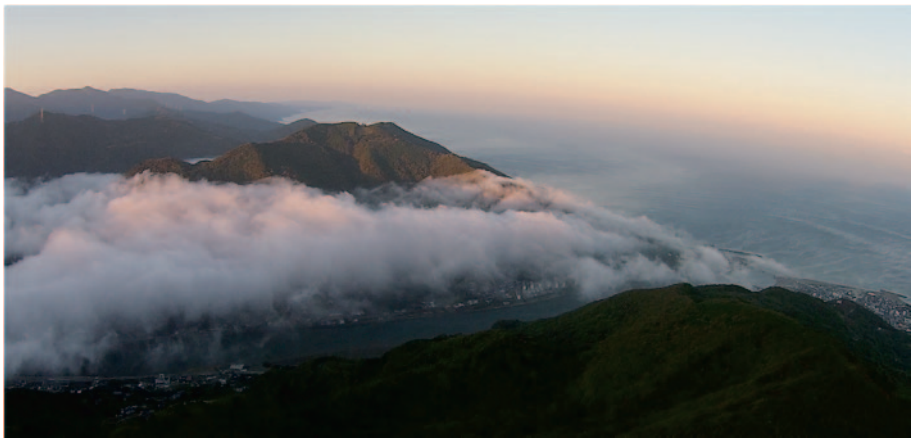

Figure 1Photograph of Hijikawa-Arashi at the estuary of Hijikwa River on 4 Nov. 2015.

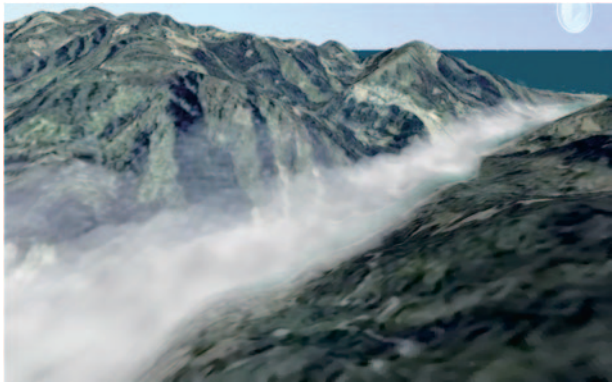

Figure 2 Simulated cloud water of Hijikawa-Arashi

**Acknowledgement**

This work is partly supported by Field 3, Strategic Programs for Innovative Research, Ministry of Education, Culture, Sports, Science and Technology of the Japanese government.

**References:**

Ohashi, Y., Terao, T., Shigeta, Y., & Ohsawa, T. (2015). In situ observational research of the gap wind "Hijikawa-Arashi" in Japan. Meteorol. Atmos. Phys., **127**, 33-48.

Saito, K., Fujita, T., Yamada, Y., Ishida, J. I., Kumagai, Y., Aranami, K., & et al. (2006). The operational JMA nonhydrostatic mesoscale model. Mon. Wea. Rev., **134**, 1266-1298.

[Day 3, 14:20-14:40]

# High cloud size dependency in the applicability of the fixed anvil temperature hypothesis using global nonhydrostatic simulations

*Akira T. Noda[1], Tatsuya Seiki[1], Masaki Satoh[1,2], and Yohei Yamada[1]

[1]Japan Agency for Marine-Earth Science and Technology, Japan

[2]Atmosphere and Ocean Research institute, The University of Tokyo, Japan

(Akira T. Noda, a_noda@jamstec.go.jp)

## 1. Introduction

Hartmann and Larson (2002) proposed a constraint of a high-cloud response to global warming, termed the fixed-anvil-temperature (FAT) hypothesis. The hypothesis states that cloud-top temperature, $T_{CT}$, remains nearly constant despite the increase in surface temperature due to global warming. Zelinka and Hartmann (2010) developed the idea and suggested that the FAT condition causes positive longwave cloud feedback by inhibiting efficient thermal emissions from the earth. In the FAT hypothesis, the anvil top height corresponds to the altitude where the radiative cooling in cloud-free regions rapidly decreases due to low saturated vapor pressure, which is determined only by temperature. The validity of the FAT hypothesis depends on the magnitude of the changes of cloud-top temperature. However, it has not been well recognized the extent to which changes can be regarded as small or large enough. Based on 7-km mesh NICAM data, we investigate the relative components of the changes of outgoing-longwave radiation (OLR) at the top of the atmosphere (TOA) by decomposing the contributions into $T_{CT}$, cloud optical thickness (or cloud emissivity, $\varepsilon$), and clear-sky OLR, $F^{CLR}$, and clarify their dependency on cloud size. For more detailed results, readers are asked to refer to Noda et al. (2016).

## 2. Formulation

To evaluate what factors contribute to the net OLR change, we derive a diagnostic equation of OLR at the TOA, $F$ (W m$^{-2}$), in terms of $T_{CT}$ (K), $\varepsilon$, and $F^{CLR}$ (W m$^{-2}$). We begin with an approximation of OLR as

$$\begin{aligned} F &\cong \sigma\varepsilon T_{CT}^{4} + F_{CB} \\ &\cong \sigma\varepsilon T_{CT}^{4} + (1-\varepsilon)F^{CLR}, \end{aligned}$$

where $F_{CB}$ (W m$^{-2}$) is the upwelling longwave radiation from the bottom level of a high cloud, and $\sigma\left(=5.67\times10^{-8}\ \mathrm{W\,m^{-2}\,K^{-4}}\right)$ is the Stefan-Boltzmann constant. The response of OLR to global warming, $\Delta$, can be approximated as

$$\begin{aligned} \Delta\overline{F}^{(i)} &\cong \left(\frac{\partial F}{\partial \varepsilon}\right)_{T_{CT},F^{CLR}} \Delta\overline{\varepsilon}^{(i)} + \left(\frac{\partial F}{\partial T_{CT}}\right)_{\varepsilon,F^{CLR}} \Delta\overline{T_{CT}}^{(i)} + \left(\frac{\partial F}{\partial F^{CLR}}\right)_{\varepsilon,T_{CT}} \Delta\overline{F^{CLR}}^{(i)} \\ &= F_{\varepsilon}\Delta\overline{\varepsilon}^{(i)} + F_{T}\Delta\overline{T_{CT}}^{(i)} + F_{F}\Delta F^{CLR(i)}, \end{aligned}$$

where

$$F_{\varepsilon} = \sigma\left(\overline{T_{CT}}^{(i)}\right)^{4} - \overline{F^{CLR}}^{(i)}, \quad F_{T} = 4\varepsilon^{(i)}\sigma\left(\overline{T_{CT}}^{(i)}\right)^{3}, \quad F_{F} = 1-\varepsilon^{(i)}.$$

An overbar with a prefix, $i$, denotes an average over $i$-th cloud area (Noda et al. 2014). Those values are hereafter shown with being binned at cloud radius. Using the above formula, one can evaluate the contributions of $\varepsilon$, $T_{CT}$, and $F^{CLR}$ to changes of $F$.

## 3. Results

Figure 1 shows contributions of changes of $T_{CT}$, $\varepsilon$, and $F^{CLR}$. From CTL to GW (Fig. 1a), OLR changes

positively by 1.0−3.5 W m$^{-2}$ for the clouds with $r$>50 km for the actual $\Delta F$. The contribution of the three terms to the net OLR change clearly varies depending on the radius. The change of cloud emissivity is largest at approximately $r$=90 km, and then decreases with increasing radius. In contrast, the effect of the changes of $T_{CT}$ becomes stronger with increasing radius. In particular, for $r$>340 km, the contribution magnitude becomes comparable to that of cloud emissivity (blue and green lines, respectively). In contrast to the above two terms, the $F^{CLR}$ contribution is very small: the term is negative at every radius, and its amplitude increases slightly with increasing cloud radius by $r$=700 km. Considering the net contributions (Fig. 1b), the changes in ε strongly contribute to the net OLR change by $r$=1800 km due to changes of smaller clouds. In contrast, the contribution of $T_{CT}$ increases gradually, nearly constantly with radius, eventually slightly exceeding that of $\varepsilon$. On this point, there is some uncertainty in the present analysis of' the detailed effects of cloud forcing, and this will need to be improved. Nonetheless, it is likely that the effects of changes in ε and $T_{CT}$ are nearly comparable with each other, and the changes in $F^{CLR}$ have a much weaker effect.

## 4. Conclusion

We have argued for the importance of the FAT hypothesis based on the high-resolution GCM data, in which cumulus parameterization was not used, particularly focusing on the dependency on high cloud size. The present study suggests that the extent to which the FAT hypothesis holds true can depend on cloud size. That is, for smaller cloud sizes (e.g., less than approximately 340 km in the present case), the contribution of $T_{CT}$ is of secondary importance, and the contribution of cloud emissivity is more important. In contrast, for clouds larger than 340 km, the contribution of cloud emissivity is comparable to that of $T_{CT}$, and thus, both of the two components become equally important. The role of $F^{CLR}$ is smaller than those of the two previous factors over the low latitudes. The changes of $F^{CLR}$ depend weakly on cloud radius. In addition, we also showed dependency of the responses of precipitable water, $\tau$, $\varepsilon$, $F_{CLR}$, and $T_{CT}$ to global warming on cloud radius.

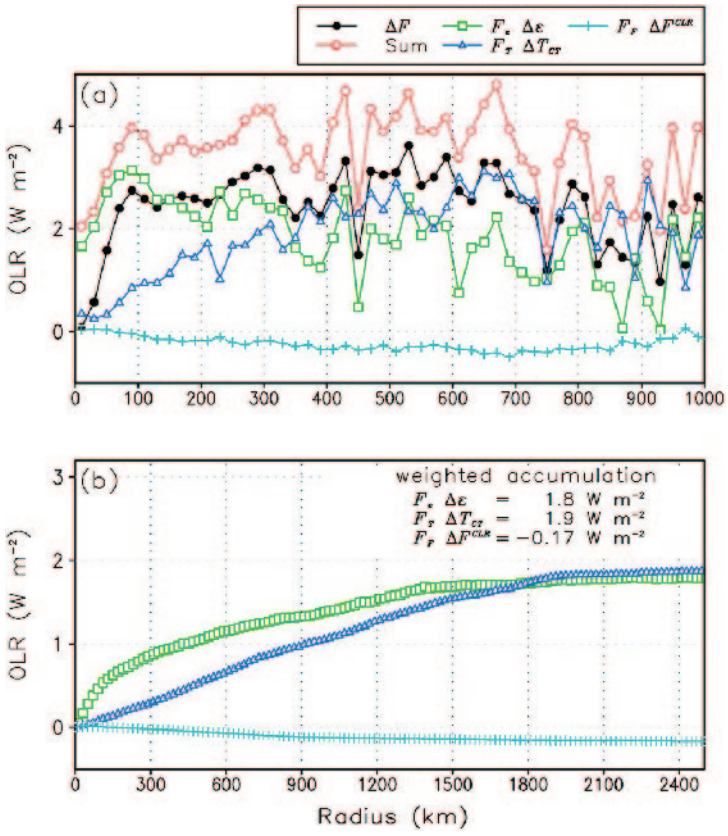


Figure 1. Budget analysis of OLR changes due to global warming binned by cloud size (20 km bins), showing (a) mean values for each cloud size and (b) their area-ratio-and-frequency-of-occurrence-weighted accumulation in the $x$ (radius) direction

## References


Hartmann, D. and K. Larson, 2002, GRL.

Noda, A. T., M. Satoh, Y. Yamada, C. Kodama, and T. Seiki, 2014, JCLI.

Noda, A. T., T. Seiki, M. Satoh, and Y. Yamada, 2016, GRL.

Zelinka, M., and D. Hartmann, 2010, JCLI.

[Day 3, 14:40-15:00]

# Large-eddy simulation of a diurnal cycle of atmospheric turbulent boundary layer flows over an urban area by coupling with a meso-scale meteorological simulation model

Hiromasa Nakayama[1], Tetsuya Takemi[2]

1. Japan Atomic Energy Agency, Ibaraki, Japan

2. Disaster Prevention Research Institute, Kyoto University, Kyoto, Japan

Email: nakayama.hiromasa@jaea.go.jp

## Abstract

The variability of atmospheric flow is induced by meteorological disturbances, terrains, and surface roughness elements. For understanding the wind system over urban areas, a numerical modeling is a useful tool. To simulate atmospheric flows in real meteorological settings, numerical weather prediction (NWP) models are commonly used. Although the accuracy of NWP models for daily weather is continuously improving, it is difficult to reproduce small-scale wind fluctuations due to the effects of urban buildings that are not explicitly represented in NWP models. For simulating turbulent winds within and over urban areas, a computational fluid dynamics (CFD) technique based on large-eddy simulation (LES) is effective. Therefore, an approach to couple the LES-based CFD model and the NWP model should be promising to simulate turbulent winds over urban areas under real meteorological conditions. In order to represent turbulent winds under real meteorological conditions by the LES model, the NWP outputs can be used as the initial and boundary conditions of the model. Here, a serious issue is encountered when imposing time-dependent turbulent inflow data for LESs from the NWP outputs, because the NWP models are not able to reproduce high-frequency turbulent fluctuations to appropriately drive LES models.

Therefore, in this study, the recycling technique using the NWP data (Nakayama et al., 2012) was used to generate turbulent inflows for LES models. In evaluating the computational approach to couple the LES and NWP models, the Joint Urban 2003 field experimental data were used. These experiments were conducted in the central district of Oklahoma City from June 28 through July 31, 2003 in the United States of America. The model used for a mesoscale meteorological simulation was the Weather Research

and Forecasting (WRF) model, the Advanced Research WRF Version 3.3.1 (Skamarock et al. 2008). We used a nesting capability to resolve the Oklahoma City region by setting two-way nested, three computational domains. The CFD model used here is based on an LES model (Nakayama et al., 2015). In the LES model, wind velocity and potential temperature data obtained by the WRF model were imposed at lateral boundaries. The surface heat fluxes were calculated using the surface potential temperature obtained by the WRF model. The inlet, spanwise, and bottom boundaries were determined by the WRF outputs with 500 m resolution linearly interpolated on the grids of the outer domain with 1-minute interval.

The LES data of wind speeds, wind directions, and potential temperature fluctuated around the WRF data from the morning to the evening. This indicates that the turbulent fluctuations by the recycling technique were successfully generated and the structure of mean flow in the meteorological field is maintained in the LES model. Compared to the observed data, the LES model is found to generally show the vertical profiles of wind speed, wind directions, and potential temperature similar to them at each measuring time, which implies that it reproduces a diurnal evolution of atmospheric boundary layers well. However, the LES model does not represent local changes in wind speeds and wind directions of the experimental data especially at the lower part of the boundary layer during some period of time. This is due to the prediction errors of the WRF data used to prescribe the LES inflow boundary. The WRF model cannot explicitly represent turbulent effects induced by urban surface geometries. Since the prediction accuracy of the LES model is highly sensitive to the inflow boundary, urban surface aerodynamic effects should be appropriately incorporated into the WRF model to accurately reproduce wind velocities at a ground level.

**References:**

Skamarock, W, C., Klemp, J, B., Dudhia, J., Gill, D, O., Barker, D, M., Duda, M, G., Huang, X., Wang, W., Powers, J, G.: A description of the Advanced Research WRF Version 3, *NCAR Tech. Note*, NCAR/TN-475+STR, 1 pp, 2008.

Nakayama H, Takemi T, Nagai H. Large-eddy simulation of urban boundary-layer flows by generating turbulent inflows from mesoscale meteorological simulations, Atmos. Sci. Lett. 2012; 13: 180–186.

Nakayama H, Takemi T, Nagai H. Development of local-scale high-resolution atmospheric dispersion model using large-eddy simulation part5: Detailed simulation of turbulent flows and plume dispersion in an actual urban area under real meteorological conditions, J. Nucl. Sci. Technol. 2016; 53: 887-908.

[Day 3, 15:00-15:20]

# Framework for Improvement by Vertical Enhancement: A Simple Approach to Improve Low and High Level Clouds in Large Scale Models

Takanobu Yamaguchi[1,2], Graham Feingold[2], Vincent E. Larson[3]

1. Cooperative Institute for Research in Environmental Sciences, University of Colorado, USA

2. NOAA Earth System Research Laboratory, USA

3. Department of Mathematical Sciences, University of Wisconsin-Milwaukee, USA

Email: tak.yamaguchi@noaa.gov

## Abstract

Low and high clouds of shallow extent are poorly represented in large-scale models such as global climate models and weather forecasting models. This is true for stratocumulus clouds and even more so for high-level cirrus clouds that reside at an altitude where vertical resolution is particularly coarse. This adversely affects, amongst others, estimation of cloud feedbacks for climate prediction and weather forecasts. Here we address vertical resolution as a reason for the failure of these models to adequately represent shallow clouds. We introduce a new methodology, the Framework for Improvement by Vertical Enhancement (FIVE). FIVE embeds a one-dimensional model, which comprises the same physical parameterizations of turbulence, convection, microphysics, and vertical advection solved in the coarse-grid host model, but implemented on a locally high vertical resolution grid. By exchanging tendencies with one another, the host and cloud models are always synchronized. The methodology is demonstrated for drizzling stratocumulus capped by a sharp inversion. First, FIVE is applied to a single column model to examine the extent to which specific physical processes, alone or in combination, require calculation at high vertical resolution for good representation of clouds. Second, a two-dimensional regional model coupled with FIVE produces results comparable to those performed with high vertical resolution. FIVE is thus expected to represent low clouds more realistically and hence reduce the low cloud bias in large-scale models. Finally we propose a number of methods that will be developed and tested to further optimize FIVE.

[Poster, P1]

# Decomposition of the large-scale atmospheric state driving downscaling

Seiya Nishizawa[1], Sachiho A. Adachi[1], Yoshiyuki Kajikawa[1,2], Tsuyoshi Yamaura[1], Kazuto Ando[1], Ryuji Yoshida[1,2], Hisashi Yashiro[1], Hirofumi Tomita[1]

1. RIKEN Advanced Institute for Computational Science, Kobe, Japan
2. Research Center for Urban Safety and Security, Kobe University, Kobe, Japan

Email: s-nishizawa@riken.jp

## Abstract

We propose a new concept for dynamical downscaling (DS) to achieve precise estimation and better understanding of regional climate change. This concept is based on the consideration of large-scale atmospheric states driving downscaling in the phase space.

The large scale state $\phi$ is decomposed into the climatology $\langle\phi\rangle$ and the deviation from it $\phi'$ (referred to as a perturbation). The climatology is further decomposed into reference climatology $\langle\phi_0\rangle$ and climate difference $\{\phi,\phi_0\}$: $\phi = \langle\phi_0\rangle + \{\phi,\phi_0\} + \phi'$, where climate difference is expressed as $\{\phi,\phi_0\} = \langle\phi\rangle - \langle\phi_0\rangle$. The large-scale states for DS are obtained through reconstruction of the independent decomposed components of climatology and perturbation, e.g., $\langle\phi_0\rangle + \{\phi_A,\phi_0\} + \phi'_B$, from two different state $\phi_A$ and $\phi_B$. The concept provides a wider possibility of obtaining large-scale states in comparison to the limited states generated by general circulation models (GCMs). This limitation of the GCMs arises from the fact that these models cannot perfectly represent the relationship between climatology and perturbation in nature.

The concept also lays the foundation for estimating the individual influences of changes in these two components on the regional climate. Through a comparison of the downscaled states driven by the large-scale states, which differ only by one component from one another, the influence of the individual components can be estimated. A comprehensive evaluation of the results obtained by different DS methods in previous studies helps us understand the contribution of various components to the total regional climate change in the future.

The importance of the individual influences is demonstrated by a downscaling experiment based on the concept. We examine the influences of these components on the regional precipitation through a comparison of the three DS simulations and a simultaneous consideration of the influences: the present climate direct DS, the future climate direct DS, and the assumed true climate pseudo global warming DS (Yoshikane et al. 2012). The result shows that the summer-time climatology of the daily precipitation becomes smaller due to the climate difference, while it becomes larger due to the perturbation change. This suggests that interpretations made by considering only the net change or the change in one component face the risk of misunderstanding the future regional climate. A simultaneous estimation considering the net and individual components is thus necessary. This result demonstrates the usefulness of the decomposition concept we propose in this study.

**References:**

Yoshikane, T., F. Kimura, H. Kawase, and T. Nozawa: Verification of the performance of the pseudo-global-warming method for future climate changes during June in East Asia, *SOLA* 2012, **8**, 133–136, doi:10.2151/sola.2012-033

[Poster, P2]

# How does utilization of high-resolution SST give impact to regional climate simulation?

Sachiho A. Adachi[1,2], Fujio Kimura[3], Hiroshi G. Takahashi[2,4]
Masayuki Hara[5], Xieyao Ma[2,6], Hirofumi Tomita[1,2]

1. RIKEN Advanced Institute for Computational Science, Japan
2. Japan Agency for Marine-Earth Science and Technology, Japan
3. Center for Computational Sciences, University of Tsukuba, Japan
4. Department of Geography, Tokyo Metropolitan University, Japan
5. Center for Environmental Science in Saitama, Japan
6. Nanjing University of Information Science & Technology, China

Email: sachiho.adachi@riken.jp

## Abstract

This study investigated the impact of the use of high resolution sea surface temperature (SST) data on estimation of surface air temperature (SAT) in the Nagoya metropolitan area using a regional climate model. Two SST data with different spatial resolution were prepared from the real-time global SST data. The high-resolution SST had little impact on the daily mean and diurnal variation of SAT, although a slight improvement was detected in coastal areas. We also estimated the impact of the areal mean bias in SST on SAT, by using two SST data with a different areal mean value of SST. The results indicated that the areal mean bias in SST data has the larger impact on the representation of SAT than the use of high resolution SST.

### 1. Introduction

To improve the representation of regional climate by a regional climate model (RCM), we need to consider two issues; the capability of the model and the accuracy of boundary conditions. Even if the model has better physical schemes and is well tuned for its target region, the reproducibility of local climate also depends on the boundary conditions of the model. There are many kinds of boundary conditions, such as land use, topography, and sea surface temperature (SST). In this study, we focus on the SST data. A lot of SST data are available to be used for a boundary condition in a RCM. These SST data have different spatial resolutions and different areal mean values. We investigated the impacts of spatial resolution and areal mean value of SST data on representation of

surface air temperature (SAT) by a RCM in the Nagoya metropolitan area.

## 2. Method

Two kind of sensitivity experiments were preformed using the weather research and forecasting (WRF) model version 3.3.1 for this study. First sensitivity experiment is to estimate the impact of spatial resolution difference of SST. The RTGSST_HR was used as the high-resolution SST, while the coarse data averaged from it, with 1˚spacing, was used as the low-resolution SST. The mean values are the same between these two SST data. Second sensitivity experiment is to estimate the impact of the difference in areal mean value. The RTGSST_HR was used as the control experiment. Another SST data was prepared; we modified RTGSST_HR data using the different mean values of SST. The difference of SST value between RTGSST_HR and the modified one is correspond to that between RTGSST_HR and NCEP reanalysis SST data. The reason why we chose NCEP reanalysis SST as the counterpart is that the differences in its mean values from RTGSST_HR were the largest among five SST data candidate.

## 3. Results

The high-resolution SST had little impact on the daily mean and diurnal variation of SAT, although a slight improvement was detected in coastal areas. On the other hand, the areal mean bias in SST data has the larger impact on the representation of SAT than the use of high resolution SST.

There is a possibility that the bias in the areal mean SST becomes a major cause of the bias in SAT. In the case that the mean SST has the bias by about 0.5-1.5 K in all the calculation domains, the influence on SAT reaches about 0.4˚C over the land. The areas where the mean SST was modified became wider, the affected land area also became wider.

## Acknowledgements:

This study was supported by FOCUS Establishing Supercomputing Center of Excellence and CREST/JST.

## References:

Adachi, S. A., F. Kimura, H. G. Takahashi, M. Hara, X. Ma, H. Tomita, 2016: Impact of high-resolution sea surface temperature and urban data on estimations of surface air temperature in a regional climate. *J. Geophys. Res. Atmos.*, doi:10.1002/2016JD024961.

[Poster, P3]

# An Idealized Numerical Experiment of Japan Sea Polar Airmass Convergence Zone

Shun-ichi Watanabe[1], Hiroshi Niino[1]

1. Atmosphere and Ocean Research Institute, the University of Tokyo, Japan

Email: watanabe-s@aori.u-tokyo.ac.jp

## Abstract

In winter, a convergence zone called Japan Sea Polar Airmass Convergence Zone (JPCZ) often appears over the Japan Sea in association with cold air outbreak from Eurasian continent (Asai 1988). Nagata (1991) showed that the land-sea thermal contrast, the blocking effect of the mountain, and the characteristic SST distribution contribute to the formation of the JPCZ. The JPCZ sometime migrates meridionally and experience intensification and weakening (Ohigashi and Tsuboki 2007). Furthermore, mesoscale cyclones often form in association with the JPCZ (Watanabe and Niino 2014). In this study, we investigate the formation process of the JPCZ by an idealized numerical experiment.

Japan Meteorological Agency Non-hydrostatic Model (JMA-NHM; Saito et al. 2006) is used for the numerical experiments.. The model domain is an f-plane of 3000 km × 2000 km at 40°N with a horizontal resolution of 5 km. The zonal boundary condition is open. The meridional and vertical boundaries are frictionless rigid walls. An idealized topography in which land and ocean occupy western and eastern sides, respectively, is assumed. In the control experiment (CNTL; Fig. 1a), the coastline is indented westward and a mountain of 2000 m height exists near the coastline. A uniform westerly of 10 m $s^{-1}$ is assumed. The vertical profile of the basic potential temperature is shown in Fig. 1c, where the stratification is so strong that the flow cannot go over the mountain. The SST

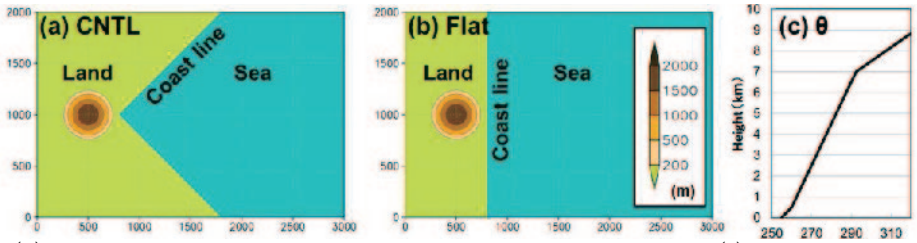


Fig. 1 (a), (b) The topography used in CNTL and FLAT, respectively. (c) The vertical profile of the basic potential temperature.

is 10 °C and the skin temperature of the land is same as the temperature at the lowest level of the model. We perform three sensitivity experiments in which the mountain is removed (NO_MT), the coastline is straight (FLAT; Fig. 1b), or fluxes from the sea surface is switched off (NO_FLUX) to examine the effect of the lower boundary.

In CNTL, a convergence zone appears leeward of the mountain between northwesterly and westerly at the northern and southern sides, respectively (Fig.2a). Moreover, several mesoscale vortices form in the convergence zone and develops as it moves downstream. In association with the formation of the mesoscale vortices, the convergence zone shifts meridionally. These characteristics agree well with the observed JPCZ. A locally warm area, which corresponds to a low pressure area, forms at the lee of the mountain (Fig.2b). Airflows are directed to the low pressure area due to the pressure gradient force, forming the convergence zone.

The convergence zone also appears in NO_MT and FLAT. In these experiments, the locally warm area are also seen, indicating such area is crucial for the formation of the convergence zone. On the other hand, the convergence zone and the warm area do not form in NO_FLAX. The air parcels coming into the warm area travel a longer fetch and obtain more heat and moisture from the sea surface due to the blocking of the mountain and/or the indented coastline, resulting in the formation of the locally warm area. Thus, these topographies contribute to the formation and maintenance of the convergence zone through a feedback process through the sea surface fluxes.

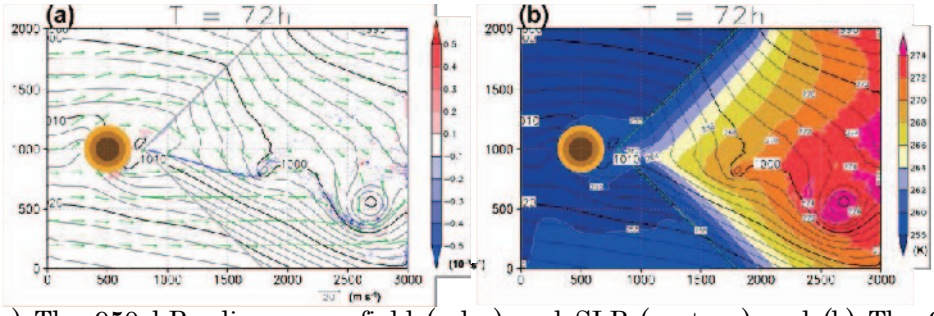


Fig. 2 (a) The 950 hPa divergence field (color) and SLP (contour) and (b) The 950 hPa temperature (color) and SLP (contour) at 72 h for CNTL.

**References:**

Asai, T: Meso-scale features of heavy snowfalls in Japan Sea coastal regions of Japan (in Japanese). *Tenki* 1988, **35**, 156-161.

Ohigashi, T., and K. Tsuboki 2007: Shift and intensification process of the Japan-Sea Polar Airmass Convergence Zone associated with the passage of a mid-tropospheric cold core. *Journal of the Meteorological Society of Japan* 2007, **85**, 633-662.

Saito, K., and Coauthors, 2006: The operational JMA nonhydrostatic mesoscale model. *Monthly Weather Review.* **134**, 1266-1298, doi:10.1175/MWR3120.1.

Watanabe, S. I. and H. Niino, 2014: Genesis and Development Mechanisms of a Polar Mesocyclone over the Japan Sea. *Monthly Weather Review*, **142**, 2248–2270.

[Poster, P4]

# Effects of environment shear on convective systems in a minimal model of QBO-like oscillation.

Hoang-Hai BUI[1,2], Eriko NISHIMOTO[1], Shigeo YODEN[1]

[1] *Department of Geophysics, Kyoto University, Kyoto, Japan*

[2] *VNU University of Science, Hanoi, Vietnam*

Email: haibh@edu.vnu.vn

## Abstract

Effects of environment shear on convective systems were studied using a minimal model of QBO-like oscillation (Yoden et al, 2014, Nishimoto et al 2016). The model is configured to run in two-dimensional (x-z) mode with periodic boundary condition, high resolution (5 km horizontally & approximately 200m vertically), and simple physics (no Coriolis effects, no convective parameterization, no diurnal and seasonal variation of solar radiation, etc.). When the radiative-convective equilibrium is established, we achieve an oscillation that shows a downward propagation of the zonal mean in the stratosphere and also the periodic variations of precipitation and convective systems.

In this study, we performed a new series of nudging experiments that nudge the wind towards zero from the surface to a nudge level. The modulation of running mean precipitation is affected in an intriguing manner: it gradually disappears as the nudge layer goes higher, reappears and be strongest at the nudge layer of 7km, then gradually disappears again (Fig.1). The results suggest two separate mechanisms of precipitation modulation in our minimal model: In the no-nudging case, strong low-level shear tends to enhance the convection and leads to larger precipitation. In the nudging case, strong wind at cloud top level and/or strong shear below the cloud top level lead to decreased precipitation. This may be a possible mechanism to understand the real-world link of the QBO and tropospheric convection.

We also perform another series of parameter-sweep experiments that uses the nudging technique to control zonal wind at the top of the model and low-level shear explicitly. The results show that the modulation of precipitation is associated with different types of convective systems in different environmental shear conditions.

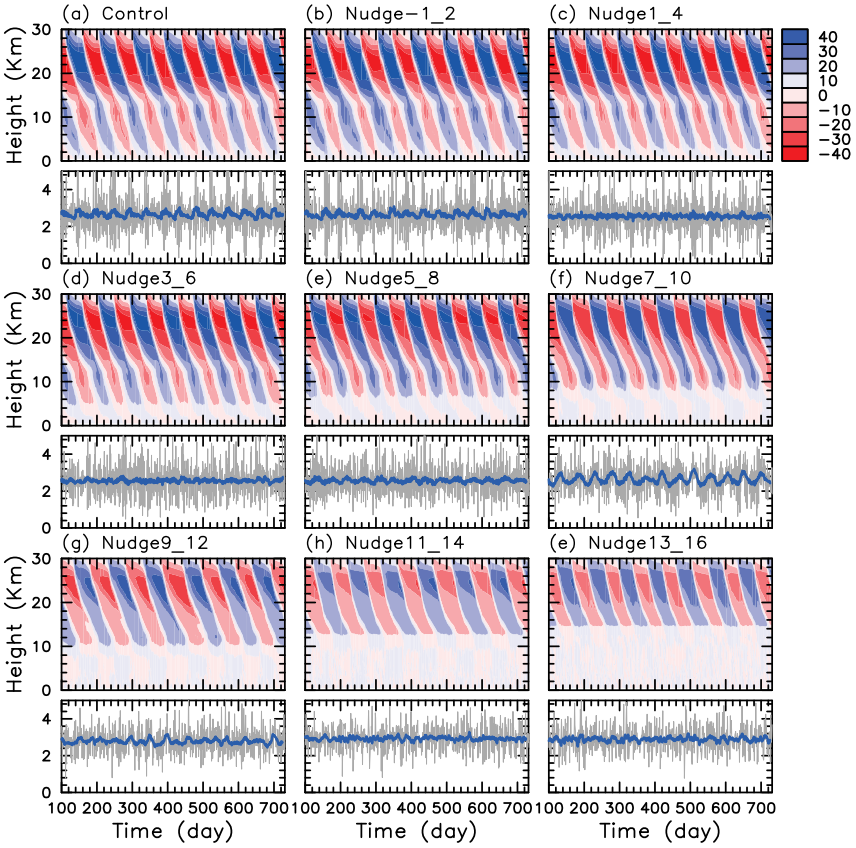


Figure 1. Zonal mean zonal wind (shaded), 1 day domain averaged rainfall (gray lines) and smoothed 1day-rainfall (blue lines) of nudging experiments.

## References:

Nishimoto, E., S. Yoden, and H.-H. Bui, 2016: Vertical Momentum Transports Associated with Moist Convection and Gravity Waves in a Minimal Model of QBO-like Oscillation. *J. Atmos. Sci.*, **73**, 2935–2957. http://journals.ametsoc.org/doi/10.1175/JAS-D-15-0265.1 (Accessed August 24, 2016).

Yoden, S., H.-H. Bui, and E. Nishimoto, 2014: A Minimal Model of QBO-Like Oscillation in a Stratosphere-Troposphere Coupled System under a Radiative-Moist Convective Quasi-Equilibrium State. *Sola*, **10**, 112–116. http://jlc.jst.go.jp/DN/JST.JSTAGE/sola/2014-023.

[Poster, P5]

# Introduction of the project 'Innovative numerical weather predictions and advanced weather disaster prevention based on damage-level estimation' and data assimilation experiment of radio occultation refractivity data by using a mesoscale LETKF system

Hiromu Seko[1]

1. Japan Agency for Marine-Earth Science and Technology / Meteorological Research Institute, Japan Meteorological Agency

Email: hseko@mri-jma.go.jp

## Abstract

### 1. Project 'Innovative numerical weather predictions and advanced weather disaster prevention based on damage-level estimation'

This project is a part of 'Advancement of meteorological and global environmental predictions utilizing observational 'Big Data' (Theme 4)' of 'The post K computer development plan of the FLAGSHIP2020 Project: Development of a wide range of applications that will address social and scientific priority issues'. The goals of this project are to show the possibilities of high accurate predictions of heavy rainfalls and tornadoes by using high-resolution numerical weather models, which resolve cloud convection cells, and the possibilities of longer leading time, which is the time between the predictions and outbreaks of heavy rainfalls or tornados. To reach these goals, the assimilation methods for big-observation data (high-frequent and high-resolution data), such as Himawari-8 rapid scan data, phased array radar data and so on, will be established in this project. In addition to the developments of data assimilation methods, improvements of numerical weather models, such as implementing the coupling effect with ocean models and refinements of micro physical processes, and developments of ensemble forecast techniques and their applications. In the latter half of this presentation, the assimilation method for Radio occultation data, one of 'Big Data', will be presented.

## 2. Data assimilation experiments of radio occultation refractivity data

An assimilation method of radio occultation (RO) data for a mesoscale Local Ensemble Transform Kalman Filter (LETKF) (Miyoshi and Aranami, 2006) system has been developed (Seko and Tsuda, 2015). There are the following two difficulties in the assimilation of RO data: (1) An assumption of uniform distribution of refractivity, which is used in the estimation of refractivity profiles at tangent points, is not always valid, and (2) path averaged data is difficult to be assimilated by LETKF system because data assimilation using LETKF is conducted by each grid point. To solve these difficulties, (1) the path averaged refractivity was reproduced from the tangent point data and (2) path-averaged refractivity was divided into the refractivity at grid points around the path by using the ensemble average and spread obtained by LETKF system. This developed method was applied to the RO data observed on 29 July 2011. The assimilation result of this RO data shows that the sign of the difference between the first guess and observation may be changed when the large mesoscale perturbation of refractivity exists around the tangent points, and that the temperature and water vapor are modified more widely when the path-averaged refractivity is assimilated. The RO data on the upstream side of low-level inflow, which is supplied to heavy rainfalls, is expected to make the leading time longer. This method will be applied in this post–K project.

## References:

Miyoshi, T., and K. Aranami: Applying a Four-dimensional Local Ensemble Transform Kalman Filter (4D-LETKF) to the JMA Nonhydrostatic Model (NHM). *SOLA*, 2006, 2, 128-131.

Seko, H., T. Tsuda: Data Assimilation Experiments of Radio Occultation Refractivity Data by using a Mesoscale LETKF System. *CAS/JSC WGNE Research Activities in Atmospheric and Oceanic Modelling*, 2015, 45, 25-26.

[Poster, P6]

# Sensitivity studies of cloud responses on SSTs in RCE experiments using a high-resolution global nonhydrostatic model

Tomoki Ohno[1], Masaki Satoh[1,2]

1. Atmosphere and Ocean Research Institute, the University of Tokyo, Japan

2. Japan Agency for Marine-Earth Science and Technology, Japan

Email: t-ohno@aori.u-tokyo.ac.jp

## Abstract

As the variation in climate sensitivity among global climate models (GCM) is largely attributable to differences in cloud feedback, better understanding of the response of clouds to climate changes provides important insights into climate science. The radiative-convective equilibrium (RCE) is one of key ingredients in order to understand the role of moist convection in the atmosphere. To reduce the uncertainties of the response of clouds to climate changes, simulations with RCE configurations are examined using a high-resolution nonhydrostatic global circulation model (the Nonhydrostatic Icosahedral Atmospheric Model; NICAM; Satoh et al., 2014). The configurations with fixed SSTs, explicit microphysics parameterizations, and no cumulus parameterization are used. Especially, the sensitivity of the high clouds, liquid water path, and ice water path to vertical grid spacings are studied using fixed SST configurations, as previous studies showed high clouds responses are different between NICAM and other coarse resolution climate models. In addition, it was found that vertical grid spacings of 400 m or less are necessary to resolve the bulk structure of cirrus clouds, we also examine sensitivities to vertical resolutions (Seiki et al., 2015).

It is found that amounts of high cloud increase as associated with the increase of SST in the simulations with different cloud microphysics schemes, although the heights of high clouds and detrainment speeds near the convective region depend on microphysics schemes used. The responses of the amount of high cloud are consistent with those of the tropical cloud of the study of Satoh et al. (2012) based on the global simulations. However, the response of the amount of high cloud in simulations with higher vertical resolutions vary with cloud microphysics schemes, although the heights of high clouds and detrainment speeds near the convective region are similar to those of simulations

with relatively lower vertical resolutions. These results indicate that differences of properties of clouds such as effective radii of hydrometeors and their dependencies for the vertical resolution are possible cause of variations of the response of clouds to climate changes. In addition, they suggest the possible existence of uncertainties of the results of studies based on the simulations with conventional GCMs which do not consider the microphysical properties.

**References:**

Satoh, M., H. Tomita, H. Yashiro, H. Miura, C. Kodama, T. Seiki, A. T. Noda, Y. Yamada, D. Goto, M. Sawada, T. Miyoshi, Y. Niwa, M. Hara, T. Ohno, S. Iga, T. Arakawa, T. Inoue and H. Kubokawa: The Non-hydrostatic Icosahedral Atmospheric Model: description and development. *Progress in Earth and Planetary Science* 2014, **1**:18. doi: 10.1186/s40645-014-0018-1

Satoh, M., S. Iga, H. Tomita, Y. Tsushima, A. Noda: Response of Upper Clouds in Global Warming Experiments Obtained Using a Global Nonhydrostatic Model with Explicit Cloud Processes. *ProgressJ. Climate,* 2012, **3**:2178–2191. doi: : 10.1175/JCLI-D-11-00152.1

Seiki, T., C. Kodama, M. Satoh, T. Hashino, Y. Hagihara, and H. Okamoto: Vertical grid spacing necessary for simulating tropical cirrus clouds with a high-resolution atmospheric general circulation model. *Geophys. Res. Lett., 42, 4150–4157, doi:10.1002/2015GL064282.*

[Poster, P7]

# Simulations of deep convection as a testbed for two non-hydrostatic models

Didier Ricard, Antoine Verrelle
CNRM (Météo-France, CNRS), Toulouse, France
Email: didier.ricard@meteo.fr

## Abstract

Three-dimensional numerical simulations of deep moist convection are used to evaluate the ability of two mesoscale models, AROME and Meso-NH at kilometer and hectometer scales (explicit convection).

AROME (Seity et al 2011) is the limited-area non-hydrostatic model at Météo-France dedicated for short-range and fine-scale numerical weather prediction. It is a spectral model using a semi-implicit (SI) temporal scheme and a semi-Lagrangian (SL) advection scheme. The current operational version has a 1.3-km horizontal resolution and 90 vertical levels (Brousseau et al. 2016).

Meso-NH (Lafore et al 1998) is a grid-point Eulerian model based on anelastic equations. This research model can simulate atmospheric motions ranging from synoptic scale down to LES.

These two mesoscale models are based on two different dynamical cores, but at kilometer resolution, the physics package is the same for both models, including a single-moment microphysical scheme (ICE3), a shallow convection scheme (EDKF), a surface scheme (SURFEX) and a 1D turbulence scheme (1.5 order closure). At higher resolution, Meso-NH can use a 3D turbulence scheme.

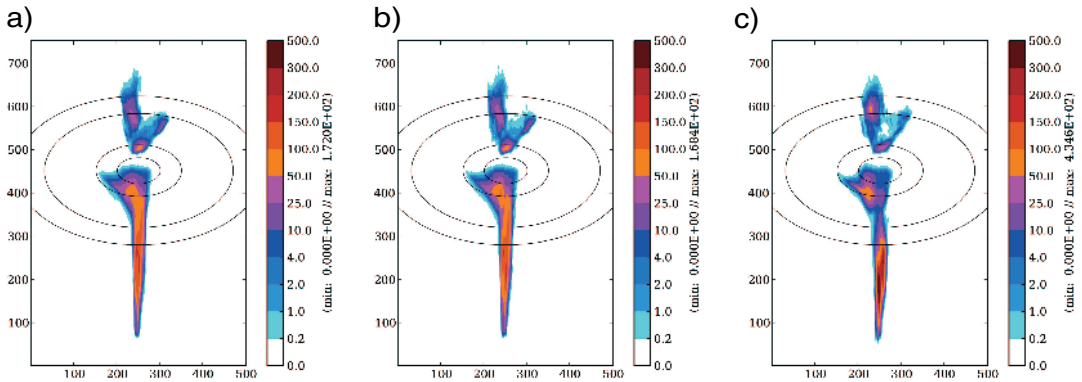


Meso-NH 1km 1D BL  Meso-NH 1km 3D BL  Meso-NH 1km 3D Deardorff

*Figure 1: 24h accumulated precipitation (between 24 and 48h) for 1-km grid spacing runs with 1D (a) and 3D (b) turbulence schemes using Bougeault-Lacarrère mixing length (BL) and 3D turbulence scheme using Deardorff mixing length (c) for the case of orographic convection. Idealized orography is represented in black lines (50 m, 100 m, 500 m, 1000 m).*

This study is based on two idealized cases of deep convection: a new case of orographic convection (Figure 1) and a classic case of supercell and multicell systems (considered in Verrelle et al, 2015) (Figure 2). Indeed, the divergence modes are important in deep convective systems with a strong interaction between the dynamical core and the physical parameterizations. Sensitivity tests to explicit diffusion and physical dissipation (shallow convection scheme, 1D or 3D turbulence scheme) as well as to time step and horizontal resolution are conducted to illustrate some damping mechanisms. The characteristics of convective systems are analyzed and the experiments are assessed using different diagnostics.

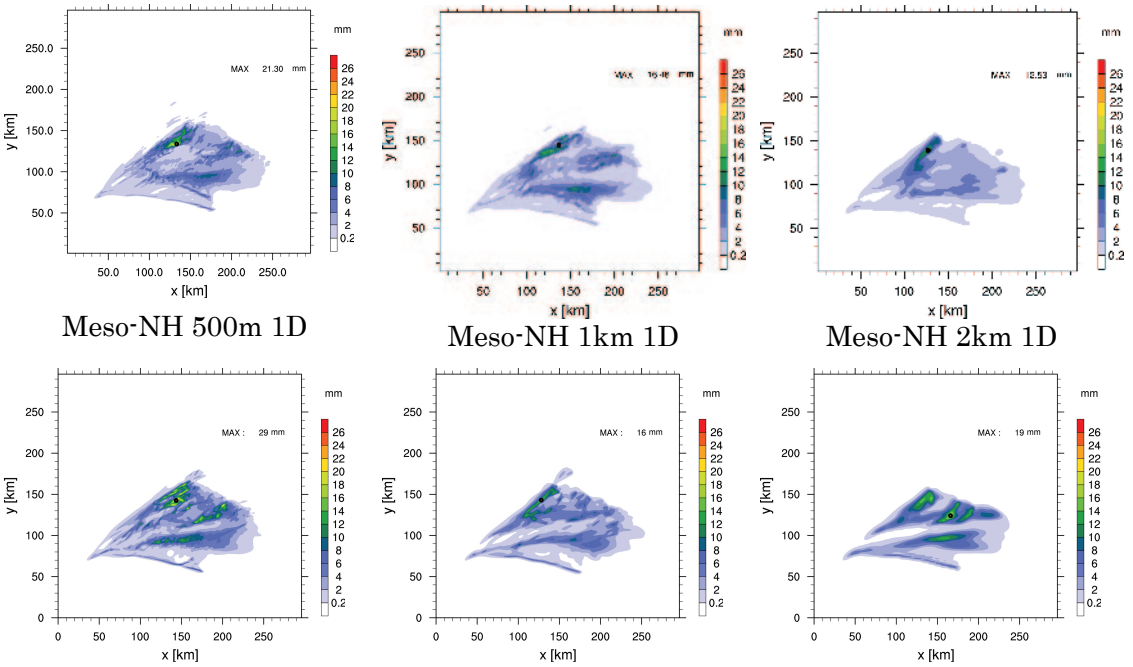


*Figure 2: Accumulated precipitation during 150 min for 500-m (left column), 1-km (center column) and 2-km (right column) grid spacing runs for Meso-NH (first line) and AROME models (second line) with a 1D turbulence scheme for the case of supercell and multicell systems.*

**References:**


Brousseau, P., Seity, Y., Ricard, D. and Léger, J., 2016: Improvement of the forecast of convective activity from the AROME-France system. *Q.J.R. Meteorol. Soc., 142: 2231–2243. doi:10.1002/qj.2822*

Lafore, J. P., J. Stein, N. Asencio, P. Bougeault, V. Ducrocq, J. Duron, C. Fischer, P. Hereil, P. Mascart, J. P. Pinty, J. L. Redelsperger, E. Richard, and J. Vila-Guerau de Arellano, 1998: The Meso-NH Atmospheric Simulation System. Part I: Adiabatic formulation and control simulations. *Annales Geophysicae, 16, 90-109*

Seity, Y., P. Brousseau, S. Malardel, G. Hello, P. Bénard, F. Bouttier, C. Lac, and V. Masson, 2011: The AROME-France Convective-Scale Operational Model. *Mon. Wea. Rev., 139, 976–991, doi: 10.1175/2010MWR3425.1*

Verrelle, A., Ricard, D. and Lac, C., 2015: Sensitivity of high-resolution idealized simulations of thunderstorms to horizontal resolution and turbulence parametrization. *Q.J.R. Meteorol. Soc., 141: 433–448. doi:10.1002/qj.2363*

[Poster, P8]

# A Computationally Cost Effective Online Nesting Procedure for Regional Atmospheric/Climate Models

Ryuji Yoshida, Tsuyoshi Yamaura, Sachiho A. Adachi, Seiya Nishizawa, Hisashi Yashiro, Yousuke Sato, and Hirofumi Tomita

RIKEN Advanced Institute for Computational Science, Kobe, Japan.

Tel: +81-78-940-5735, E-mail: ryoshida@riken.jp

## Abstract

For a down-scaling experiment in the regional atmospheric/climate models, a nesting system is necessary component. Nesting system has two types of procedure; offline nesting and online nesting. Since each nested domain is calculated sequentially in offline nesting, the intermediate files are necessary to transfer data from parent domain to child domain. Online nesting has merits against offline nesting in updating interval of boundary data and un-necessity of intermediate files. Michalakes (1997) implemented online nesting as an extension from offline nesting. The conventional online nesting (CNV) procedure is available in a lot of regional models.

However, is the CNV the best implementation of online nesting from the view of computational performance? In the CNV, the whole computational nodes manage all of the nested-domains as a single group. Recently, a task-management procedure of online nesting has been implemented in the National Centers for Environmental Prediction (NCEP) Nonhydrostatic Multi-Scale Model on the B grid (NMMB, DiMego et al. 2011; Janjic and Gall 2012). In the new procedure, computational nodes are split into multiple groups, and each group manage only one domain. Therefore, time integration for each domain can be executed simultaneously. However, the computational performance of the new procedure has not yet been investigated. In this study, we proposed a cost-effective online nesting procedure (CONeP), and investigated the computational performance comparing with the CNV by using the K computer. CONeP can execute domain calculations simultaneously similarly to the NMMB, and also allow to flexible experimental settings, e.g. number of vertical layers is variable among nested domains. We implemented CONeP to the SCALE-RM (Nishizawa et al. 2015; Sato et al. 2015), which is a regional atmospheric model developed by RIKEN AICS. We evaluated the computational performance with the triple nested domains. Detail experimental settings are shown in Table 1. For the calculation, 100 nodes of the K computer were used in both the CNV and CONeP. In CONeP, the nodes were divided into three groups,

and assigned to each domain; 4, 16 and 80 nodes for Domain 1, 2, and 3, respectively. The elapsed times of a 1,350-s time integration for the CNV case was 21.3 s. On the other hand, it was 16.6 s for the CONeP case, and approximately 22% faster than CNV with the same number of computational nodes. Thus, CONeP has better computational performance than CNV. CONeP has more advantage with an increasing number of nested domains. CONeP allow for users to assign an optimal node number to each domain to gain the best computational performance.

Table 1: Experimental settings

| settings | CNV | CONeP |
|---|---|---|
| horizontal grid numbers for all domains | 80 x 80 | 80 x 80 |
| horizontal grid space (domain 1, 2, 3) [km] | (27, 9, 3) | (27, 9, 3) |
| vertical layers (domain 1, 2, 3) | (48, 64, 80) | (48, 64, 80) |
| time interval (domain 1, 2, 3) [s] | (27, 9, 3) | (27, 9, 3) |

**References:**

DiMego Geoff D., Z. Janjic, T. Black, E. Rogers, M. Pyle, J. Du, H.-Y. Chuang, B. Ferrier, and D. Jovic, 2011: UPDATE ON WRF IN NCEP OPERATIONS, the 12th WRF Users' Workshop, ftp://ftp.emc.ncep.noaa.gov/wd20vxt/NMMB-tutorial/NMMB_tutorial_nesting.pptx

Janjic, Z. I., and R. Gall, 2012: Scientific documentation of the NCEP Nonhydrostatic Multiscale Model on the B Grid (NMMB). Part 1: Dynamics. NCAR Tech. Note, NCAR/TN-4891STR, 75 pp.

Michalakes, J., 1997: RSL: A Parallel Runtime System Library for Regional Atmospheric Models with Nesting, to appear in proceedings of the IMA workshop Structured Adaptive Mesh Refinement Grid Methods, March 12-13, Minneapolis, 1997.

Nishizawa S., H. Yashiro, Y. Sato, Y. Miyamoto, and H. Tomita, 2015: Influence of grid aspect ratio on planetary boundary layer turbulence in large-eddy simulations, Geosci. Model Dev., 8, 3393–3419, doi:10.5194/gmd-8-3393-2015.

Sato Y., S. Nishizawa, H. Yashiro, Y. Miyamoto, Y. Kajikawa, and H. Tomita, 2015: Impacts of cloud microphysics on trade wind cumulus: which cloud microphysics processes contribute to the diversity in a large eddy simulation?, Prog. Earth Planet. Sci., 2, 23, doi:10.1186/s40645-015-0053-6.

[Poster, P9]

# Development of the stretch-atmosphere and ocean model to study air-sea interaction associated with tropical cyclone.

Hiroyasu Kubokawa[1], Masaki Satoh[1,2], Takashi Arakawa[3], Hiroyasu Hasumi[1,2,4]

1. Atmosphere and Ocean Research Institute, the University of Tokyo, Japan

2. Japan Agency for Marine-Earth Science and Technology, Japan

3. Research Organization for Information Science and Technology

4. National Institute of Polar Research

Email: kubok@aori.u-tokyo.ac.jp

## Abstract

The tropical cyclones approached near Japan bring the large impacts on our lives. While the track of tropical cyclone is mainly controlled by wind fields associated with the Pacific high, development is influenced by heat flux from that oceans. Recently, global nonhydrostatic atmospheric model (Nonhydrostatic Icosahedral Atmospheric Model, NICAM) is used to simulate the tropical cyclones or characteristics of deep convection. However, to simulate the tropical cyclones more reality, we should develop the atmosphere-ocean coupling model.

We select the stretched-version NICAM (Tomita et al., 2008) as an atmospheric model and also select the CCSR Ocean Component Model (COCO) as an ocean model. The Stretch-NICAM saves computational resources by focusing on a specific region at high resolution. The horizontal resolution becomes coarser for the region outside the target region, but in this study we are only interested in the local results within the target region. The horizontal spacing of stretched-version NICAM and COCO is about 7 km and 1 degree grid, respectively. The horizontal grid configuration is difference between stretched-version NICAM and COCO. Here we insert the coupler model (called Jcup) between the these models and exchange of fluxes in Jcup every 1 hr. The initial condition of the NICAM is prepared by NCEP Tropospheric Analysis data. Initial data of COCO is prepared by COCO-3D data. Here, COCO-3D data is calculated by periodically forcing by ERA-interim data.

In this study, we chose the tropical cyclone generated at 28 August 2004 near Japan and investigate the air-sea interaction associated with the tropical cyclone. The model integration was performed with 7 days. We also perform the NICAM calculation (not coupled) to investigate the influence of ocean. Here, we use the some types sea surface temperature data as an initial condition. To compare the real ocean, we also use the 4-dimensional Ocean Reanalysis dataset (FORA) and Argo floats data.

Our new model shows that the reduction of the sea surface temperature associated with tropical cyclone is large about 1 K compared with FORA data. In the presentation, we will show the results about the boundary layer and state in the sea.

**References:**

Tomita, H. (2008), A stretched icosahedral grid by a new grid transformation. *J. Meteor. Soc. Japan*, **86A**, 107–119, doi:10.2151/jmsj.86A.107.

[Poster, P10]

# A comparison of precipitations reproduced with regional reanalysis assimilating only conventional observations and dynamical downscaling

Shin Fukui[1,2], Toshiki Iwasaki[1], Kazuo Saito[2], Hiromu Seko[2], Masaru Kunii[2],

1. Tohoku University, Japan

2. Meteorological Research Institute, Japan

Email: fukui@wind.gp.tohoku.ac.jp

## 1. Introduction

Long-term consistent and high-resolution three dimensional atmospheric datasets are invaluable to investigate past local extreme events and effects of climate change. For this purpose, the dynamical downscaling approach is widely applied to the global analyses. The dynamical downscaling reproduces dynamically consistent fields, the reproduced field variables sometimes includes significant errors. This is because the lateral boundary conditions do not fully control the inner variabilities. The regional reanalysis is expected to generate more accurate fields with dynamical consistency. To keep the long-term consistency, the data for the assimilation are only conventional observations, which have been established for about 60 years such as surface observations at weather stations and upper observations with radiosondes. The system is assessed comparing dynamical downscaling regarding precipitation.

## 2. Experimental design

As the assimilation system, we adopt the local ensemble transform Kalman filter (LETKF; Hunt et al. 2007) implemented in the JMA's Nonhydrostatic Model (NHM; Saito et al. 2007). A double nesting procedure is conducted in JRA-55 (Kobayashi et al. 2015). The inner model covers the whole Japan with 5-km grid spacing, while the outer model covers the East Asia with 25-km grid spacing. The observation data for the assimilation are surface pressure reported as SYNOP, SHIP and BOUY, and upper wind, temperature and relative humidity reported as TEMP and PILOT. The experimental period is set to August 2014. As the comparison, two kinds of dynamical downscaling approaches using the NHM without assimilation. In the one downscaling (DS1), the time integration is performed with spectral boundary coupling over the experimental period. In the other (DS2), the 12-hour integrations are conducted from the interpolated coarse model outputs every 6 hours.

## 3. Comparison with the dynamical downscalings

The comparison is conducted in terms of bias scores (BI) and threat scores (TS) of 6-hourly accumulated precipitation reproduced with 5-km grid spacing NHM against JMA's radar/raingauge analysed precipitation data (R/A). The BIs of the results of 5km NHM-LETKF (LET) are about 0.6, which is comparable to the BIs of DS2 and less than the BIs of DS1. The initial conditions in LET are too smooth because they are obtained from ensemble means of perturbed forecasts, while they do not have the resolution gap as in DS2. LET and DS2 have some problems about spin-up, while DS1 does not have the problem due to the continuous integration over long term. The BIs of all the simulations are less than 1 independently of the thresholds. This result implies that the NHM double-nested in JRA-55 underestimates the precipitation in the warm season in Japan. The TSs of LET is around 0.3 when the threshold is larger than 5 mm/6h. They are better than the TSs of DS2 when the threshold is larger than 25 mm/6h and are significantly improved compared with the TSs of DS1. In LET, the errors accompanied by the internal variabilities that are not fully controlled only by the boundary conditions are suppressed with the assimilation, while the errors grow in DS1.

## 4. Summary

Assimilating the conventional observations with the NHM-LETK improves the precipitation pattern over two kinds of dynamical downscaling approaches. However, the system underestimates the precipitation due to weaker spin-up. It suggests that amplitudes of analysis and lateral boundary perturbations should be tuned carefully. Whether using LETKF or not, the precipitation is underestimated. The problem should be also tackled in terms of the model itself and boundary conditions.

## References:

Hunt, B. R., E. J. Kostelich, and I. Szunyogh: Efficient data assimilation for spatiotemporal chaos: A local ensemble transform Kalman filter. *Physica D*, **230**, 112-126, 2007.

Kobayashi, S., Y. Ota, Y. Harada, A. Ebita, M. Moriya, H. Onoda, K. Onogi, H. Kamahori, C. Kobayashi, H. Endo, K. Miyaoka, and K. Takahashi: The JRA-55 Reanalysis: General specifications and basic characteristics. J. *Meteor. Soc. Japan*, **93**, 5-48, 2015.

Saito, K., J. Ishida, K. Aranami, T. Hara, T. Segawa, M. Narita, and Y. Honda: Nonhydrostatic atmospheric models and operational development at JMA. *J. Meteor. Soc. Japan*, **85**, 271-304, 2007.

[Poster, P11]

# Assimilation Experiments of Himawari-8 Rapid Scan Atmospheric Motion Vectors

Michiko Otsuka[1], Masaru Kunii[1], Hiromu Seko[1], Kazuki Shimoji[2] and Koji Yamashita[3]

1. Meteorological Research Institute, Japan Meteorological Agency, Japan

2. Meteorological Satellite Center, Japan Meteorological Agency, Japan

3. Numerical Prediction Division, Japan Meteorological Agency, Japan

Email: motsuka@mri-jma.go.jp

## Abstract

Himawari-8 has been operating rapid scan observations around Japan every 2.5 minutes. Rapid Scan Atmospheric Motion Vectors (RS-AMV) are derived from image triplets at 5-min interval taken from 2.5-min rapid scans with the improved retrieval algorithm involving newly developed tracking and height assignment methods (Shimoji 2014). This study aims to investigate the impact of RS-AMVs on the prediction of mesoscale phenomena such as local heavy rainfalls by utilizing them into mesoscale data assimilation.

First, the data quality and the characteristics of observation errors of RS-AMVs were examined using the statistics of differences from JMA mesoscale analyses, radiosonde and wind profiler observations and NHM (JMA non-hydrostatic model) forecasts. The results of comparisons with JMA mesoscale analyses and upper air observations during the month of August 2015 revealed that the overall quality of RS-AMV was good enough to be assimilated in spite of different error characteristics at different pressure levels in different channels. RS-AMVs in three water vapor channels showed larger root mean square vector differences than those in visible or infrared channels and had a slight positive bias in wind speed. Low level RS-AMVs including winds over land in visible and infrared channels also seemed to be in good agreement with wind profiler observations. Then, we estimated horizontal and inter-band correlations of observation errors based on the statistics of covariances of first-guess departures (RS-AMV minus NHM forecast wind). The average correlation for low-level RS-AMVs was below 0.2 around 200 km, while the correlations of mid- and high-level

RS-AMVs were still high at the same distance. It is necessary to consider these possible spatial correlations of observation errors when assimilating such high-density data as RS-AMVs. As for the inter-band correlations, the correlations were higher in pairs of RS-AMVs at higher levels without depending on certain band combinations.
Next, several data assimilation experiments using NHM-LETKF (Kunii 2014) or JNoVA (JMA Non-hydrostatic Model Based Variational Data Assimilation System) were conducted. On a heavy rainfall case in summer of 2015 , the impact of RS-AMV was slightly positive in wind forecasts especially in early forecast hours and at lower levels, while in rainfall forecasts, slightly positive in case of light rain but negative in heavy rain. Different experiments were conducted on the same case with each using a different resolution of smoothing or different bands in the formation of super observations, and rainfall forecast scores from each experiment were compared with each other. It seemed that low level winds had more positive impact than winds at mid- and high- levels in that case. The experiments on other cases will be presented in the workshop.

Now that Himawari-8 rapid scan operations have been bringing more data with unprecedented density and frequency, it is necessary to find the most efficient way to utilize RS-AMVs for maximum benefits in assimilation. We still need further investigation in the methods of data selection, QC, or settings of data thinning and observation errors in order to take advantage of these high resolution RS-AMVs.

**References:**

Kunii M., 2014: Mesoscale data assimilation for a local severe rainfall event with the NHM-LETKF system. *Wea. Forecasting*, 29, 1093-1105.

Shimoji, K., 2014: Motion tracking and cloud height assignment methods for Himawari-8 AMV, *Proceedings of 12th International Winds Workshop* (Available online at http://www.eumetsat.int/website/home/News/ConferencesandEvents/PreviousEvents/DAT_2441511.html accessed on 20 September 2016)

[Poster, P12]

# 4D-EnVAR with iterative calculation of non-linear model

Sho Yokota[1], Masaru Kunii[1], Kazumasa Aonashi[1], and Seiji Origuchi[2]

1. Meteorological Research Institute, Japan Meteorological Agency, Japan

2. Fukuoka Aviation Weather Station, Japan Meteorological Agency, Japan

E-mail: syokota@mri-jma.go.jp

## 1 . Introduction

Hybrid 4D-VAR and 4D-EnVAR are two popular ensemble-based variational data assimilation methods. Although Hybrid 4D-VAR iteratively calculates non-linear observation operator (*H*) and forecast model (*M*) and the ensemble-based forecast error covariance is reflected in the analyses, Hybrid 4D-VAR requires large development and computational costs. The costs of 4D-EnVAR are smaller than those of Hybrid 4D-VAR because 4D-EnVAR does not use adjoint of tangent linear forecast model. However, 4D-EnVAR analyses are generally worse than Hybrid 4D-VAR probably because 4D-EnVAR does not iteratively calculate non-linear *H* and *M*.

Yokota et al. (2016) developed 4D-EnVAR with observation space localization that iteratively calculates non-lenear *H*, and showed that this method can make better analyses than 4D-LETKF (Hunt et al. 2007) using SPEEDY model (Molteni 2003). We improve this 4D-EnVAR to iteratively calculate *M* as well as *H*, and show that this 4D-EnVAR can make better analyses than previous one.

## 2 . Formulation

In 4D-EnVAR with observation space localization (hereafter, EnVAR), $\overline{\boldsymbol{x}_t^a}$ (analysis at time slot $t$) is transformed to $\boldsymbol{w}_j$ as

$$\overline{\boldsymbol{x}_t^a} = \overline{\boldsymbol{x}_t^f} + \sum_{j=1}^{m} \delta \boldsymbol{x}_{j,t}^f \circ \boldsymbol{w}_j, \tag{1}$$

where $\overline{\boldsymbol{x}_t^f}$ and $\delta \boldsymbol{x}_{j,t}^f$ are ensemble mean and ensemble perturbation (member *j*), respectively, of first guess at time *t*, and $\boldsymbol{w}_j$ is optimized by minimizing the cost function (see Yokota et al. 2016). The formulation of 4D-EnVAR with iterative calculation of *M* as well as *H* (hereafter, EnVAR_M) is same as EnVAR except that

$$\overline{\boldsymbol{x}_t^a} = M_t\left(\overline{\boldsymbol{x}_0^a}\right) = M_t\left(\overline{\boldsymbol{x}_0^f} + \sum_{j=1}^{m} \delta \boldsymbol{x}_{j,0}^f \circ \boldsymbol{w}_j\right) \tag{2}$$

is used for transformation to $\boldsymbol{w}_j$ instead of Eq. (1), where $M_t$ is the forecast model for time $t$.

## 3 . Single-observation assimilation experiments

We compared 80-member EnVAR and EnVAR_M with single-observation assimilation experiments using SPEEDY model. At the end of 6-hour assimilation window, single observation was assimilated to (180°E, 20°N) where zonal wind $u$ = -9.6 [m $s^{-1}$] and relative humidity *RH* = 65.6 [%]. When $u$ = 5.0 [m $s^{-1}$] was assimilated, analyses of $u$ are -2.6 m $s^{-1}$ in EnVAR and -0.6 m $s^{-1}$ in EnVAR_M at the observation point (Fig. 1a,b). When *RH* = 30.0 [%] was assimilated, analyses of *RH* are 49.9 % in EnVAR and 42.4 % in EnVAR_M (Fig. 1c,d). These means that EnVAR_M makes analyses that are closer to the observation than EnVAR.

## 4 . Observation system simulation experiments (OSSEs)

We also conducted OSSEs using 80-member SPEEDY model. In the OSSEs, observations of zonal and meridional winds, temperature, relative humidity, and surface pressure, which were created by adding random errors to "true" values (results of free-run simulation) at 2-hour intervals at radiosonde-like points, were assimilated. Biases and root mean square errors (RMSEs) from "true" values are smaller in the forecasts from EnVAR_M analyses than those from EnVAR analyses (Fig. 2). However, EnVAR_M with the small number of ensemble members is not necessarily better than EnVAR because of the difficulty of minimizing non-linear cost function of EnVAR_M.

## 5 . Summary

We developed 4D-EnVAR with iterative calculation of $M$ as well as $H$. Iteratively calculating $M$ is effective to make better analyses. As a next step, we will be applied this method to the mesoscale non-hydrostatic model.

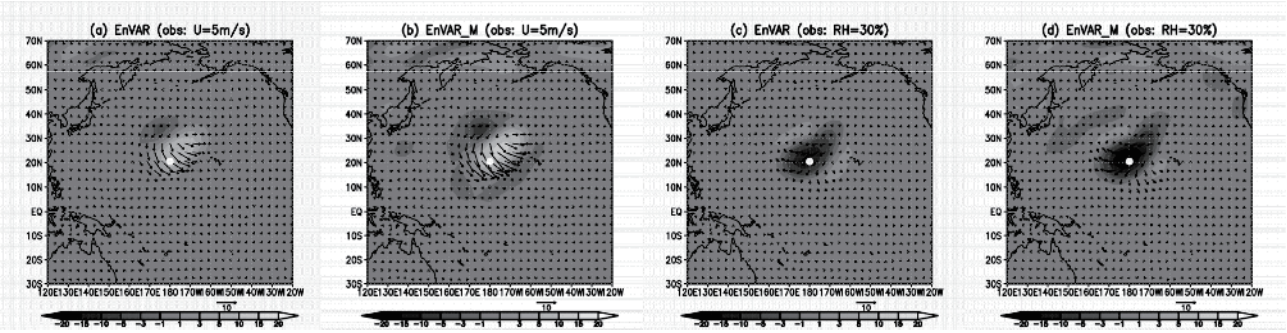


Fig. 1 (a)(c) EnVAR and (b)(d) EnVAR_M analysis increments of $u$ (arrows, m $s^{-1}$) and $RH$ (shade, %) at the end of assimilation window when (a)(b) $u = 5.0$ [m $s^{-1}$] and (c)(d) $RH = 30.0$ [%] were assimilated.

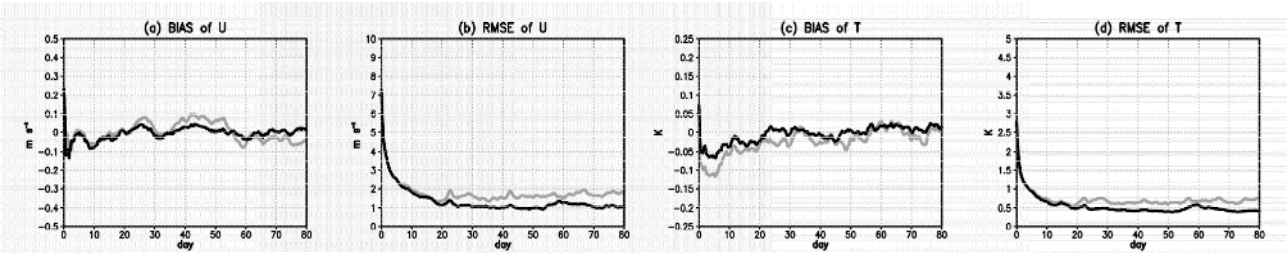


Fig. 2 Time series of (a)(c) bias and (b)(d) RMSE of the ensemble means of (a)(b) zonal wind and (c)(d) temperature of every-6-hour ensemble forecasts from EnVAR (gray) and EnVAR_M (black) analyses.

**Acknowledgements**

The SPEEDY model, developed by Franco Molteni and Fred Kucharski, and SPEEDY-LETKF, developed by Takemasa Miyoshi, were used for assimilation experiments. The source code developed by Numerical Prediction Division, Japan Meteorological Agency was used for minimizing the cost function. This study was supported in part by "Social and scientific priority issues (Theme 4) to be tackled by using post K computer of the FLAGSHIP2020 Project" (ID: hp150289, hp160229).

**References**

Hunt, B. R., E. J. Kostelich, and I. Szunyogh: Efficient data assimilation for spatiotemporal chaos: A local ensemble transform Kalman filter. *Phys. D*, 2007, **230**, 112–126.

Molteni, F.: Atmospheric simulations using a GCM with simplified physical parametrizations. I: Model climatology and variability in multi-decadal experiments. *Clim. Dyn.*, 2003, **20**, 175–191.

Yokota, S., M. Kunii, K. Aonashi, and S. Origuchi: Comparison between four-dimensional LETKF and ensemble-based variational data assimilation with observation localization. *SOLA*, 2016, **12**, 80–85.

[Poster, P13]

# Evaluations of cloud properties in NICAM using CALIPSO and CloudSat

Woosub Roh[1], Masaki Satoh[1,2]

1. Atmosphere and Ocean Research Institute, the University of Tokyo, Japan

2. Japan Agency for Marine-Earth Science and Technology, Japan

Email: ws-roh@aori.u-tokyo.ac.jp

## Abstract

The evaluation of cloud and precipitation is important in high-resolution models such as NICAM. These models are generally defined as nonhydrostatic models with horizontal grid spacing sufficiently fine to be able to explicitly simulate individual cloud systems. For clouds, NICAM more realistically represents microphysical processes, such as the consistent treatment of precipitating hydrometeors, compared with general circulation models (GCMs), and they calculate the time evolution, structure, and life cycle of cloud systems.

We evaluated thermodynamic phases of clouds in a NICAM using Joint simulator and a Cloud-Aerosol Lidar and Infrared Pathfinder Satellite Observation (CALIPSO) lidar. For the evaluation, we developed the simulator of depolarization ratio in Joint simulator. We compared and analyzed two simulations using two microphysics schemes such as NICAM Single-moment Water 6 (NSW6, Tomita 2008b) and the modified NSW6 (Roh and Satoh 2014). We followed the methodology, which developed by Yoshida et al. (2010) to enables discrimination of vertically resolved cloud particle types based on depolarization ratio and a new parameter estimated from two attenuated backscattering coefficients in neighboring layers. We evaluate the effects of microphysics on the cloud statistics using and in NICAM based on CALIPSO signals.

The NICAM was carried out using a regional version of NICAM with a stretched grid (Tomita 2008a), minimum resolution is 2.4 km horizontal resolution and most of resolutions are under 5 km. The integration time is from 00 UTC 1 to 18 UTC 5 January 2007. The first 18 ours are used for the spin up time. The NICAM simulations were initialized with National Centers for Environmental Prediction (NECP) data with one degree resolution for winds, temperature, relative humidity, and geopotential data. The

sea surface temperature is fixed. We tested two microphysics schemes: the first is the original NSW6 (Tomita 2008b, herein CON), and the second is the modified NSW6 (Roh and Satoh 2014, herein MODI). The sensor simulators used are the EarthCARE Active Sensor Simulator (Okamoto et al. 2007) in Joint simulator. A merged dataset for CloudSat CPR radar and CALIPSO lidar is used. (Hagihara et al. 2010, hereafter, CSCA-MD). In order to increase the sample size, the CSCA-MD for the month of January 2007 is compared to the simulation.

We will investigate the microphysical processes related to supercooled water clouds and effects of supercooled water clouds on radiative properties and dynamics of atmosphere over a globe. We also try to consider the effects of ice clouds with 2D plates in a satellite simulator.

**References:**


Hagihara, Y., H. Okamoto, and R. Yoshida, 2010: Development of a combined CloudSat-CALIPSO cloud mask to show global cloud distribution. *J. Geophys. Res.*, **115**, D00H33, doi:10.1029/2009JD012344.

Okamoto, H., T. Nishizawa, T. Takemura, H. Kumagai, H. Kuroiwa, N. Sugimoto, I. Matsui, A. Shimizu, A. Kamei, S. Emori, and T. Nakajima, 2007: Vertical cloud structure observed from shipborne radar and lidar,: mid-latitude case study during the MR01/K02 cruise of the R/V Mirai, *J. Geophys. Res*, 112, D08216, doi:10.1029/2006JD007628.

Roh, W., and M. Satoh, 2014: Evaluation of Precipitating Hydrometeor Parameterizations in a Single-Moment Bulk Microphysics Scheme for Deep Convective Systems over the Tropical Central Pacific. *J. Atmos. Sci.*, **71,** 2654-2673.

Tomita, H., 2008a: A stretched grid on a sphere by new grid transformation. *J. Meteor. Soc. Japan*, **86A**, 107-119.

Tomita, H., 2008b: New microphysics with five and six categories with diagnostic generation of cloud ice. *J. Meteor. Soc. Japan*, **86A**,121-142.

Yoshida, R., H. Okamoto, Y. Hagihara, and H. Ishimoto, 2010: Global analysis of cloud phase and ice crystal orientation from cloud-aerosol lidar and infrared pathfinder satellite observation (CALIPSO) data using attenuated backscattering and depolarization ratio, *J. Geophys. Res.,* 115, D00H32, doi:10.1029/2009JD012334.

[Poster, P14]

# Impacts of spatial grid resolution on the cloud cover of marine shallow cumulus

Yousuke Sato[1,2], Shin-ichiro Shima[2], Hirofumi Tomita[1]

1. RIKEN Advanced Institute for Computational Science, Japan

2. Graduated School of Simulation Studies, University of Hyogo, Japan

Email: yousuke.sato@riken.jp

## Abstract

This study investigated impacts of grid resolution on shallow cumulus simulated by a lagrangian cloud microphysical model (LCM) coupled with a large eddy simulation (LES) model. Since LES models are powerful tool to simulate small scale phenomena including shallow clouds, they have been used as a reference solution when improving cloud parameterization in general circulation models (GCMs). (e.g., Golaz et al., 2007; Kogan, 2013). However, the impacts of spatial resolution on simulated clouds should be concerned to verify the reliability of LES models as discussed by many previous studies (e.g., Cheng et al., 2010; Yamaguchi and Randall, 2012). Matheou et al. (2011) indicated that the numerical convergence for cloud cover, which is critical parameter for radiative process in GCMs, was not achieved with their finest grid resolution of 10m grid spacing.

In this study, a series of sensitivity simulations of shallow maritime cumulus were carried out to clarify the grid resolution required to obtain numerical convergence of cloud cover. The horizontal (vertical) grid resolution was swept from 100 m (80m), which was the same as the BOMEX, to 6.25m (5m) without changing grid aspect ratio. A LCM called Super Droplet Method (SDM; Shima et al., 2009) was used to reduce the uncertainties derived from cloud microphysical parameterization and numerical diffusion. The experimental setup was based on Barbados Oceanographic and Meteorological Experiment (BOMEX; Siebesma et al., 2003).

Results of the experiments indicated that the cloud cover increased with fining grid spacing, and the numerical convergence was achieved with the horizontal (vertical) grid resolution with 12.5 m (10m) in view of cloud cover. The small scale upward velocity and small amount of surface precipitation, which was only resolved with fine grid resolution, were critical to reproduce the accurate cloud cover.

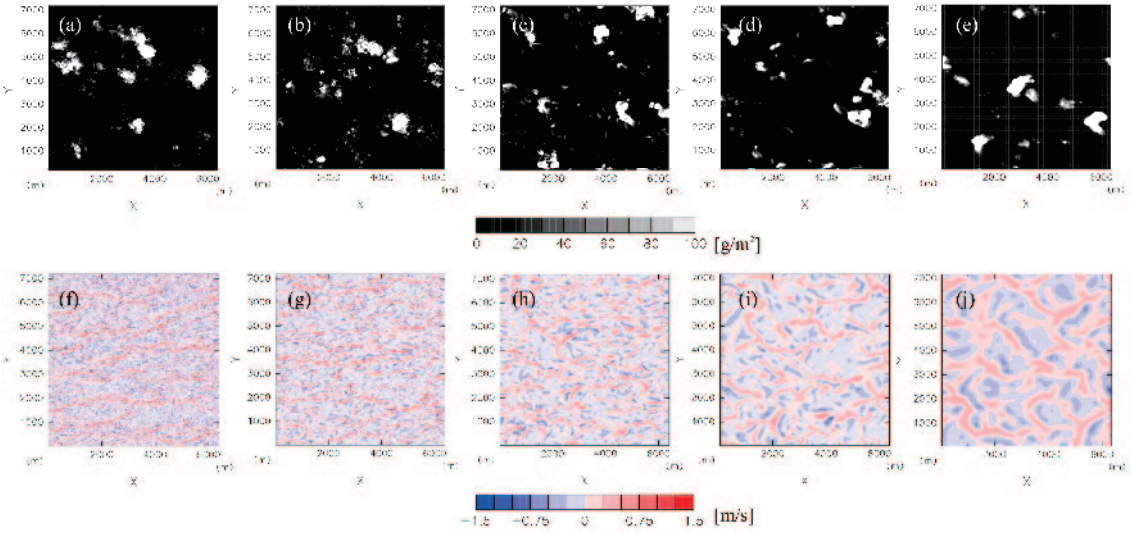


Figure 1: (a-e) Liquid water path and (f-j) vertical velocity on $z = 50$ m at $t = 21000$ sec simulated with grid resolution of (a,f) 6.25m, (b,g) 12.5m, (c,h) 25m, (d,i) 50m, and (e,j) 100m.

**References:**

Cheng, A., K.-M. Xu, and B. Steven, Effects of resolution on the simulation of boundary-layer clouds and the partition of kinetic energy to subgrid scales, *J. Adv. Model. Earth Syst.*, 2010, **2**, 3, doi:10.3894/JAMES.2010.2.3.

Golaz, J.-C., V. E. Larson, J. a. Hansen, D. P. Schanen, and B. M. Griffin, Elucidating model inadequacies in a cloud parameterization by use of an ensemble-based calibration Framework, *Mon. Wea. Rev.*, 2007, **135**, 4077–4096

Kogan, Y., A Cumulus cloud microphysics parameterization for cloud-resolving models, *J. Atmos. Sci.*, 2013, **70**, 1423–1436

Matheou, G., D. Chung, L. Nuijens, B. Stevens, and J. Teixeira, On the fidelity of large-eddy simulation of shallow precipitating cumulus convection, *Mon. Wea. Rev.* 2010, **139**, 2918–2939

Shima, S., K. Kusano, A. Kawano, T. Sugiyama, and S. Kawahara, The super-droplet method for the numerical simulation of clouds and precipitation: a particle-based and probabilistic microphysics model coupled with a non-hydrostatic model, *Q. J. R. Meteorol. Soc.*, 2009, **135**, 1307–1320

Siebesma, A. et al., A large-eddy simulation intercomparison study of shallow cumulus convection, *J. Atmos. Sci.*, 2003, **60**, 1201–1219.

Yamaguchi, T., and D. a Randall, Cooling of entrained parcels in a large-eddy simulation, *J. Atmos. Sci.*, 2012, **69**, 1118–1136

[Poster, P15]

# Initiation processes and structures of intraseasonal variability simulated in an aqua-planet

Daisuke Takasuka[1], Masaki Satoh[1]

1. Atmosphere and Ocean Research Institute, the University of Tokyo, Japan

## 1. Introduction

In the tropics, large-scale and intraseasonal convective activities represented by the Madden-Julian Oscillation (MJO) are often organized over the ocean. Previous studies suggest that MJO onset can be influenced by circumnavigating Kelvin-wave signals radiated from the previous MJO event (e.g., Matthews 2008), accumulation of moisture in the middle atmosphere (e.g., Nasuno et al. 2015), or mechanical forcing from the extratropical region (e.g., Zhao et al. 2013). It is, however, difficult to discuss the essential role in initiation or organization processes of MJO in the real world because of its complicated situations such as land-sea masks or seasonality. In addition, it is unclear why the MJO exists as another mode distinguished from moist-Kelvin wave signals. Therefore, we discuss the selection and initiation processes of the MJO-mode in comparison with moist-Kelvin wave signals using idealized aqua-planet experiments with different SST distributions.

## 2. Model description and experimental design

The Nonhydrostatic Icosahedral Atmospheric Model (NICAM) was used to conduct aqua-planet experiments. The horizontal grid spacing was about 56 km uniformly. The model top was set to 40 km, with 40 vertical layers. The solar insolation was fixed to that in the equinox condition. We conducted three experiments with different fixed-SST distributions; one was the zonally uniform SST with a maximum of 27℃ along the equator (UNIFORM), and the others were forced by a zonal wavenumber one patch (30°N/S) superimposed on the UNIFORM, whose amplitudes at the equator were 2K and 4K (2KW1 and 4KW1, respectively). The cloud scheme was explicitly used in spite of relatively coarse resolution because it can improve a representation of the relationship between the moisture, convection, and large-scale dynamics. All experiments run for 10 years from the result of 3-yr integration from a state of rest and constant temperature.

## 3. Detection of convective intraseasonal variability

We confirm a dominant intraseasonal variability (ISV; period: 20−100 days) with different characteristics in each experiment. In order to detect those ISV in terms of convective activities, we construct the detective method using only outgoing longwave radiation (OLR) data. An EOF analysis of OLR anomalies (0°−360°, 30°N/S) filtered for the zonal wave number more than one and 20−100 days period yields two spatial EOF patterns representing eastward propagation with the intraseasonal time scale. Then, 20−100 days filtered OLR anomalies have been projected onto the corresponding EOFs and PC1 and PC2 are normalized. The phase space spanned by these two PCs and OLR anomalies averaged over the initiation region defined from the phase composite qualitatively are used to detect the initiation of ISV in each experiment.

## 4. Results

Figure 1 shows the time-longitude diagrams of lagged-composite 10°N/S OLR and U850

anomalies (Day 0: the initiation date of ISV). In the 2KW1, convective signals in phase with low-level convergence propagate eastward at less than 5 m/s, which is associated with MJO-like disturbances. In the UNIFORM, on the other hand, convective signals are in phase with westerly anomalies and their phase speed is much faster than in the 2KW1. These signals can be regarded as moist-Kelvin waves. We can also recognize that the convective signals in the 4KW1 are slightly faster that in the 2KW1. These results suggest the zonal non-uniformity of the SST distribution is necessary for the existence of the MJO-mode, and that the amplitude of the zonal SST gradient may have influence on the mechanism of propagation of the MJO-mode.

Initiation and organization processes of the MJO-mode are investigated in the 2KW1 which internally produces MJO-like disturbances well. The moisture accumulation in the middle troposphere caused by the horizontal advection is obvious prior to the organization of MJO-like disturbances. It helps to make the favorable condition for deep convection. The horizontal advection seems to be related to the Rossby response to negative heating anomalies over the warm pool. In addition, negative sea level pressure anomalies propagating from the previous MJO-like event approach the western side of the warm pool and lead to the convergence in the planetary boundary layer, which can trigger the convective initiation. Moreover, the budget analysis of the variance of frozen moist static energy anomalies (e.g., Wing and Emanuel 2014) suggest that the positive feedback of the latent heat flux and longwave radiation can efficiently operate during the former and latter period of the organization of MJO-like disturbances respectively.

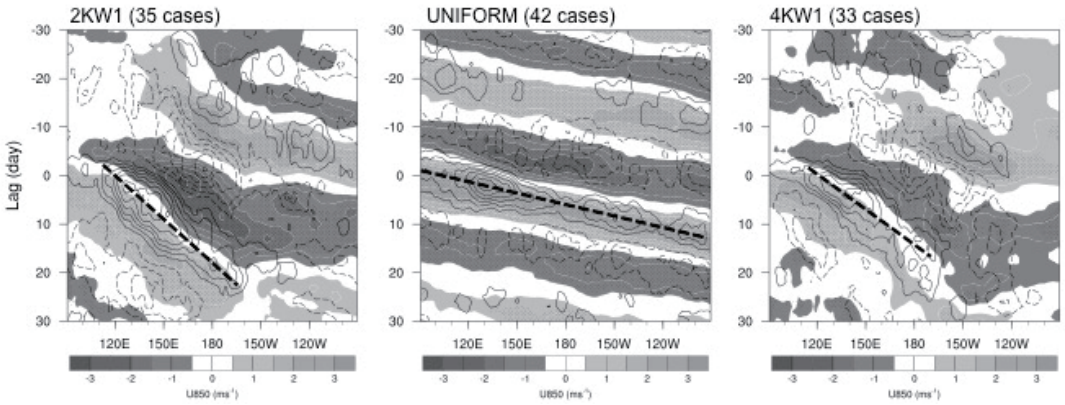


Fig. 1. Time-longiture diagrams of lagged-composite OLR (contours) and U850 (shaded) anomalies

**References:**

Matthews A. J.: Primary and successive events in the Madden-Julian Oscillation, *Quart. J. Ray. Meteorol. Soc.*, 2008, **134**, 439−453

Nasuno, T., T. Li, and K. Kikuchi: Moistening processes before the convective initiation of Madden–Julian oscillation events during the CINDY2011/DYNAMO period., 2015, *Mon. Wea. Rev.*, **143**, 622–643

Wing A. A. and K. A. Emanuel: Physical mechanisms controlling selfaggregation of convection in idealized numerical modeling simulations., 2014, *J. Adv. Model. Earth Syst.*, **6**: 59–74

Zhao, C.-B., T. Li, and T. Zhou: Precursor signals and processes associated with MJO initiation over the tropical Indian Ocean., 2013, *J. Climate*, **26**, 291–307

[Poster, P16]

# Global 7-km mesh nonhydrostatic Model Intercomparison Project for improving TYphoon forecast (TYMIP-G7)

Masuo Nakano[1], Akiyoshi Wada[2], Masahiro Sawada[2], Hiromasa Yoshimura2, Ryo Onishi[1], Shintaro Kawahara[1], Wataru Sasaki[1], Tomoe Nasuno[1], Munehiko Yamaguchi[2], Takeshi Iriguchi[2], Masato Sugi[2], and Yoshiaki Takeuchi[2]

1. Japan Agency for Marine-Earth Science and Technology, Japan

2. Meteorological Research Institute, Japan Meteorological Agency, Japan

Email: masuo@jamstec.go.jp

## Abstract

Recent advances in high-performance computers facilitate operational numerical weather prediction by global hydrostatic atmospheric models with horizontal resolution ~10 km. Given further advances in such computers and the fact that the hydrostatic balance approximation becomes invalid for spatial scales < 10 km, development of global nonhydrostatic models with high accuracy is urgently needed.

The Global 7-km mesh nonhydrostatic Model Intercomparison Project for improving TYphoon forecast (TYMIP-G7; Nakano et al. 2016) is designed to understand and statistically quantify the advantage of high-resolution nonhydrostatic global atmospheric models for improvement of tropical cyclone (TC) prediction. The 137 sets of 5-day simulations using three next-generation nonhydrostatic global models with horizontal resolution 7 km, and conventional hydrostatic global model with horizontal resolution 20 km are run on the Earth Simulator. The three 7-km mesh nonhydrostatic models are the nonhydrostatic global spectral atmospheric Model using Double Fourier Series (DFSM; Yoshimura, 2012), Multi-Scale Simulator for the Geoenvironment (MSSG; Takahashi et al., 2006, 2013), and Nonhydrostatic ICosahedral Atmospheric Model (NICAM; Satoh et al. 2014). The 20-km mesh hydrostatic model is the operational Global Spectral Model (GSM; Japan Meteorological Agency, 2013) of the Japan Meteorological Agency.

Compared with the 20-km mesh GSM, the 7-km mesh models reduce systematic errors of TC track and intensity predictions but still have difficulties in predicting rapid TC

intensification. The benefits of the multi-model ensemble method are confirmed to be valid for the 7-km mesh nonhydrostatic global models. Whereas the three 7-km mesh models reproduce a typical axisymmetric mean inner-core structure such as primary and secondary circulations, simulated TC structures and their intensity in each case are very different among the models. Moreover, the simulated track is not always better than that of the 20-km mesh GSM. These results suggest that development of more sophisticated initialization techniques and model physics is needed for further improvement of TC prediction.

**References:**


Japan Meteorological Agency: Outline of the operational numerical weather prediction at the Japan Meteorological Agency. Appendix to WMO technical progress report on the global data-processing and forecasting system and numerical weather prediction, 2013, 188p.http://www.jma.go.jp/jma/jma-eng/jma-center/nwp/outline2013-nwp/index.htm.

Nakano, M., A. Wada, M. Sawada, H. Yoshimura, R. Onishi, S. Kawahara, W. Sasaki, T. Nasuno, M. Yamaguchi, T. Iriguchi, M. Sugi, and Y. Takeuchi: Global 7-km mesh nonhydrostatic Model Intercomparison Project for improving TYphoon forecast (TYMIP-G7): Experimental design and preliminary results, *Geosci. Model Dev. Discuss.* 2016, under revision, doi:10.5194/gmd-2016-184.

Satoh, M., H. Tomita, H. Yashiro, H. Miura, C. Kodama, T. Seiki, A. T. Noda, Y. Yamada, D. Goto, M. Sawada, T. Miyoshi, Y. Niwa, M. Hara, T. Ohno, S. Iga, T. Arakawa, T. Inoue and H. Kubokawa: The Non-hydrostatic Icosahedral Atmospheric Model: description and development. *Progress in Earth and Planetary Science* 2014, **1**:18. doi: 10.1186/s40645-014-0018-1

Takahashi, K., X. Peng, R. Ohnishi, T. Sugimura, M. Ohdaira, K. Goto. and H. Fuchigami: Multi-Scale Weather/Climate Simulations with Multi-Scale Simulator for the Geoenvironment (MSSG) on the Earth Simulator. *Ann. Rep. Earth Simulator Center,* 2006, April 2006–March 2007, pp.27–33, ISSN 1348–5822.

Takahashi K., R. Onishi, Y. Baba, S. Kida, K. Matsuda, K. Goto. and H. Fuchigami: Challenge toward the prediction of typhoon behaviour and down pour. *J. Phys.: Conference Series*, 2013, **454**:012,072.

Yoshimura, H.: Development of a nonhydrostatic global spectral atmospheric model using double Fourier series. *CAS/JSC WGNE Research Activities in Atmospheric and Ocean Modeling*, 2012, **42**, 3.05-3.06.

[Poster, P17]

# Future projection of extratropical cyclone simulated by a 14 km mesh global atmospheric model

Chihiro Kodama[1], Bjorn Stevens[2], Thorsten Mauritsen[2], Tatsuya Seiki[3] and Masaki Satoh[3,1]

1. Japan Agency for Marine-Earth Science and Technology, Japan

2. Max Planck Institute for Meteorology, Germany.

3. Atmosphere and Ocean Research Institute, the University of Tokyo, Japan

Email: kodamac@jamstec.go.jp

## Abstract

Changes in the extratropical cyclones due to global warming are investigated using 14 km mesh global non-hydrostatic atmospheric model, NICAM (Satoh et al. 2014). Present and future climate runs (Kodama et al. 2015; Satoh et al. 2015) were performed for 25-30 years each with bulk cloud microphysics scheme instead of convection scheme. Detection and tracking algorithms are applied to the model output as well as reanalysis data to obtain statistical features of the extratropical cyclones. Structural changes of the extratropical cyclones are analyzed by compositing each variable at the cyclone center.

The model simulates fine structure of the extratropical cyclone (Figure 1). Statistical features simulated by the model in terms of mean sea level pressure (MSLP), low-level wind speed and longevity are comparable to those obtained from JRA-55 reanalysis (Figure 2). Mean structure of the extratropical cyclone including precipitation is also simulated. Geographical distribution of storm-track is captured, though significant positional bias exists, especially over the North Pacific.

The model projects a poleward shift of the storm-track and a slight reduction of the number of extratropical cyclones due to global warming, which is consistent with the previous studies. Mean precipitation and low-level wind speed around the extratropical cyclone are enhanced (especially in the Southern Hemisphere for low-level wind speed) but MSLP is not significantly decreased. One key aspect of the future projection in this study is an enhancement of the vertical wind, which corresponds to the increased ice water path and cloud radiation effect by longwave radiation. Further analysis in terms

of the characteristic feature of the extratropical cyclone such as warm conveyer belt is necessary to understand future projection of the extratropical cyclone by high-resolution global non-hydrostatic atmospheric model.

**References:**

Kodama, C., Y. Yamada, A. T. Noda, K. Kikuchi, Y. Kajikawa, T. Nasuno, T. Tomita, T. Yamaura, H. G. Takahashi, M. Hara, Y. Kawatani, M. Satoh and M. Sugi: A 20-year climatology of a NICAM AMIP-type simulation. *J. Meteor. Soc. Japan*, 2015, **93**, 393-424, doi: 10.2151/jmsj.2015-024.

Satoh, M., H. Tomita, H. Yashiro, H. Miura, C. Kodama, T. Seiki, A. T. Noda, Y. Yamada, D. Goto, M. Sawada, T. Miyoshi, Y. Niwa, M. Hara, T. Ohno, S. Iga, T. Arakawa, T. Inoue and H. Kubokawa: The Non-hydrostatic Icosahedral Atmospheric Model: description and development. *Progress in Earth and Planetary Science*, 2014, **1**:18, doi: 10.1186/s40645-014-0018-1.

Satoh, M., Y. Yamada, M. Sugi, C. Kodama and A. T. Noda: Constraint on future change in global frequency of tropical cyclones due to global warming. *J. Meteor. Soc. Japan*, 2015, **93**, 489-500, doi: 10.2151/jmsj.2015-025.

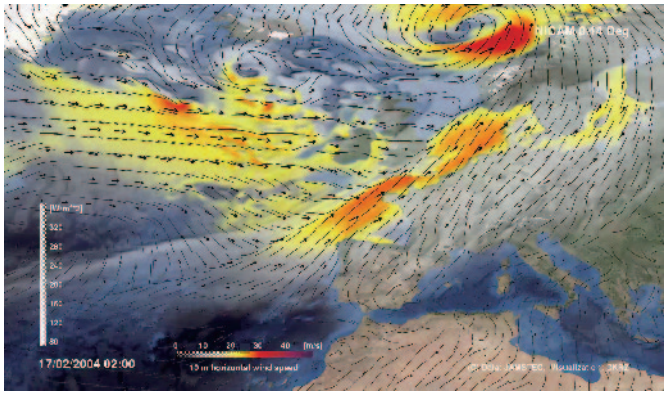


Figure 1: The most intense extratropical cyclone in the Northern Hemisphere in the present climate simulation. 10 m wind speed and vector (shading and arrow) and outgoing longwave radiation (white) are shown.

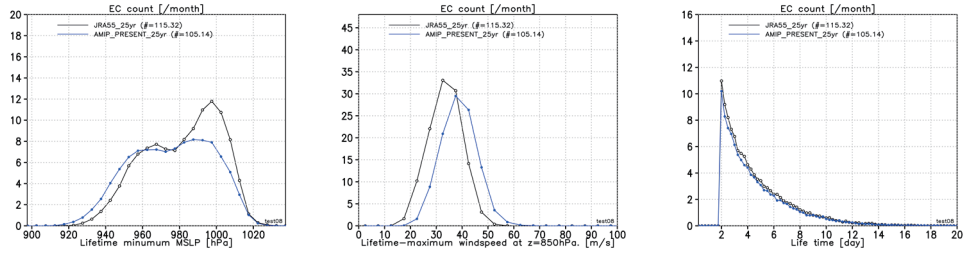


Figure 2: Histogram of the extratropical cyclone per month binned by the lifetime minimum MSLP (left), lifetime-maximum wind speed at 850 hPa (center) and longevity (right). Black and blue lines show results from JRA-55 reanalysis and present climate simulation, respectively.

[Poster, P18]

# RCEMIP: Radiative Convective Equilibrium Model Inter-comparison Project

Masaki Satoh[1], Tomoki Ohno[1], Allison Wing[2], Sandrine Bony[3], and Bjorn Stevens[4]

1. Atmosphere and Ocean Research Institute, the University of Tokyo, Kashiwa, Japan
2. Lamont-Doherty Earth Observatory, Columbia University, Palisades, NY, USA
3. Laboratoire de Météorologie Dynamique, IPSL, CNRS, Paris, France
4. Max-Planck Institute for Meteorology, Hamburg, Germany

Email: satoh@aori.u-tokyo.ac.jp

## Abstract

Radiative Convective Equilibrium Model Inter-comparison Project (RCEMIP) is proposed. Radiative-convective equilibrium (RCE) is referred to as atmospheric quasi statistical balance between convection and radiation processes (Manabe and Strickler 1964). Historically, RCE has been argued mainly with one-dimensional models, but in recent years more computationally intensive numerical calculations of RCE have been conducted with three-dimensional numerical models with explicitly resolved convection and domain lengths of 100-1000 km. A simple horizontally uniform boundary condition is prescribed with a constant sea surface temperature (SST) or a slab ocean model with uniform solar insolation. Since clouds are a most ambiguous part of climate models, the simple framework of RCE is suitable for understanding how clouds are simulated in numerical models. RCE is also useful to clarify the sensitivities of clouds to the details of cloud schemes implemented in numerical models (e.g., Satoh and Matsuda 2008). A number of RCE numerical studies have been conducted until recently with their own various configurations. One category is RCE on the sphere either with or without a cumulus parameterization scheme (e.g., Popke et al., 2013; Arnold and Randall, 2015; Reed et al., 2015; Bony et al., 2016; Satoh et al., 2016; Ohno and Satoh, 2016). The other category is RCE with regional models in an arbitrary domain size , primarily with explicitly resolved convection (e.g., Wing and Cronin 2016; Silvers et al. 2016). In order to systematically understand differences or similarities of various model results, a more coordinated framework for RCE numerical studies is demanded as “RCEMIP”. Possible choices for experimental settings of RCE are listed as follows:

- Geometry: sphere / plane (square or channel)
- Domain size: Earth radius R / length=40,000 km × factor (e.g., 0.1–1.0)
- Horizontal resolution: $\Delta x$ = 1–10 km for explicit convection, or coarser

resolution (1–2 degree) with a cumulus parameterization

- Boundary condition: fixed SST (e.g., 296, 300, 304K) or a slab ocean
- $CO_2$: a current value or increased (e.g., $4\times CO_2$)
- Physics dependency: cloud microphysics, turbulence, radiation,; switch on/off of cumulus parameterization
- Interactive radiation or non-interactive, with/without clouds
- With or without diurnal cycle
- Without rotation, or with rotation

Among a lot of varieties listed above, we will discuss the experimental design of RCEMIP, scientific targets, and how to proceed. One strength of RCEMIP is the numerous scientific questions that could be explored, such as better understanding of uncertainties of climate sensitivities and changes in clouds and circulations, or convective aggregation, associated with global warming.

**References:**


Arnold, N. P., and D. A. Randall, 2015: Global-scale convective aggregation: Implications for the Madden-Julian Oscillation. *J. Adv. Model. Earth Syst.*, **7**, 1499-1518.

Bony, S. et al., 2016: Thermodynamic control of anvil cloud amount. *PNAS*, **113**, 8927-8932.

Manabe, S., and R. F. Strickler, 1964: Thermal equilibrium of the atmosphere with a convective adjustment. *J. Atmos. Sci.*, **21**, 361-385.

Ohno, T., and M. Satoh, 2016: Sensitivity studies of cloud responses on SSTs in RCE experiments using a high-resolution global nonhydrostatic model. The 4th International Workshop on Nonhydrostatic Models., Hakone, Japan. Nov. 30 - Dec. 2, 2016.

Popke, D. et al., 2013: Climate and climate change in a radiative-convective equilibrium version of ECHAM6. *J. Adv. Model. Earth Syst.*, **5**, 1-14.

Reed, K. et al., 2015: Global Radiative–Convective Equilibrium in the Community Atmosphere Model, Version 5. *J. Atmos. Sci.*, **72**, 2183-2197.

Satoh, M., and Y. Matsuda, 2009: Statistics on high-cloud areas and their sensitivities to cloud microphysics using single-cloud experiments. *J. Atmos. Sci.*, **66**, 2659-2677.

Satoh, M. et al., 2016: Structure of tropical convective systems in aqua-planet experiments: Radiative-convective equilibrium versus the Earth-like experiment. *SOLA*, **12**, 220-224.

Silvers, L. G. et al., 2016: Radiative convective equilibrium as a framework for studying the interaction between convection and its large-scale environment. *J. Adv. Model. Earth Syst.*, **8**, 1330–1344.

Wing, A. A., and T. W. Cronin., 2016: Self-aggregation of convection in long channel geometry. *Q. J. Roy. Meteor. Soc.,* **142**, 1-15.

**Participants**

| | | |
|---|---|---|
| Sachiho Adachi | RIKEN Advanced Institute for Computational Science | sachiho.adachi@riken.jp |
| Hoang Hai Bui | Kyoto University | haibuihoang@gmail.com |
| Luis Adriano Chongue | Doshisha University | chongue.chongueluis@gmail.com |
| Shin Fukui | Tohoku University | fukui@wind.gp.tohoku.ac.jp |
| Akimoto Ginga | Japan Meteorological Agency | ginga.akimoto@met.kishou.go.jp |
| Wojciech Grabowski | NCAR | grabow@ucar.edu |
| Akihiro Hashimoto | Meteorological Research Institute | ahashimo@mri-jma.go.jp |
| Takumi Honda | RIKEN Advanced Institute for Computational Science | takumi.honda@riken.jp |
| Yasutaka Ikuta | Japan Meteorological Agency | yiktpleza5@yahoo.co.jp |
| Junshi Ito | Meteorological Research Institute | junshi@aori.u-tokyo.ac.jp |
| Toshiki Iwasaki | Tohoku University | iwasaki@wind.gp.tohoku.ac.jp |
| Teruyuki Kato | Meteorological Research Institute | tkato@mri-jma.go.jp |
| Takuya Kawabata | Meteorological Research Institute | tkawabat@mri-jma.go.jp |
| Kohei Kawano | Japan Meteorological Agency | k_kawano@met.kishou.go.jp |
| Kazuyoshi Kikuchi | University of Hawaii | kazuyosh@hawaii.edu |
| Chihiro Kodama | Japan Agency for Marine-Earth Science and Technology | kodamac@jamstec.go.jp |
| Shunji Kotsuki | RIKEN Advanced Institute for Computational Science | shunji.kotsuki@riken.jp |
| Hiroyasu Kubokawa | Atmosphere and Ocean Research Institute, University of TOkyo | kubok@aori.u-tokyo.ac.jp |
| Kengo Matsubayashi | Japan Meteorological Agency | kengomatsubayashi@met.kishou.go.jp |
| Celio Matuele | Doshisha University | celiomatuele@gmail.com |
| John McGregor | CSIRO | John.McGregor@csiro.au |
| Tomoki Miyakawa | Atmosphere and Ocean Research Institute, The University of Tokyo | miyakawa@aori.u-tokyo.ac.jp |
| Takemasa Miyoshi | RIKEN Advanced Institute for Computational Science | takemasa.miyoshi@riken.jp |
| Hugh Morrison | National Center for Atmospheric Research | morrison@ucar.edu |
| Christopher Moseley | Max-Planck-Institute for Meteorology | christopher.moseley@mpimet.mpg.de |
| Kozo Nakamura | Japan Agency for Marine-Earth Science and Technology | nakamura@jamstec.go.jp |
| Masuo Nakano | Japan Agency for Marine-Earth Science and Technology | masuo@jamstec.go.jp |
| Hiromasa Nakayama | Japan Atomic Energy Agency | nakayama.hiromasa@jaea.go.jp |
| Tomoe Nasuno | Japan Agency for Marine-Earth Science and Technology | nasuno@jamstec.go.jp |
| Hiroshi Niino | Atmosphere and Ocean Research Institute, The University of Tokyo | niino@aori.u-tokyo.ac.jp |
| Yuki Nishikawa | Atmosphere and Ocean Research Institute, The University of Tokyo | y_nishi@aori.u-tokyo.ac.jp |
| Seiya Nishizawa | RIKEN Advanced Institute for Computational Science | s-nishizawa@riken.jp |
| Akira Noda | Japan Agency for Marine-Earth Science and Technology | a_noda@jamstec.go.jp |
| Tomoki Ohno | Atmosphere and Ocean Research Institute, The University of Tokyo | t-ohno@aori.u-tokyo.ac.jp |
| Chia Rui Ong | Earth and Planetary Science, The University of Tokyo | ong.chiarui@eps.s.u-tokyo.ac.jp |
| Ryo Onishi | Japan Agency for Marine-Earth Science and Technology | onishi.ryo@jamstec.go.jp |
| Michiko Otsuka | Meteorological Research Insitute | motsuka@mri-jma.go.jp |
| Mike Pritchard | University of California, Irvine | mspritch@uci.edu |
| David Randall | Colorado State University | randall@atmos.colostate.edu |
| Didier Ricard | CNRM (Meteo-France / CNRS) | didier.ricard@meteo.fr |
| Woosub Roh | Atmosphere and Ocean Research Institute, The University of Tokyo | ws-roh@aori.u-tokyo.ac.jp |
| Kazuo Saito | Meteorological Research Institute | ksaito@mri-jma.go.jp |
| Yousuke Sato | RIKEN Advanced Institute for Computational Science | yousuke.sato@riken.jp |
| Masaki Satoh | Atmosphere and Ocean Research Institute, The University of Tokyo | satoh@aori.u-tokyo.ac.jp |
| Thomas Schwitalla | University of Hohenheim | thomas.schwitalla@uni-hohenheim.de |
| Tatsuya Seiki | Japan Agency for Marine-Earth Science and Technology | tseiki@jamstec.go.jp |
| Hiromu Seko | Meteorological Research Institute | hseko@mri-jma.go.jp |
| Chung-Hsiung Sui | National Taiwan University | sui@as.ntu.edu.tw |
| Daisuke Takasuka | Atmosphere and Ocean Research Institute, The University of Tokyo | takasuka@aori.u-tokyo.ac.jp |
| Kazushi Takemura | Kyoto University | k_takemura@kugi.kyoto-u.ac.jp |
| Koji Terasaki | RIKEN Advanced Institute for Computational Science | koji.terasaki@riken.jp |
| Eigo Tochimoto | Atmosphere and Ocean Research Institute, The University of Tokyo | tochimoto@aori.u-tokyo.ac.jp |
| Hirofumi Tomita | RIKEN Advanced Institute for Computational Science | htomita@riken.jp |
| Lian-Ping Wang | Japan Agency for Marine-Earth Science and Technology | lwang@udel.edu |

| | | |
|---|---|---|
| Shun-ichi Watanabe | Atmosphere and Ocean Research Institute, The University of Tokyo | watanabe-s@aori.u-tokyo.ac.jp |
| Chien-Ming Wu | National Taiwan University | mog@as.ntu.edu.tw |
| Yoshinori Yamada | Meteorological Research Institute | yyamada@mri-jma.go.jp |
| Takanobu Yamaguchi | CIRES CU / NOAA ESRL | tak.yamaguchi@noaa.gov |
| Hisashi Yashiro | RIKEN Advanced Institute for Computational Science | h.yashiro@riken.jp |
| Takuya Yasui | Japan Meteorological Agency | t_yasui@met.kishou.go.jp |
| Sho Yokota | Meteorological Research Institute | syokota@mri-jma.go.jp |
| Ryuji Yoshida | RIKEN Advanced Institute for Computational Science | ryoshida@riken.jp |

Organized by
Atmosphere and Ocean Research Institute (AORI), The University of Tokyo
RIKEN, Advanced Institute for Computational Science (AICS)
Research Group on Non-hydrostatic Numerical Models, Meteorological Society of Japan

Supported by
Japan Meteorological Agency
Center for Earth Surface System Dynamics (CESD),
Atmosphere and Ocean Research Institute (AORI), The University of Tokyo
The Virtual Laboratory for the Earth's Climate Diagnostics Program (VL)
RIKEN, Advanced Institute for Computational Science (AICS)
FOCUS Establishing Supercomputing Center of Excellence
FLAGSHIP2020 Project, Priority Issue 4
Meteorological Society of Japan
Japan Geoscience Union
SGI Japan, Ltd.